2016

Functional Consequences of mtDNA Methylation on Mitochondrial Transcription Factor Binding and Transcription Initiation

Elliot N. Burton
Virginia Commonwealth University

FUNCTIONAL CONSEQUENCES OF MTDNA METHYLATION ON MITOCHONDRIAL TRANSCRIPTION FACTOR BINDING AND TRANSCRIPTION INITIATION

A thesis submitted in partial fulfillment of the requirements for the degree of Master of Science at Virginia Commonwealth University

by

ELLIOT BURTON
Bachelor of Science, James Madison University, 2011

Advisor: Shirley M. Taylor, PhD
Associate Professor
Department of Microbiology and Immunology

Virginia Commonwealth University
Richmond, Virginia
February, 2016

Acknowledgement

I would like to recognize some of the individuals who had an impact on my life during my graduate education. First, I would like to thank Dr. Shirley Taylor for the opportunity to work with her. I would also like to thank my committee members, Dr. Rita Shiang and Dr. Joyce Lloyd for their guidance.

Thank you to all the members of the Taylor and Moran laboratories, past and present, for their camaraderie and support, both scientific and personal: Dr. Timothy Lochmann, Dr. Lisa Shock, Dr. Prashant Thakkar, Joyce Balinang, Jason Robinson, Shannon Hendrick, John Strang, Dr. Catherine Bell, Dr. Stuti Agarwal, Dr. Chen Yang, and Charles Lyons. I would also like to acknowledge the National Science Foundation for the funding that made this research possible.

Finally, I would like to thank my friends and family, especially my wife, Sarah, for their unwavering love and support, without which none of this would be possible.

Table of Contents

Abstract

FUNCTIONAL CONSEQUENCES OF MTDNA METHYLATION ON MITOCHONDRIAL TRANSCRIPTION FACTOR BINDING AND TRANSCRIPTION INITIATION

Elliot Burton, B.S.

A thesis submitted in partial fulfillment of the requirements for the degree of Master of Science at Virginia Commonwealth University

Virginia Commonwealth University, 2016

Major Advisor: Shirley M. Taylor, PhD
Associate Professor, Department of Microbiology and Immunology

The role of cytosine modifications on nuclear transcription has been well characterized, but the function of DNA methylation in the mitochondrial genome has not been determined. Previous studies conducted by the Taylor laboratory have shown overexpression of the mitochondrial isoform of DNMT1 leads to strand-specific changes in gene expression. Here, we show that increased mtDNMT1 expression leads to an increase in the polycistronic transcript encoding the ND1 and Cox1 sequences. In order to understand the mechanistic basis of these changes, we investigated the effects of CpG methylation in the heavy strand promoter on transcription initiation and TFAM binding. Methylation was found to increase transcription initiation from HSP1 and result in larger TFAM:DNA complexes forming at lower protein concentrations. Our data suggest a functional role for cytosine methylation in the mitochondria, which we propose may have an effect on oxidative phosporylation and cellular function.

Introduction

Epigenetics: an overview

Epigenetics is the study of heritable changes in gene expression that are not due to changes in the DNA sequence [1]. Although DNA is often represented as linear and protein-free, in the nucleus it is heavily condensed to form chromatin. This is achieved through several layers of compaction. The most basic unit of compacted DNA and protein is the nucleosome, which consists of ~165 base pairs of DNA wrapped around a histone hetero-octamer [2]. This repeating motif results in five to tenfold compaction of the DNA, but makes the DNA sequence less accessible to regulatory proteins [2]. These nucleosomes are then coiled into a 30 nm fiber, which form higher order structures that result in the formation of the metaphase chromosome [2]. Different modifications of the exposed histone tails are correlated to compacted, silenced chromatin (heterochromatin) or open, actively transcribed chromatin (euchromatin).

Epigenetic modifications are also present on the DNA itself in the form of cytosine modifications [1]. Cytosines in cytosine-guanine (CpG) dinucleotides can be modified with methyl (5mC) or hydroxymethyl (5hmC) groups, which are associated with compaction and transcriptional silencing [1] or active demethylation and expression[3] of a region, respectively. CpG methylation patterns are established during mammalian development by DNA methytransferases (DNMT) 3a and 3b [4] and maintained through cell division by DNMT1, but there is functional overlap between the different enzymes [5]. 5mC is converted to 5hmC by the

ten-eleven translocation (TET) family of enzymes [6]. Cytosine methylation can recruit methyl binding proteins (MBDs), which in turn recruit histone-modifying enzymes, resulting in the perpetuation of allele transcription states [7].

The effects of cytosine modifications on transcription are fairly well understood for the nuclear genome, but there is a second source of genetic information in the cell, the mitochondrial genome, and the effects of CpG modification in this separate genome are not understood.

The Mitochondrial Genome

Each mitochondrion contains between 1 and 15 copies of the mitochondrial genome [8], and human cells can contain hundreds to one thousand mitochondria [9]. Accordingly, the number of mitochondrial genomes per cell can vary, but mitochondrial DNA (mtDNA) represents about 1% of the total DNA in a cell [10]. However, mitochondrial DNA contains the genes encoding essential components of the electron transport chain, making its regulation and expression necessary for normal energy homeostasis.

The mitochondrial genome is a 16,569 bp circular DNA encoding 2 rRNAs, 22 tRNAs, and 13 proteins (Figure 1). These genes are distributed across both strands of the genome, which are referred to as the light and heavy strands due to their different buoyant densities in cesium chloride gradients [11]. The heavy strand encodes the two rRNAs, 14 tRNAs and 12 of the 13 proteins, while the light strand encodes a single protein (ND6) and the remaining 8 tRNAs [12]. The mitochondrial genome lacks introns, but contains a noncoding region, called the D-loop, that includes transcriptional promoters and the origin of replication for the heavy strand [13].

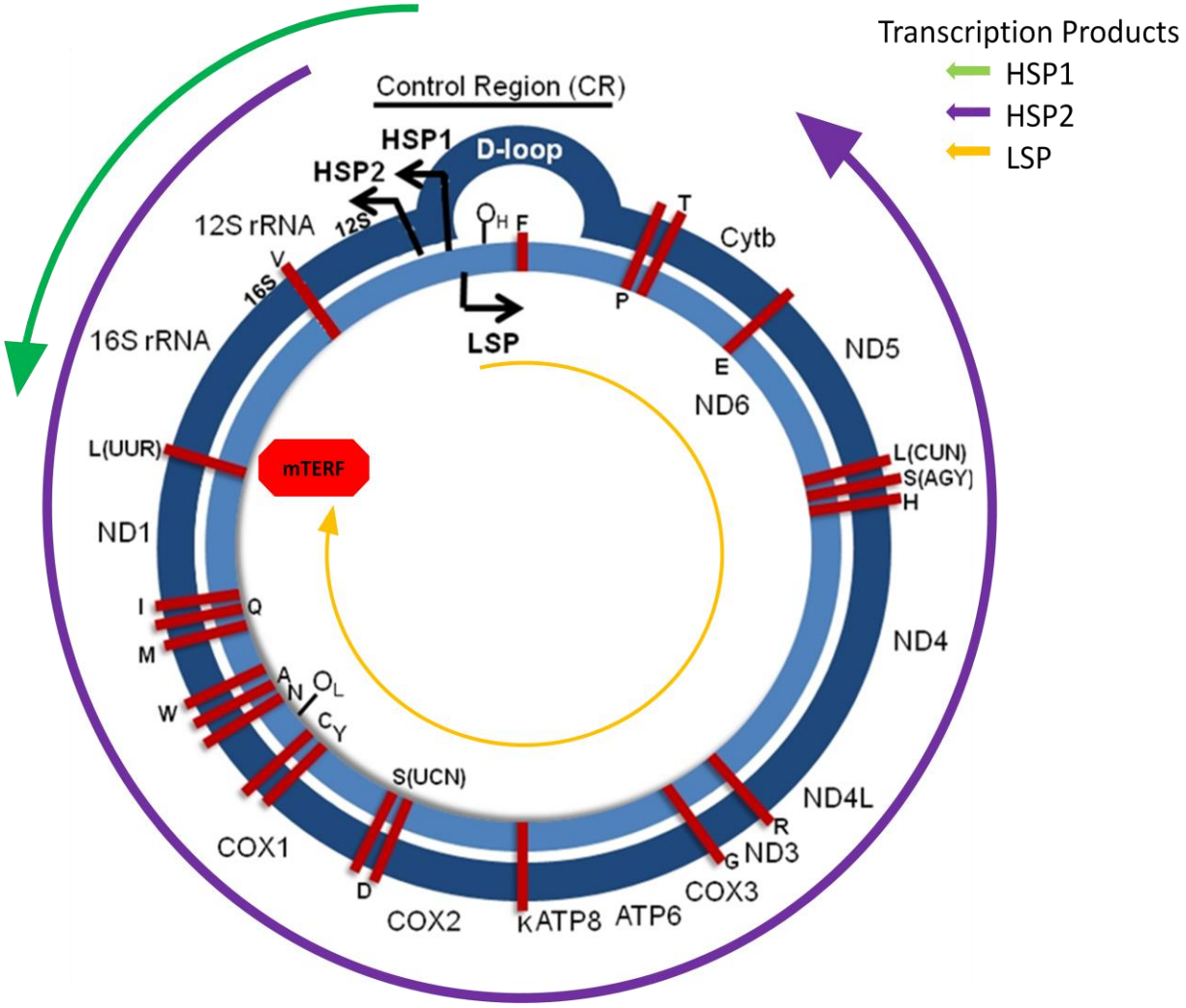

Figure 1. Diagram of the mitochondrial genome and polycistronic transcription products. The heavy strand is depicted in dark blue and the light strand is depicted in light blue. The red lines depict the tRNA genes. The mTERF binding site is shown by the red octagon. The polycistronic messages produced by transcription initiation at the three promoters are depicted by the arrows.

Mitochondrial Transcription

Transcription of the mitochondrial genome occurs in a strand-specific manner and produces polycistronic primary messages [14] that are then processed to form the mature rRNAs, mRNAs, and tRNAs [15]. Transcription is initiated at one of three promoters: two heavy strand promoters (HSP1 and HSP2) and one light strand promoter (LSP). HSP2 and LSP produce polycistronic messages that contain almost all of the respective strand, while transcription initiated at HSP1 results in a shorter polycistronic message containing the two rRNAs, terminating at the 3' end of the 16s rRNA gene [14]. The existence of HSP2 has been debated, and though transcription can be initiated from this promoter *in vitro*, it has been found to be more than 100-fold less efficient at transcription initiation than HSP1 under identical conditions [28]. It has been hypothesized that only HSP1 is used *in vivo* and that early termination of transcription immediately downstream of the 16s rRNA may better explain the higher levels of the rRNAs than mRNAs observed in mitochondria [32].

The machinery responsible for mitochondrial transcription is distinct from the nuclear transcriptional machinery. The single mitochondrial RNA polymerase (POLRMT) is a nuclear-encoded, single-subunit enzyme that is homologous to bacteriophage T3 and T7 RNA polymerases, rather than the multi-subunit nuclear RNA polymerases [16]. While the single-subunit RNA polymerase of T7 phage is functional without any accessory proteins [17], this is not the case for POLRMT, which requires mitochondrial transcription factor A (TFAM) and mitochondrial transcription factor B2 (TFB2M) (Figure 2) [18].

TFB2M and the paralogous enzyme TFB1M show primary sequence similarity to bacterial rRNA dimethyltransferases, and phylogenetic analysis suggests that the TFBM factors were derived from the genome of the mitochondrial endosymbiont [17]. While TFB1M

primarily functions as a mitochondrial rRNA methyltransferase [19], TFB2M is less efficient as a methyltransferase [20] and is a much more active transcription factor *in vitro* than TFB1M [18]. TFB2M was shown to be the more active TFBM protein in mitochondrial transcription in *Drosophila* through RNAi knockdown – reduction of TFB2M resulted in a decrease in mitochondrial transcription [21] while reduction of TFB1M did not [22]. These data suggest that TFB2M is the TFBM factor primarily involved in the mitochondrial transcription initiation complex.

TFAM is a member of the high mobility group (HMG) superfamily of DNA binding proteins. It is composed of two HMG box domains which bind the minor groove of promoter DNA, creating two kinks in the DNA and forcing it to undergo a U-turn [23]. These HMG box domains are separated by a linker region and followed by a C-terminal tail, which is essential for activation of transcription [24]. The HMG box domains of TFAM can also bind nonspecifically to non-promoter DNA, and in addition to transcription initiation, TFAM also packages the mitochondrial genome into a more compact, less active form, referred to as a nucleoid [25].

TFAM is the first component of the mitochondrial transcription machinery to bind the promoter region [26]. POLRMT is then recruited to the promoter region through protein-protein interactions with the C-terminal end of TFAM and protein-DNA interactions with upstream sequence [27]. TFB2M then binds to POLRMT and the promoter sequence and melts the transcription start site, initiating transcription [28]. These interactions have been most clearly characterized for LSP, and to a lesser degree, HSP1 [28]. However, the binding of TFAM may have a different effect on transcription initiation from HSP2 [28,29]. *In vitro* assays using equimolar concentrations of template, TFAM, TFB2M, and POLRMT have shown that

transcription initiated from HSP2 results in 100-fold less run-off product than transcription initiated from

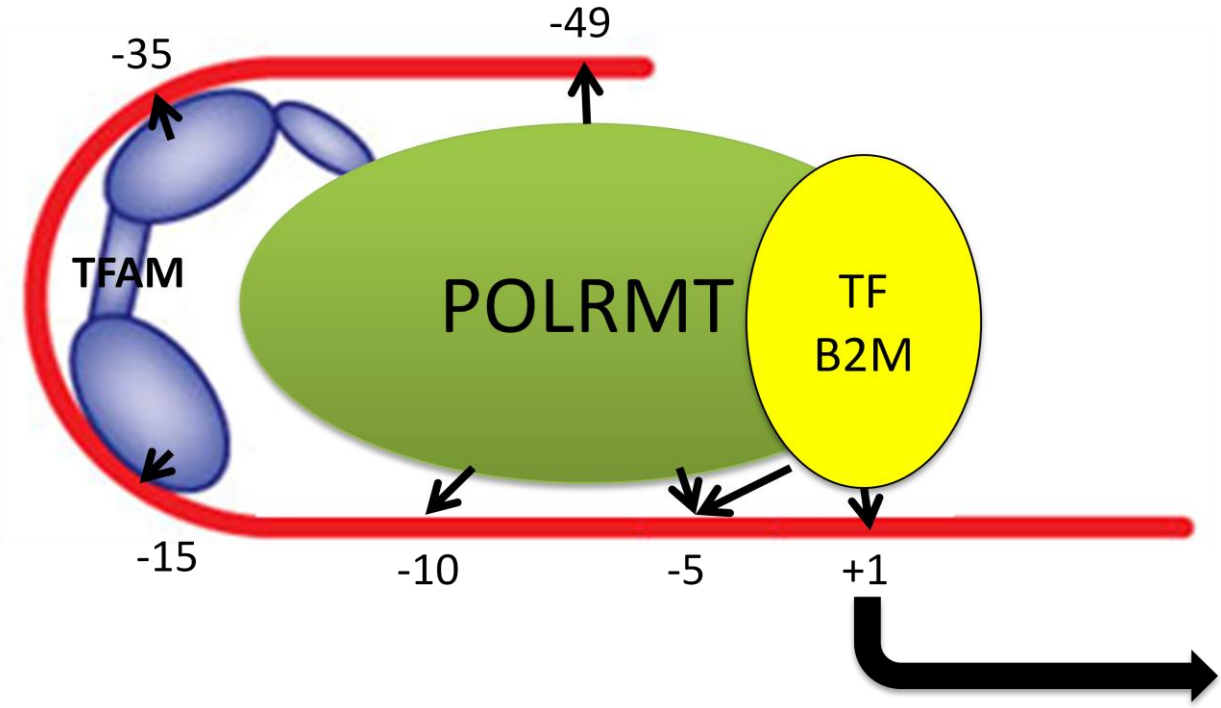

Figure 2. Assembly of the transcription initiation complex at LSP. Transcription begins at +1. The numbers and arrows represent points of protein/DNA interactions upstream of the promoter, based on crosslinking studies [27].

HSP1 under identical conditions [28]. Removing TFAM from the same *in vitro* reaction does not result in a change in transcription from HSP2 [28], indicating that it is not essential. Similar studies using a HSP2 template with a shorter transcribed sequence found that adding TFAM to the reaction resulted in reduced transcription [29], indicating that TFAM may be a repressor of transcription from HSP2. In addition to its role in mitochondrial transcription initiation, TFAM also serves as a packaging protein by binding non-specifically to the mitochondrial genome and compacting it into nucleoids [30]. The mechanism by which the degree of TFAM-mediated compaction is regulated in different mtDNA molecules, allowing active transcription from some and the formation of nucleoids from others, has not yet been determined.

The study of transcription termination in mitochondria has focused largely on one protein, the mitochondrial transcription termination factor 1 (mTERF1). mTERF1 binds in the Leu tRNA coding region of the mitochondrial genome and was originally shown to terminate *in vitro* transcription originating from HSP1 [31]. However, recent knock out studies in mice suggest that the primary role of mTERF *in vivo* is to prevent transcription interference at LSP from unterminated elongation complexes and transcription of antisense rRNAs [32]. Supporting this is the observation that mTERF terminates transcription from the light strand more effectively than transcription from the heavy strand [32].

Mitochondrial DNA Replication

Transcription from LSP is not only important for mitochondrial DNA expression, but also plays a role in the replication of the mitochondrial genome. POLRMT can generate RNA primers used by DNA polymerase γ (pol γ) to initiate mtDNA replication from LSP [33]. Other proteins essential for replication of the mitochondrial genome are replicative helicase Twinkle,

which unwinds and melts the double-stranded DNA, and mitochondrial single-stranded DNA-binding protein (mtSSB), which stabilizes single-stranded DNA produced by Twinkle before replication occurs [34].

Several models for mitochondrial DNA replication currently exist. The oldest model is based on electron microscopy of replicating mtDNA molecules [35] and pulse-chase labeling studies [36] demonstrating asynchrony in the synthesis of the light and heavy strands, and is referred to as the strand-displacement model [37]. This model proposes that replication begins at the heavy strand origin of replication in the D-loop. As replication of the heavy strand proceeds, the light strand is displaced and maintained as single-stranded DNA until the light strand origin of replication is made available via strand displacement. Light strand replication then proceeds. This model suggests that mitochondrial DNA replication is unidirectional, continuous, and asynchronous [34].

More recent studies have demonstrated the presence of RNA intermediates incorporated in the lagging strand [38, 39], leading to the development of the RNA Incorporated ThroughOut the Lagging Strand, or RITOLS model [34]. This model suggests that both strands are replicated simultaneously and unidirectionally, with RNA replication intermediates that are later processed into DNA. A second model, called the strand-coupled model [34], suggests that the RNA intermediates act as primers for coupled leading and lagging strand synthesis [40].

Interestingly, TFAM has been shown to have a potential impact on mitochondrial replication beyond its role in the synthesis of replication primers as part of the transcription machinery. A small increase in TFAM expression (~2-fold) *in vivo* results in an increase in the number of copies of the mitochondrial genome [41], but forced overexpression has been shown to result in mitochondrial DNA depletion in HEK293 cells [42]. These observations, combined

with *in vitro* data showing that TFAM-packaged nucleoids can block replication [43] suggest that TFAM binding plays a role in determining which mitochondrial genomes are available for replication, as well as which are engaged in transcription.

Early Reports of Mitochondrial Methylation

DNA methyltransferase activity was detected in the mitochondria of higher-order eukaryotes in 1971 [44], suggesting that mitochondrial DNA could contain 5mC. Two years later, both methyltransferase activity and the presence of 5mC were demonstrated to be present in the mitochondria of cultured mouse and hamster cells by *in vivo* incorporation of [methyl-^{3}H]methionine into the mitochondrial genome in the form of 5mC [45]. The spectrophotometric detection of 5mC in mitochondrial DNA isolated from beef heart was also published that year [46]. However, in 1974, two papers were published that failed to detect 5mC in the mitochondrial DNA of *Xenopus laevis*, HeLa cells [47], and *Paramecium aurelia* [48], beginning a controversy over the existence of mitochondrial DNA methylation that continues to impact the field. Later studies went on to show that mitochondrial 5mC occurs at CpG dinucleotides [49], as it does in the nucleus, and that the CpG dinucleotide is under-represented in animal mitochondrial genomes, indicating CpG suppression, also as in the nucleus [50]. While these early studies demonstrated the presence of methylation in mitochondrial DNA and methyltransferase activity, they failed to identify the enzyme responsible.

DNA methyltransferases

DNA methyltransferases methylate DNA by transferring a methyl group from S-adenosyl-L-methionine (SAM) to the 5-position of cytosine residues [51]. In the nucleus, three

DNA methyltransferases are responsible for establishing and maintaining DNA methylation. DNMT1 is considered to be a maintenance methyltransferase, as it has a 5- to 30-fold preference for hemimethylated substrates [52]. DNMT3a and 3b are considered *de novo* methyltransferases, responsible for establishing methylation patterns during development [53]. Despite these classifications, there is evidence for functional overlap between DNMT1 and 3a/b [54]. All three of these genes have been shown to be essential for viability in mouse knockout experiments. Loss of DNMT1 leads to lethality at E9.5 [55]. Loss of DNMT3b results in lethality at E14.5-18.5 [53], and loss of DNMT3a results in mice that appear normal at birth, but which die at about 4 weeks [53]. The early lethality resulting from loss of DNMT1 may be due to effects on cell division, as catalytic inactivation of DNMT1 in human cancer cells has been shown to result in severe mitotic defects and cell death [56]. These knockout and loss of function studies demonstrate the essential nature of DNA methyltransferases and, by extension, 5mC, in mammalian cells.

Identification of mitochondrial cytosine modifying enzymes

In 2011, Shock et al. reported a mitochondrial isoform of DNA methyltransferase 1 (mtDNMT1) [57]. A conserved ORF upstream of the reported DNMT1 translation start site was predicted to form a mitochondrial target sequence, and DNMT1 was shown to be present in mitochondria through immunoblotting [57. The putative MLS was shown to transport GFP to the mitochondria using confocal microscopy [57]. It had been previously reported that p53 has a repressive effect on expression of DNMT1 through specific DNA binding [58]. Interestingly, loss of p53 was shown to preferentially upregulate the mitochondrial isoform of DNMT1; a 6-fold increase in mtDNMT1 transcription was observed upon loss of p53, while the nuclear

isoform increased 3-fold [57]. Upregulation of mtDNMT1 has gene-specific effects on mitochondrial transcription [57], indicating that 5mC may be involved in regulating the transcription of the mitochondrial genome. MEF cells lacking p53 were found to overexpress ND1, the first protein coding gene on the heavy strand following the rRNA genes [57]. Light strand transcription was also found to be altered; ND6 is underexpressed in p53 knockout cells [57]. These changes in transcription may be due to an increase in transcription from HSP2, or a decrease in termination of HSP1 transcription, resulting in increased production of downstream messages.

Shock et al. also demonstrated the presence of 5hmC in mitochondrial DNA [57]. In the nucleus, the ten-eleven-translocation (TET) enzymes catalyze the conversion of 5mC to 5hmC [59], and two of the TET family members, TET1 and TET2 have been reported to be present in the mitochondria of HeLa cells [60] and cerebellar granule neurons [61]. Studies in the Taylor laboratory demonstrated protease-resistant Tet2, but not Tet1 immunoreactivity in human and mouse cell mitochondria (Thakkar, PhD dissertation, VCU 2013). Confocal microscopy indicated that Tet1 did not colocalize with mitochondria. These data indicate that Tet2 is likely the enzyme responsible for conversion of 5mC to 5hmC in this organelle. In addition to DNMT1, DNMT3a [62] and DNMT3b [61] have been reported to localize to the mitochondria after detection in cell fractionation followed by immunoblotting, but this has not been shown consistently [57, 61]. Recent enzymatic studies using mitochondrial lysates generated from mouse embryonic stem cells in which the different DNMTs have been knocked out suggest that DNMT3b, but not DNMT3a, plays a role in mitochondrial DNA methylation (Figure 3) (Shock, unpublished data).

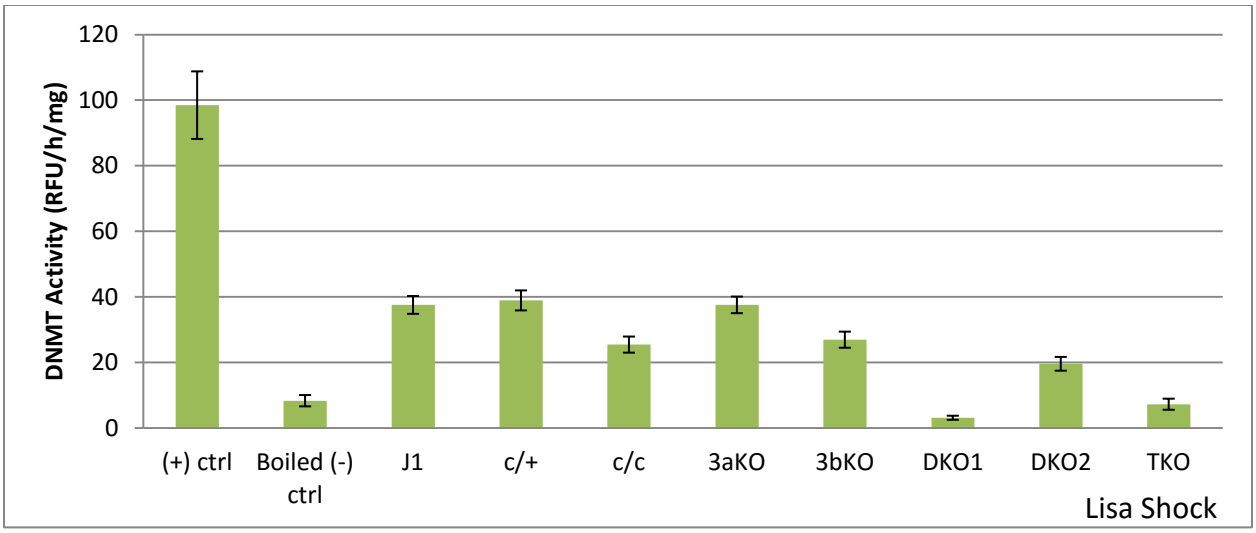

Figure 3. Enzymatic activity assays performed by Dr. Lisa Shock suggest DNMT3b may be active in mitochondria. The mouse ES cell lines used in this study were generated by Li, et al. [64, 65]. The catalytic domains of the DNMTs were deleted through gene targeting by homologous recombination. J1 cells are wild-type for DNMT1, while c/+ and c/c cells are heterozygous and homozygous knockout lines, respectively. DNMT3a and 3b homozygous knockouts were also investigated, in addition to two clones of a 3a/3b double knockout line (DKO1 and 2). In the triple knockout cells (TKO), all three DNMTs were catalytically knocked out. Dr. Shock isolated and trypsin treated mitochondria from these cell lines prior to lysis, then used the Fluorometric EpiQuik DNMT Activity Assay Ultra (Epigentek) to measure the DNMT activity of 10 μg of the mitochondrial proteins. The data show that loss of DNMT1 or DNMT3b results in a decrease in the DNMT activity of the mitochondrial extracts. Loss of all three DNMTs results in methylation activity similar to the boiled wild-type extract which serves as a negative control.

Through immunoprecipitation of DNA using 5mC and 5hmC specific antibodies (meDIP) [57] and qPCR, Dr. Lisa Shock demonstrated that loss of p53 in HCT116 cells led to increased CpG modification across the mitochondrial promoters (Figure 4) (Shock, unpublished data). A roughly two-fold enrichment in modification of HSP1 and LSP was detected in immunoprecipitation reactions with 5mC and 5hmC in cells overexpressing mtDNMT1 due to loss of p53. This change in modifications at the mitochondrial promoters presents a possible mechanism by which overexpression of mtDNMT1 results in the transcriptional changes previously observed [57]. However, this technique cannot be used to determine which CpG residues are modified; bisulfite sequencing of the mitochondrial genome would be necessary to obtain this information.

One factor that complicates the analysis of mitochondrial modifications through PCR-based methods is the presence of nuclear insertions of mitochondrial origins, or NUMTs. These pseudogenes represent portions of mitochondrial DNA incorporated into the nuclear genome and are thought to be a product of the non-homologous end joining (NHEJ) repair method of double-strand DNA breaks [66]. Through incorporation of mitochondrial DNA that has escaped to the nucleus, NHEJ repair can be performed without the deletion of nuclear DNA [66]. PCR amplification of total cellular DNA with primers generated from mtDNMA sequence might therefore amplify NUMTs in the nuclear genome, rather than true mtDNA sequences. Therefore amplification primers should be tested against cells devoid of mitochondrial DNA (rho zero) to confirm specificity. The human genome contains 33 NUMTs that share over 80% sequence similarity to the corresponding mitochondrial sequence and are longer than 500 bp [67]. This may have an effect on mitochondrial methylation studies because nuclear CpG sites are 60-90% methylated [68], compared to the 2-5% of CpGs estimated to be methylated by nearest neighbor

analysis in mitochondria [49]. This 10-fold higher degree of methylation in the nucleus could affect mitochondrial methylation analysis if NUMT contamination is present. To prevent this, future experiments analyzing mitochondrial DNA modification may need to be performed using isolated mitochondrial DNA [57], as opposed to total DNA.

Possible mechanisms of mtDNA modification action

Despite the recent interest in mitochondrial epigenetics, no mechanistic studies demonstrating a causal relationship between altered methylation and changes in mitochondrial transcription have been published. In the nucleus, DNA methylation can recruit histone deacetylase-containing complexes to further silence transcription [63], but mitochondria do not contain histones, and there is to date no evidence for the presence of methyl binding proteins in mitochondria. The mitochondrial genome is packaged into nucleoids by the cross-strand binding of TFAM in a transcription independent manner [25]. Changes in the methylation status of mitochondrial DNA could affect TFAM binding and have an effect on transcription by changing the accessibility of the DNA due to changes in nucleoid formation.

Methylation of the D-loop could also affect the binding of TFAM to the different promoters. TFAM has been shown to promote transcription from HSP1, but inhibit transcription from HSP2 [29]. Methylation of the D-loop could affect the ability of TFAM to bind to or bend the promoters, changing the ratio of bound TFAM without altering the amount of TFAM in the mitochondria. Because mitochondria usually contain more than one genome [8], differential methylation could allow for separate individual genomes to be performing independent functions, such as transcribing from different promoters within the same organelle or undergoing replication. The work described in this thesis attempts to better understand the effects of

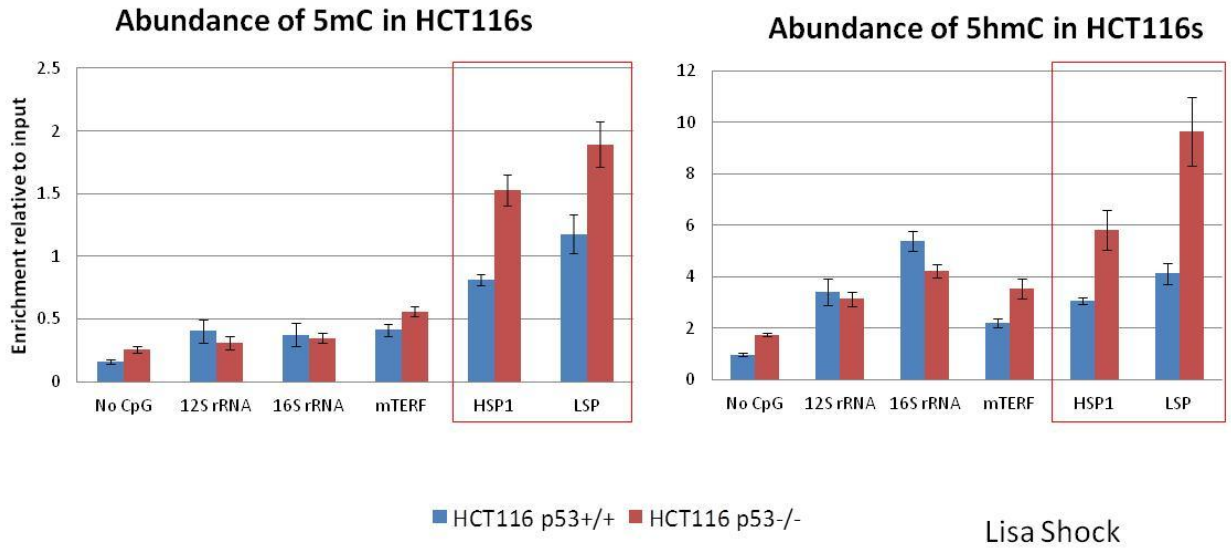

Figure 4. Loss of p53 leads to increased CpG modification in mitochondrial promoters. The above data was generated by Dr. Lisa Shock. Total DNA was isolated from HCT116 cells with and without p53. The DNA was sheared by sonication, then precipitated with antibodies specific for 5mC or 5mcC. The immunoprecipated DNA was then evaluated by qPCR with primers specific for different regions of the mitochondrial genome. The largest changes were observed in the HSP and LSP regions of the mitochondrial genome, as indicated by the red boxes.

mtDNMT1 overexpression on transcription and the effect of CpG methylation on the interaction of mTERF and TFAM with cognate mtDNA sequences. It was hypothesized that overexpression of mtDNMT1 and resulting increases in cytosine methylation would affect transcription by altering the interaction of transcription factors with the mitochondrial genome. This hypothesis was tested by

1) Examining the effect of overexpression of mtDNMT1 through loss of p53 on mitochondrial gene expression by RT-qPCR and generating a cell line in which the mitochondrial isoform of DNMT1 was overexpressed without the loss of p53
2) Determining the effects of DNA modifications on the interaction of mTERF and TFAM with mitochondrial DNA through electophoretic mobility shift assays (EMSA) and fluorescence polarization (FP)

Chapter 2: Role of mitochondrial DNA methylation in control of mitochondrial transcription

Introduction

Mitochondrial transcription is initiated from the D-loop, a non-coding regulatory region that contains the promoters for the light and heavy strands [13]. Transcription occurs in a strand-specific manner, resulting in the synthesis of polycistronic messages [14] that are processed to form the mature rRNAs, mRNAs, and tRNAs [15]. Transcription of the light strand is initiated at a single promoter, referred to as LSP, and results in a polycistronic message that contains most of the strand, terminating before entering the 16s coding sequence [14]. This termination is thought to be due to the binding of mTERF1 in the Leu tRNA coding region, which prevents transcription of antisense rRNAs [32]. Transcription of the heavy strand is initiated at one of two promoters, HSP1 or HSP2. HSP2 is located within the Phe tRNA coding sequence, and transcription initiated at this promoter results in a polycistronic message encoding most of the heavy strand, including 12 of the 13 protein coding sequences contained in the mitochondrial genome [14]. HSP1 is located upstream of the Phe tRNA coding sequence. When transcription is initiated from HSP1, a shorter polycistronic message is produced which contains the two rRNAs and is terminated by mTERF binding in the Leu tRNA coding region [14].

5mC [45, 46, 57] and 5hmC [57] have been detected in mitochondrial DNA, but the effect of these cytosine modifications on transcription has not been extensively studied. In the nucleus, 5mC is associated with repression of transcription [1], while 5hmC is associated with demethylation and active expression [3], but because the proteins that form the mitochondrial

transcription initiation complex are different from those in the nucleus, cytosine modifications may not have the same effect on transcription from the mitochondrial genome.

Shock et al. found that loss of p53 in MEF cells resulted in an increase in the amount of the mitochondrial isoform of DNMT1 produced relative to wild-type cells [57]. A similar effect was observed in HCT116 cells, and this increase in mtDNMT1 through loss of p53 was correlated to an increase in 5mC and 5hmC at the promoter regions of the mitochondrial genome (Figure 1-4) (Lisa Shock, unpublished data). To determine what effect these changes have on mitochondrial transcription, cDNA was generated for p53 null and wild-type MEF cells using random hexamers, and qPCR was performed using primers specific for several mRNA sequences [57]. No changes were observed in the amount of Cox1 or ATP6 message present, but the amount of ND1 in p53 null cells was increased, and the amount of ND6 was decreased [57]. These changes suggested that the effect of mtDNMT1 overexpression on mitochondrial transcription was strand-specific, because ND1 is the first protein coding gene on the heavy strand, directly downstream from the termination site, and ND6 is the only protein coding gene on the light strand.

The experimental method used to determine the effect of increased mtDNMT1 expression on mitochondrial transcription was further refined by Dr. Prashant Thakkar, through the use of strand-specific cDNA synthesis. Mitochondrial transcription occurs in a strand-specific manner, and random hexamer primed cDNA synthesis will result in reverse transcription of messages from both strands. qPCR analysis of the resulting cDNA will give an average of the level of transcription across both strands. To generate strand-specific cDNA, a single primer specific for the ATP6 region of the mitochondrial genome was used to prime the reverse transcription reaction. Light-strand cDNA was synthesized in one reaction, and heavy-strand

cDNA was synthesized in another. These reactions were then evaluated by qPCR separately, using primers specific for each ORF. Using this method, an increase in Cox1, the second protein coding gene on the heavy strand was detected in addition to a more substantial 3-fold increase in ND1 (Figure 2-1) (Prashant Thakkar, unpublished data). A difference in ND6 was not detected using the strand-specific method (Figure 2-1) (Prashant Thakkar, unpublished data), suggesting that the primary effect of increased mtDNMT1 expression due to loss of p53 is on heavy strand transcription.

This method of cDNA synthesis allowed Dr. Thakkar to analyze the transcription of the two strands separately, but only polycistronic message was represented. ND1 and Cox1 transcripts will only be reverse transcribed using ATP6 primers if the precursor messages have not been processed into mature mRNAs [15] (see Figure 2-2b for a schematic representation). In order to capture both polycistronic and mature transcripts, strand-specific cDNA synthesis primers must be used to reverse transcribe the individual messages. These strand-specific, gene-specific cDNA reactions can then be analyzed by qPCR using nested primers specific for each gene.

The previous studies performed in the Taylor laboratory and described above used p53 null and wild-type cells to study the effects of mtDNMT1 overexpression on mitochondrial transcription. Loss of p53 results in overexpression of the mitochondrial isoform of DNMT1 [57], but expression of the nuclear DNMT1 is also increased [58]. The proteins that form the transcription initiation complex are nuclear-encoded [16], and previous studies demonstrated that p53 shRNA-mediated knockdown in primary human fibroblasts resulted in a decrease in TFAM protein [69]. In order to determine if the observed effects on mitochondrial transcription are due

to increased mtDNMT1 and not a product of p53 loss or increased nuclear DNMT1 expression, a cell line overexpressing only the mitochondrial isoform must be generated.

Previous students in the Taylor laboratory generated an expression vector containing a cDNA clone of DNMT1 including the mitochondrial leader sequence. In addition, the translational start site of the nuclear isoform was mutated to ATC, to prevent transcription of the nuclear isoform from this construct. HEK293 cells were transfected with this construct in order to determine how mitochondrial DNA modification and transcription would be affected.

It was hypothesized that changes in mitochondrial DNA modifications would lead to changes in mitochondrial transcription and function. To test this hypothesis, mitochondrial transcription was analyzed in a gene specific-strand specific fashion in p53 -/- and +/+ MEF and HCT116 cells. HEK293 cells were transiently and stably transfected with mtDNMT1 overexpression vectors to study the effect of increased mtDNMT1 in a p53 wild-type background. Increased mtDNMT1 due to loss of p53 was found to alter transcription of the heavy strand on the polycistronic level, and a DNMT1 overexpression construct was found to transiently express in mitochondria, but that expression was lost over time.

Methods

Cell culture

HEK293 and wild-type and p53 null MEF cells were grown at 37˚C in 10% CO_2 in DMEM (Gibco/Life Technologies) with 10% FBS. HCT116 p53 +/+ and HCT116 p53 -/- cells were grown at 37˚C in 5% CO_2 in RPMI 1640 medium (Gibco/Life Technologies) with 10% FBS. All cells were fed 48 hours prior to harvesting, then trypsinized and replated 24 hours prior to harvesting to ensure uniform distribution of cell cycle traverse.

RNA isolation

Cells from 2 sub-confluent 150 mm dishes were washed twice with PBS (Gibco/Life Technologies) and resuspended in 6 mL TRIzol Reagent (Life Technologies). After a 5 minute room temperature incubation, 1.2 mL of chloroform were added to the sample, which was then shaken for 15 seconds. After a 2 minute incubation at room temperature, the sample was centrifuged at 12,000 x g for 15 minutes at 4˚C. The colorless aqueous phase was transferred to a clean tube, and an equal volume of chloroform was added. The sample was then shaken for 15 seconds and centrifuged at 12,000 x g for 15 minutes at 4˚C. The aqueous phase was then transferred to a clean tube. 3 mL of 100% isopropanol were added to the aqueous phase and the sample was incubated at room temperature for 10 minutes, then centrifuged at 12,000 x g for 10 minutes at 4˚C. The supernatant was removed, and the pellet was washed with 6 mL of 75% ethanol. After centrifuging at 7,500 x g for 5 minutes at 4˚C, the wash was discarded and the pellet was air dried for 5 minutes at room temperature. The RNA was then resuspended in 100 µL of HPLC H_20 and the concentration was determined using a ND-1000 NanoDrop spectrophotometer. The RNA was stored at -80˚C.

First Strand cDNA Synthesis

First strand cDNA was synthesized using the SuperScript ™ First-Strand Synthesis kit (Invitrogen). 5 µg of RNA were mixed with 1 µL of 10 mM dNTP mix, 1 µL of specific primer or 1 µL of random hexamers, and HPLC H_2O to bring the reaction volume to 10 µL. The reactions were incubated at 65˚C for 5 minutes, then placed on ice for at least 1 minute. 9 µL of

a 2x reaction mix containing 2 µL of 10X RT buffer, 4 µL of 25 mM $MgCl_2$, 2 µL of 0.1 M DTT, and 1 µL of RNaseOUT™ (40 U/µl) were added to the RNA mixtures, followed by 1 µL of SuperScript™ II RT. Control reactions without RT were also performed, using 1 µL of HPLC H_2O. Reactions primed with random hexamers were incubated at 25˚C for 10 minutes, and all reactions were incubated at 42°C for 50 minutes. The reactions were terminated at 70°C for 15 minutes then cooled on ice. 1 µL of RNase H was added to each reaction, which were then incubated at 37°C for 20 minutes. The cDNA was stored at -20°C.

End point PCR

End point PCR was performed using HotStarTaq Master Mix (Qiagen). For each reaction, 12.5 µL of HotStarTaq, 9.5 µL of HPLC H_2O, and 1 µL of a 10 µM working stock of both the forward and reverse primers were mixed. 1 µL of cDNA was added to each reaction. The reactions were run in a DNA Engine PTC-200 thermal cycler (Bio-Rad). The reactions were incubated at 95°C for 5 minutes before cycling. Each cycle consisted of a 30 second melting step at 95°C, a 30 second annealing step based on the melting temperature of the primers (typically between 55°C and 65°C) (see Table 1-1 and 1-2), and a 1 minute extension step at 72°C. The total number of cycles run was between 25 and 40 cycles. A 40 cycle reaction was performed to confirm cDNA synthesis, and a 25 cycle reaction was performed to qualitatively assess differences in transcript levels before qPCR was performed. After cycling, the reactions were held at 72°C for 5 minutes, then stored at 4°C. The PCR products were visualized on a 1% agarose gel in 1x TAE with ethidium bromide. 5 µL of the PCR reactions were mixed with 1 µL 6x DNA loading buffer containing bromophenol blue and run at 100V for 50 minutes. The gels were viewed using UV transillumination.

qPCR

qPCR was performed using Quantitect SYBR Green PCR mix (Qiagen). For each reaction, 12.5 µL of Quantitect SYBR Green PCR mix, 9.5 µL of HPLC H_2O, and 1 µL of a 10 µM working stock of both the forward and reverse primers were mixed (see Table 1-1 and 1-2). 1 µL of cDNA was added to each reaction, and each reaction was performed in triplicate. The reactions were run on a BioRad DNA Engine Peltier thermal cycler fitted with a Chromo4 Real-Time Fluorescence Detector attachment. The reactions were incubated at 95°C for 5 minutes before cycling. Each cycle consisted of a 30 second melting step at 95°C, a 30 second annealing step based on the melting temperature of the primers (typically between 55°C and 65°C) (see Table 1-1 and 1-2), and a 1 minute extension step at 72°C. 40 cycles were performed, and an absorbance measurement was taken after each cycle. After 40 cycles, a melting curve was generated by raising the temperature from 40°C to 90°C in 1°C increments. Each temperature was held for 1 second, and an absorbance measurement was performed. The data was analyzed using OpticonMonitor3 software.

Transfection

24 hours before the transfection, $9x10^5$ HEK293 cells were plated per well of a 6 well plate. One hour before the transfection, fresh medium was added to the cells. For each well, 3 µL of PolyJet (SignaGen) was diluted in 50 µL of serum-free DMEM. The plasmids containing the DNMT1 constructs were also diluted in 50 µL of DMEM. For transfections used to evaluate the levels of transient expression of the constructs, 2 µg of plasmid were used. For transfections that would be used to generate stable cell lines, 1 µg of plasmid was used. The diluted PolyJet

was added to the diluted DNA and the mixture was incubated for 15 minutes at room temperature. Following the incubation, the PolyJet/DNA mixture was added drop-wise to the medium in each well and mixed. The plates were returned to the incubator, and the PolyJet-containing medium was replaced with DMEM containing 10% FBS and 1% Pen/Strep after 18 hours.

To generate stable cell lines, the transfected cells were trypsinized and replated in 150 mm dishes 48 hours after the transfection. The cells were grown in DMEM containing 10% FBS, 1% Pen/Strep, and 2 mg/mL G418 until discreet colonies formed. Colonies were then selected and grown in selective media until enough cells were available to perform cell fractionation. Transiently transfected cells were harvested 48 hours after the transfection by washing each well twice with cold PBS, then adding 100 µL of SDS Lysis buffer (62.5 mM Tris pH 6.8, 5% glycerol, 2% SDS, 5% β-mercaptoethanol, and 1x complete protease inhibitor cocktail (Roche)). The cell lysate was stored at -80°C.

Cell Fractionation

Cells were plated into two 150 mm dishes 24 hours before the fractionation. The cells were washed twice with cold PBS, pH 7.4, then scraped from the plate, transferred to a 15 mL conical tube (Falcon), and placed on ice. 5% of the cells were transferred to another tube and spun down at 900 x g for 5 minutes and resuspended in 5x weight/volume of SDS lysis buffer.

The remaining cells were pelleted at 900 x g for 5 minutes and resuspended in 3mL of mitochondrial homogenization buffer (0.25M sucrose, 10mM Tris-HCl, pH7.0, 1mM EDTA, pH 6.8) containing 1 tablet of Complete EDTA-free Protease Inhibitor Cocktail tablets (Roche) per 25 mL of homogenization buffer. The resuspended cells were transferred to a 7mL glass dounce

homogenizer (Wheaton) on ice and incubated for 5 minutes. The cells were homogenized with 15 strokes and centrifuged at 900 x g for 5 minutes at 4°C. The supernatant was transferred to a clean 15 mL conical tube. The pellet containing unbroken cells and nuclei was resuspended in 3 mL of homogenization buffer, and the process was repeated for a total number of three times. After the three rounds of douncing, the collected supernatant was centrifuged at 900 x g for 5 minutes at 4°C to remove any additional unbroken cells and nuclei. The supernatant from this centrifugation was transferred to a 14 mL round-bottom tube (Falcon) and centrifuged at 10,000xg for 15 minutes at 4°C to pellet the mitochondria.

Nuclei were isolated from the pellet containing nuclei and unbroken cells by resuspending the pellet in 3 mL of nuclear buffer (0.25 M sucrose, 10 mM $MgCl_2$). The resuspended pellet was layered over a 3 mL sucrose cushion (0.88 M sucrose, 0.5 mM $MgCl_2$) and centrifuged at 2800 x g for 5 min. The pellet was resuspended in 5x weight/volume of SDS lysis buffer.

Cytosolic proteins were isolated from 5 mL of the supernatant from the mitochondrial pellet. 5 mL of 20% TCA were added, and the mixture was incubated on ice for 20 minutes. After this incubation, the mixture was centrifuged at 6000 x g for 15 minutes. The pellet was washed three times with 1 mL of acetone and centrifugation at 6000 x g for 5 minutes. The pellet was air-dried on ice for 5 minutes before being resuspended in 10x weight/volume of SDS lysis buffer.

The mitochondrial pellet was washed with 1 mL of mitochondrial homogenization buffer without protease inhibitors and resuspended in 20x weight/volume of Trypsin digestion buffer (10mM HEPES-KOH, pH 7.4, 250mM sucrose, 0.5mM EGTA, 2mM EDTA, 1mM DTT). Trypsin-EDTA (Gibco) was added to a final concentration of 10 µg/mL and the samples were

incubated at room temperature for 20 minutes with occasional mixing. Bovine trypsin inhibitor (Sigma) was added to a final concentration of 10 µg/mL , mixed, and incubated on ice for 10 minutes. The mitochondria were then pelleted again by centrifugation at 10000 x g for 10 minutes at 4°C. The pellet was washed twice with 1 mL of mitochondrial homogenization buffer containing protease inhibitors and 10 µg/mL bovine trypsin inhibitor. The pellet was then lysed in 10x weight/volume of SDS lysis buffer.

Immunoblotting

The protein concentration for each lysate was determined using a Bradford assay (Bio-Rad) comparing the lysates to a standard curve generated using known concentrations of BSA. Lysates were loaded onto SDS-PAGE gels. For immunoblots comparing whole cell lysates, 40 µg of protein were loaded. For immunoblots of fractionation experiments, fractions were loaded to obtain equal signal with compartment specific antibodies (whole cell lysate: 70 µg, nuclear lysate: 20 µg, cytosolic lysate: 25 µg, mitochondrial lysate: 18 µg). The appropriate volume of lysate was diluted with an equal volume of 2x Laemmli buffer (Bio-Rad) with 5% 2-mercaptoethanol. The samples were boiled for 5 minutes before being loaded onto the gel. 5 µL of Precision Plus Dual Color pre-stained protein ladder (BioRad) were also loaded. The gels were run in 1L of 1x running buffer (25mM Tris base, 250mM glycine, 0.1% SDS) at 150V for approximately one hour at room temperature.

After running, gels were transferred to an Immobilon-FL PVDF membrane. 1x transfer buffer was prepared by mixing 100mL of 10x transfer buffer with SDS (16.879g TrisHCl, 17.299g Tris Base, 144.134g Glycine, 10g SDS in 1L total volume) with 200mL of 100% MeOH and 700mL H2O. The transfer buffer, tank, and sponges were placed at 4°C for 1 hour prior to

transfer. The SDS-PAGE gel was washed with MilliQ H_2O and equilibrated in 1x transfer buffer for 15 minutes at 4°C. The membrane was soaked in 100% methanol for 1 minute, washed with MilliQ H_2O for 2 minutes, and equilibrated in 1x transfer buffer for 15 minutes at 4°C. The transfer was assembled by opening a clear and black transfer plate and placing it with the black plate down. One of the soaked sponges was placed on the black plate and rolled flat to remove potential air bubbles. 3 sheets of Whatman paper were then individually soaked in chilled transfer buffer and placed on the sponge, each being rolled flat to remove air bubbles. The gel was then floated onto the third sheet of Whatman paper and gently rolled flat. The membrane was placed on top of the gel, air trapped between the gel and membrane was removed by rolling. Three additional sheets of Whatman paper were placed on top of the membrane as before, followed by a second soaked sponge. The plate was then closed, locked, and placed in the black and red transfer holder so that the black plate faced the black side of the holder. The holder was placed into the tank, which had been equilibrated in an ice bath, and filled with 1x transfer buffer. The tank was then placed on ice. The transfer unit was plugged into a power supply and set to run at 100V for 1 hour. After 1 hour, the transfer apparatus was disassembled and the gel and membrane were washed in MilliQ water for about 2 minutes. The gel was stained with Bio-Safe Coomassie Stain (Bio-Rad) for 30 minutes to check for complete transfer. The membrane was soaked in 100% methanol for 1 minute, then stained with Ponceau S (Bio-Rad) to visualize the transferred proteins by incubating the membrane in the solution for 5 minutes then rinsing off the background staining with MilliQ H_2O.

The membrane was then blocked in StartingBlock T20 (ThermoFisher Scientific) on a platform shaker for 1 hour at room temperature or overnight at 4°C to prevent nonspecific antibody binding. Primary antibodies were then applied to the membrane, diluted in

StartingBlock T20 according to the optimized conditions for each antibody (see Table 1-3), with gentle shaking for 1 hour. The primary antibody was removed and membrane was washed with 1x TBS-T (0.5M Tris-HCl, pH 7.5, 0.14M NaCl, 2.7mM KCl and 0.1% Tween 20) three times for 5 minutes each with vigorous shaking. Secondary antibodies were then applied to the membrane, diluted in StartingBlock T20 according to the optimized conditions for each antibody (see Table 1-3), with gentle shaking for 1 hour. The primary antibody was removed and membrane was washed with 1x TBS-T three times for 10 minutes each with vigorous shaking. All secondary antibodies were conjugated with horseradish peroxidase, so proteins were detected using the SuperSignal West Dura (Pierce) Chemiluminescent Substrate kit according to manufacturer's instructions. Blots were developed using autoradiography film (ISC Bioexpress) and a Konica SRX-101A developer or the Li-Cor Odyssey system.

Results

Loss of p53 results in an increase in polycistronic heavy strand message in MEF and HCT116 cells

RNA was isolated from isogenic WT and p53 -/- MEFs and first strand cDNA was generated using strand specific primers specific for the ATP6 coding region of the mitochondrial genome. RT-qPCR was then performed on this cDNA using primers specific for the ND1 and Cox1 genes. Expression levels were normalized to cDNA generated using random hemaxers and amplified using primers specific for 18s rRNA. This experiment was first performed by Prashant Thakkar (Fig. 2-1A) and repeated (Fig. 2-1B) to check for the same trend. These data show that

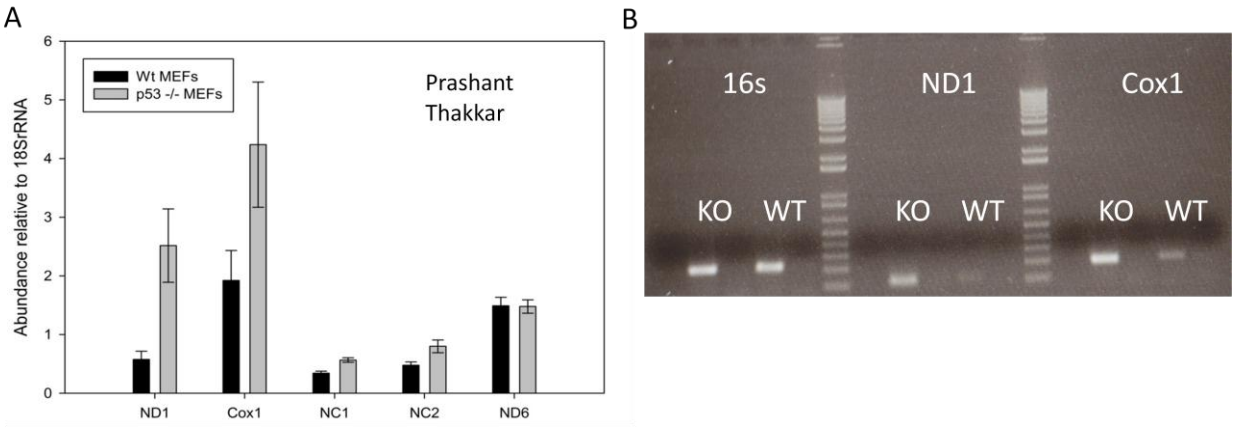

Fig 2-1. Effect of loss of p53 is on the level of the polycistronic transcript. (A) qPCR performed by Prashant Thakkar on strand specific polycistronic cDNA generated from MEF cells. Loss of p53 results in increased levels of ND1 and Cox1. (B) End-point PCR using the same method as (A), demonstrating the same trend.

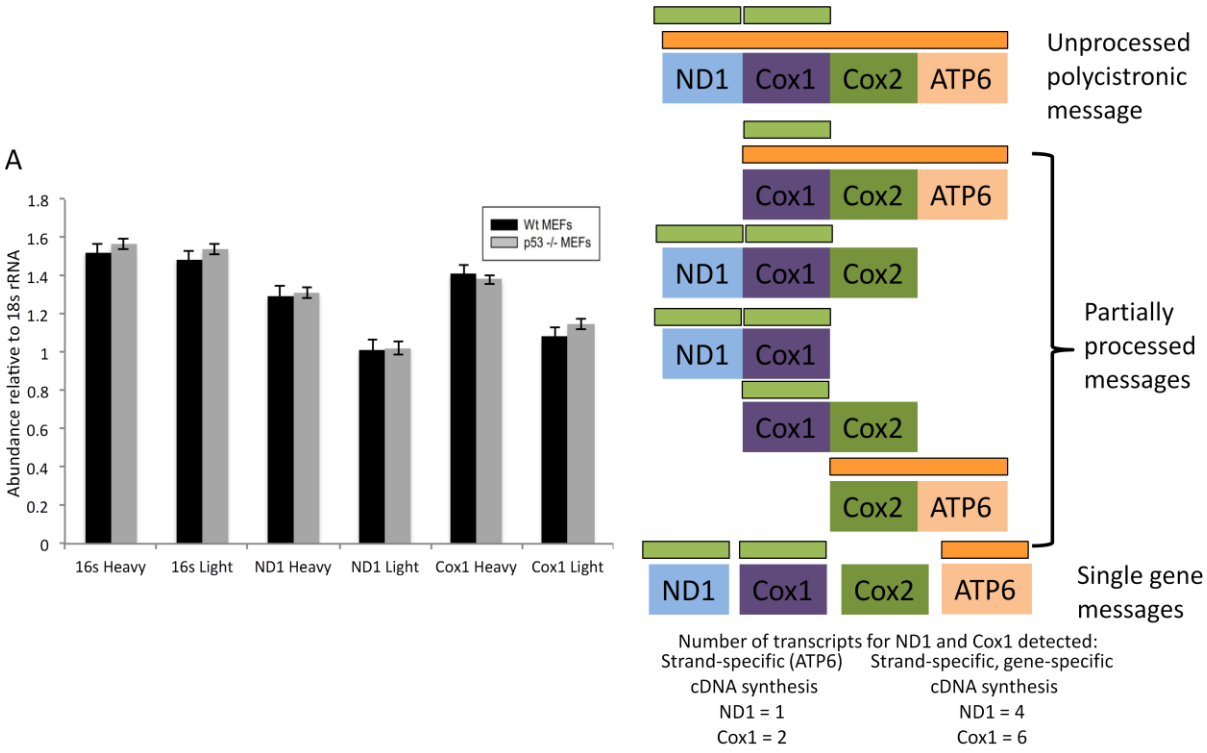

Fig 2-2. A) qPCR on cDNA generated in a strand-specific, gene-specific manner to capture both polycistronic and mature messages (n=2, combined data). No significant difference in total transcript levels is observed. B) A graphical comparison of the strand-specific and strand-specific gene-specific cDNA synthesis methods. The orange bars represent cDNA generated by the strand-specific ATP6 primers and the green bars represent the cDNA generated by the strand-specific, gene-specific primers.

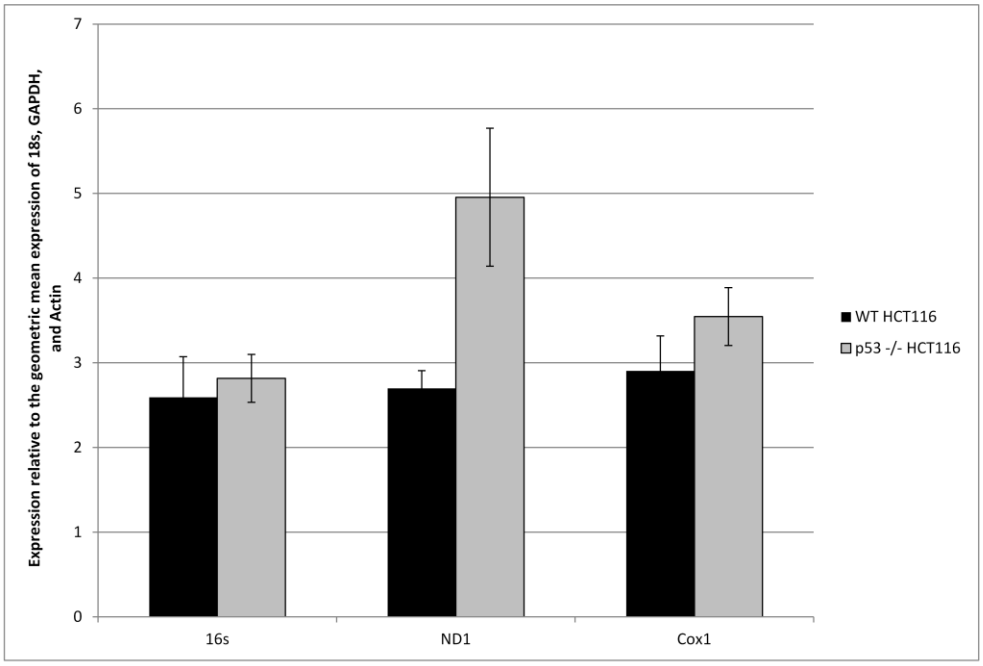

Fig 2-3. Effect of loss of p53 on polycistronic transcript in HCT116 cells is similar to MEFs. A qPCR performed on strand-specific polycistronic cDNA. Error bars represent SEM of technical triplicate data points, n=1.

there is an increase in polycistronic message containing transcript from ND1 and Cox1 in cells which overexpressed mtDNMT1 due to loss of p53.

In order to measure the level of mature mRNA within mitochondria, RNA isolated from WT and p53 -/- MEFs was used to generate cDNA using strand-specific cDNA primers placed within each individual ORF. RT-qPCR was then performed on this cDNA using nested primers specific for the ND1 and Cox1 genes. Data generated in this fashion suggested that there was no difference in the amount of ND1 and Cox1 transcripts present in WT and p53 -/- MEFs (Fig. 2-2a). The difference in cDNA generated by the methods used in Figure 2-1 and 2-2a is graphically represented in Figure 2-2b. The strand-specific method using primers specific for ATP6 would only generate ND1 and Cox1 cDNA in messages that have not yet been processed. The strand-specific gene specific method would capture both polycistronic and mature messages. The differences in the data presented in Figures 1 and 2 suggested that the effect of p53 loss on transcription was at the level of production of the polycistronic transcript, which has been shown by others to be short lived [70].

To determine if the effect of p53 loss and resulting mtDNMT1 overexpression on mitochondrial transcription was specific to MEFs or a more general phenomenon, RNA was isolated from WT and p53 -/- HCT116. First strand cDNA was generated using strand specific primers specific for the ATP6 coding region so the effect of loss of p53 on polycistronic message could be evaluated. RT-qPCR was then performed on this cDNA using primers specific for the 16s, ND1, and Cox1 genes (Fig. 2-3). Expression levels were normalized to the geometric mean of the expression of 18s, GAPDH, and Actin, which were amplified from cDNA generated using random hexamers. These data showed a similar trend to the data generated from MEFs, specifically that ND1 transcript levels were increased in p53 -/- cells. This suggests that the

effect of p53 loss and resulting mtDNMT1 overexpression on mitochondrial transcription is not a cell-line specific phenomenon.

The effect of loss of p53 on transcription is not due to changes in TFAM expression

Previous studies demonstrated that shRNA-mediated knockdown of p53 in primary human fibroblasts resulted in a decrease in TFAM protein [69]. It was therefore possible that the increased gene-specific transcription observed in Figures 1 and 2 could be due to changes in the amount of TFAM present in p53 -/- cells. Whole cell lysates were prepared from WT and p53 -/- HCT116 cells, and a immunoblot was performed using antibodies specific for p53, TFAM, and $H3K4me^3$, which served as a loading control (Fig. 2-4). No difference was observed in the level of TFAM in p53 -/- cells, indicating that the effect of the loss of p53 on transcription was not due to changes in the amount of TFAM protein present.

A mtDNMT1 construct can be transiently expressed in mitochondria

Previous studies used p53 null cells to analyze the effect of increased mtDNMT1 on mitochondrial transcription [57]. Loss of p53 also results in increased nuclear DNMT1 expression, which may have an effect on the nuclear-encoded transcription machinery [16]. To evaluate the impact of increased mtDNMT1 expression on mitochondrial transcription in isolation, expression constructs were generated to drive overexpression of the mitochondrial isoform only. Several DNMT1 constructs were used in this study, and they are depicted in Figure 2-5. A construct beginning with the ATG that has been identified as the translational start site for the nuclear isoform was used as a control (nuclear DNMT1). An expression construct for the mitochondrial isoform of DNMT1 had been generated by previous students in the Taylor

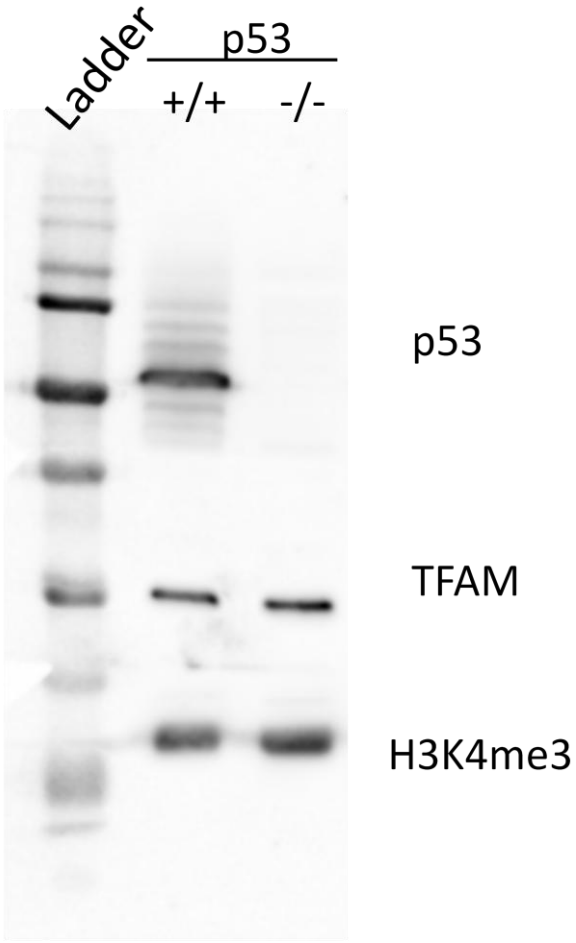

Fig 2-4. Loss of p53 does not alter TFAM expression in HCT116 cells. Immunoblot on p53 null and WT HCT116 cells shows that TFAM expression is not changed by loss of p53 in HCT116 cells (n=2, representative image). H3K4me^3 serves as a loading control.

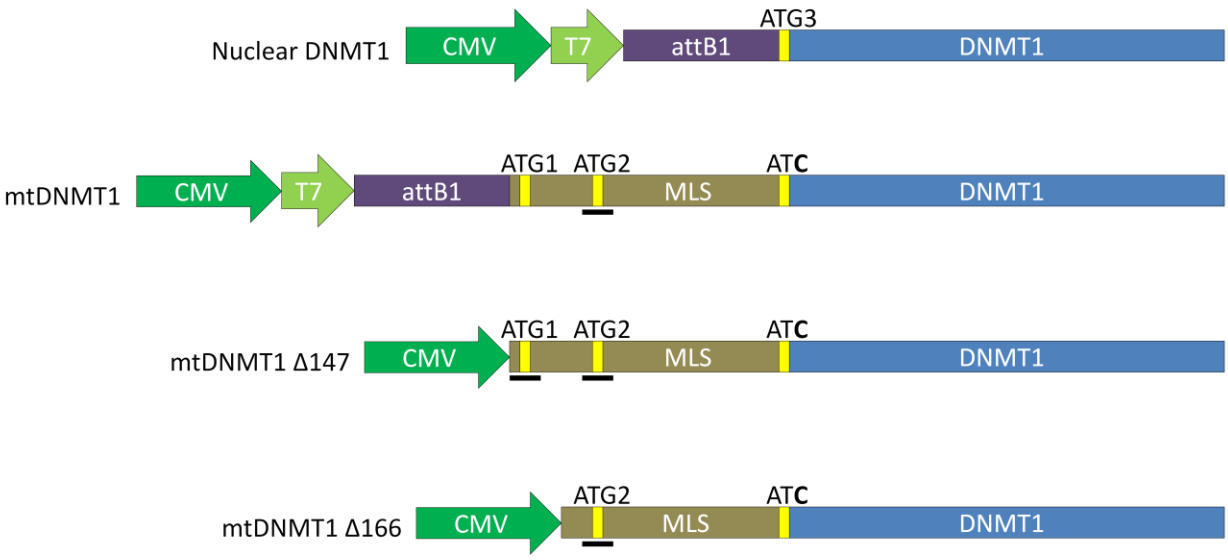

Fig 2-5. A schematic of DNMT1 constructs for nuclear and mitochondrial expression used in this study. Not drawn to scale. ATG3 represents the published transcription start site for nuclear DNMT1. These constructs were generated in the pDEST40 vector, and each carries a C-terminal V5 epitope tag.

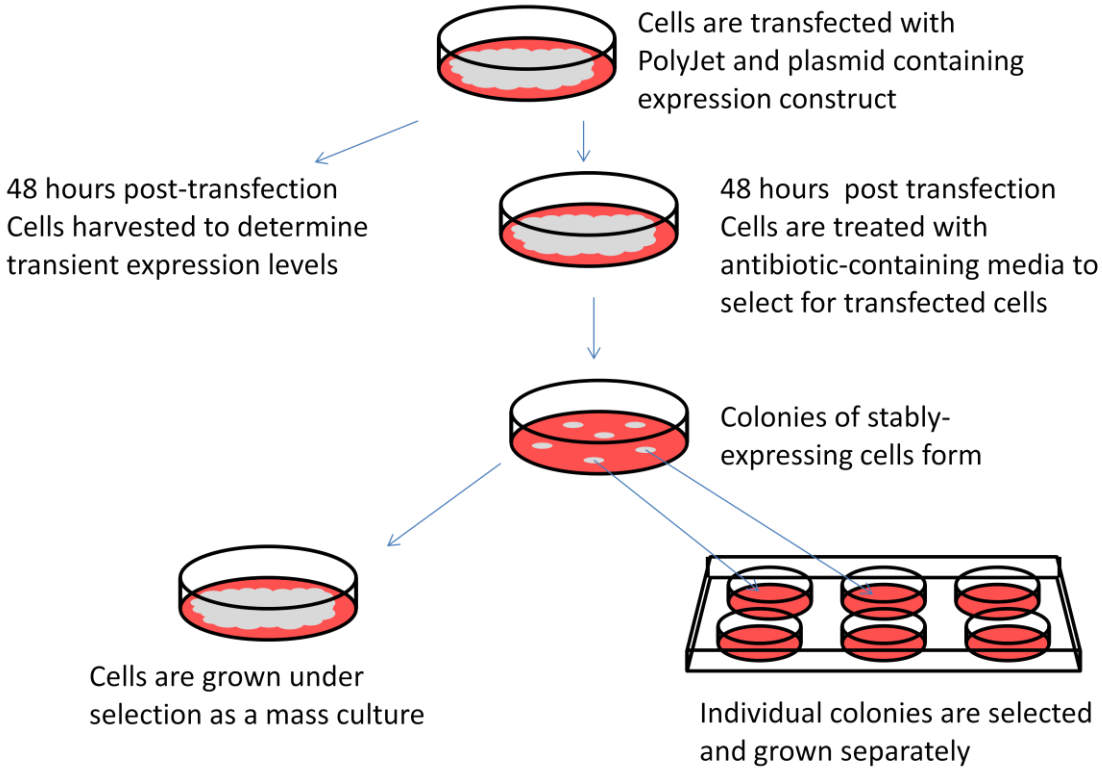

Fig 2-6. Schematic showing the workflow for the generation of cells transiently and stably expressing the DNMT1 constructs, as well as the separation of stably expressing mass cultures and stably expressing clones.

laboratory. This construct contained the mitochondrial leader sequence upstream of the nuclear translational start ATG (ATG3), which had been mutated to ATC (Ile), eliminating the translational start site. The sequence surrounding one of the upstream ATGs, referred to as ATG2, was altered to better match the Kozak consensus sequence. This construct was further altered by the VCU Molecular Biology Core Facility to generate the mtDNMT1 Δ147 and Δ166 constructs. In the Δ147 construct, the sequence between the CMV promoter and the first ATG (ATG1) of the mtDNMT1 coding sequence, which contained a T7 promoter and an attB1 recombination site, was removed and the sequence surrounding ATG1 was altered to better match the Kozak consensus sequence. In the Δ166 construct, the sequence between the CMV promoter and the second ATG (ATG2) of the mtDNMT1 coding sequence was removed. All of the constructs contained a C-terminal V5 epitope tag, which allowed for analysis of the exogenously expressed protein separately from endogenous DNMT1.

The nuclear DNMT1, Δ147, and Δ166 constructs were used to transiently transfect HEK293 cells, as well as generate stable mass cultures and clones, as shown in Figure 2-6. Whole cell and mitochondrial lysates were generated from transiently transfected cells and mitochondrial localization was investigated by immunoblotting (Fig. 2-7). The Δ166 construct was found to localize to the mitochondria, while the Δ147 construct was not detected in mitochondrial lysates, suggesting that ATG2 may be the translational start site for the mitochondrial isoform of DNMT1. This is the position of the conserved p53 and NRF1 regulatory elements [57].

Mass cultures of cells expressing the Δ166 construct were fractionated to generate whole cell, nuclear, cytoplasmic, and mitochondrial lysates (Fig. 2-8). At an early passage (passage 3), V5 signal was detected in all of the cell compartments, including the mitochondria. At a later

passage (passage 10), the mass cultures were again fractionated and very little V5 signal was observed in the mitochondrial compartment (Fig. 2-8). This suggests that passaging of the cells resulted in a loss of mitochondrial expression of DNMT1. A similar effect was observed in stable clones (Fig. 2-9). Stable clones were generated from a transfection of HEK293 cells with the Δ166 construct, but many of the clones did not show V5 expression in the whole cell lysates by passage 3. By passage 5, cellular fractionation of stable clone 3 showed very little V5 signal in the mitochondrial compartment. This suggests that overexpression of mtDNMT1 may be detrimental and selected against in cell culture.

The mtDNMT1 Δ147 and Δ166 proteins were also present in the nuclear compartment of the stably expressing cells (Fig. 2-8 and 2-9). This is due to the presence of a nuclear localization signal (NLS) within the coding sequence of DNMT1. A construct was designed to replace the NLS with a nuclear export signal (NES) (Fig. 2-10). We first attempted to switch the MLS for DNMT1 with that for TFAM, to more efficiently target DNMT1 to the mitochondria, and then to mutate the NLS to a NES. The construct was assembled through Gibson assembly of PCR amplification products of the desired sequences, but the construct was found to be highly recombinogenic, even in Stbl3 *E. coli* cells (Invitrogen). Thus, the expression construct was not able to be generated at this time.

Discussion

Loss of p53 affects mitochondrial transcription on the polycistronic level

Strand specific, polycistronic analysis of mitochondrial transcription in p53 null and wild-type MEF cells showed an increase in ND1 and Cox1 messages in p53 null cells expressing 6-fold higher DNMT1 (Figure 2-1a), but this change was not observed when only mature

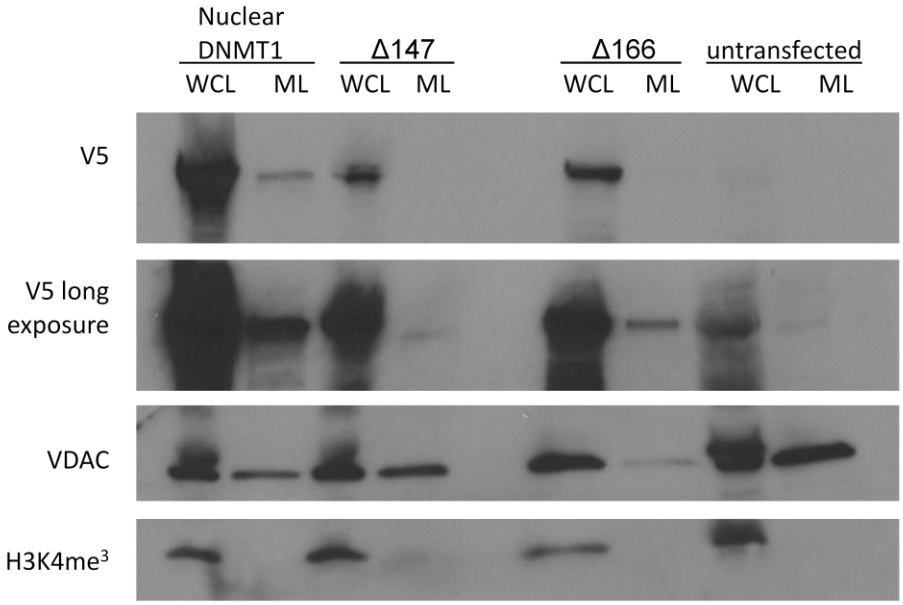

Fig 2-7. Transient expression of mtDNMT1. Cells transiently transfected with nuclear, Δ147, and Δ166 mtDNMT1 constructs were fractionated into whole cell and mitochondrial lysates, then analyzed by immunoblot (n=1). V5 indicates the DNMT1 construct, VDAC is a mitochondrial marker, and H3K4me^3 is a nuclear marker.

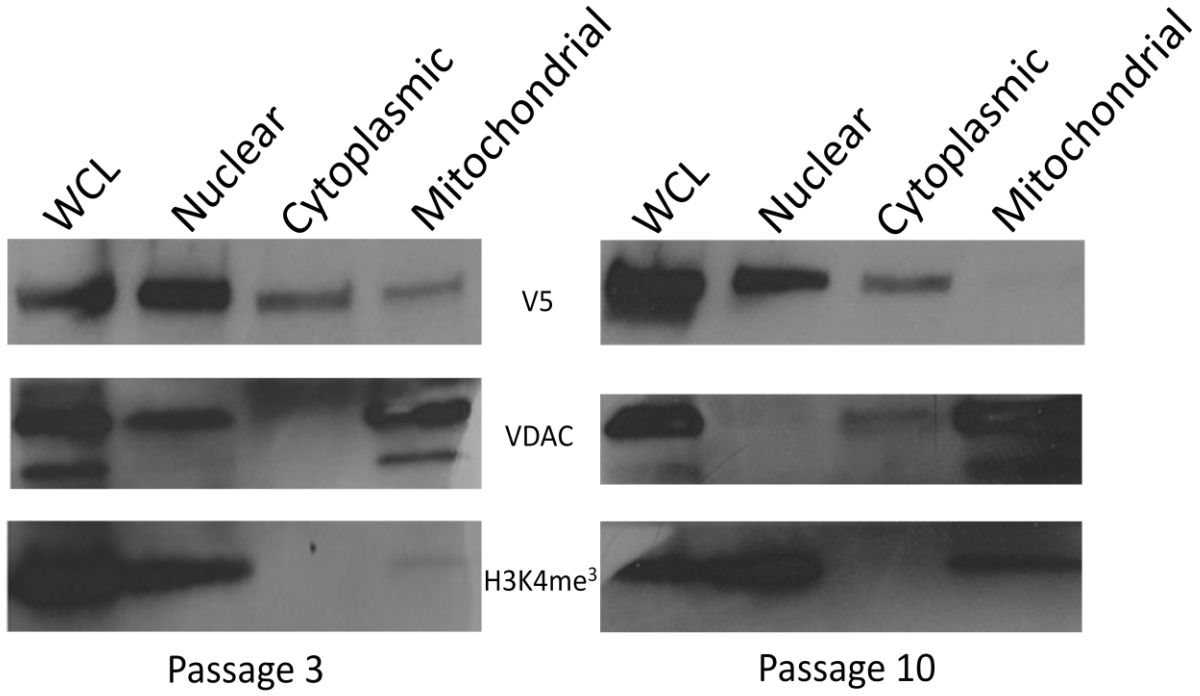

Fig 2-8. Mitochondrial expression of Δ166mtDNMT1 is lost over time in mass cultures under selection. Cells transfected with Δ166 mtDNMT1 constructs and grown in selective media were fractionated into whole cell, nuclear, cytoplasmic and mitochondrial lysates, then analyzed by immunoblot (n=1). V5 indicates the DNMT1 construct, VDAC is a mitochondrial marker, and $H3K4me^3$ is a nuclear marker.

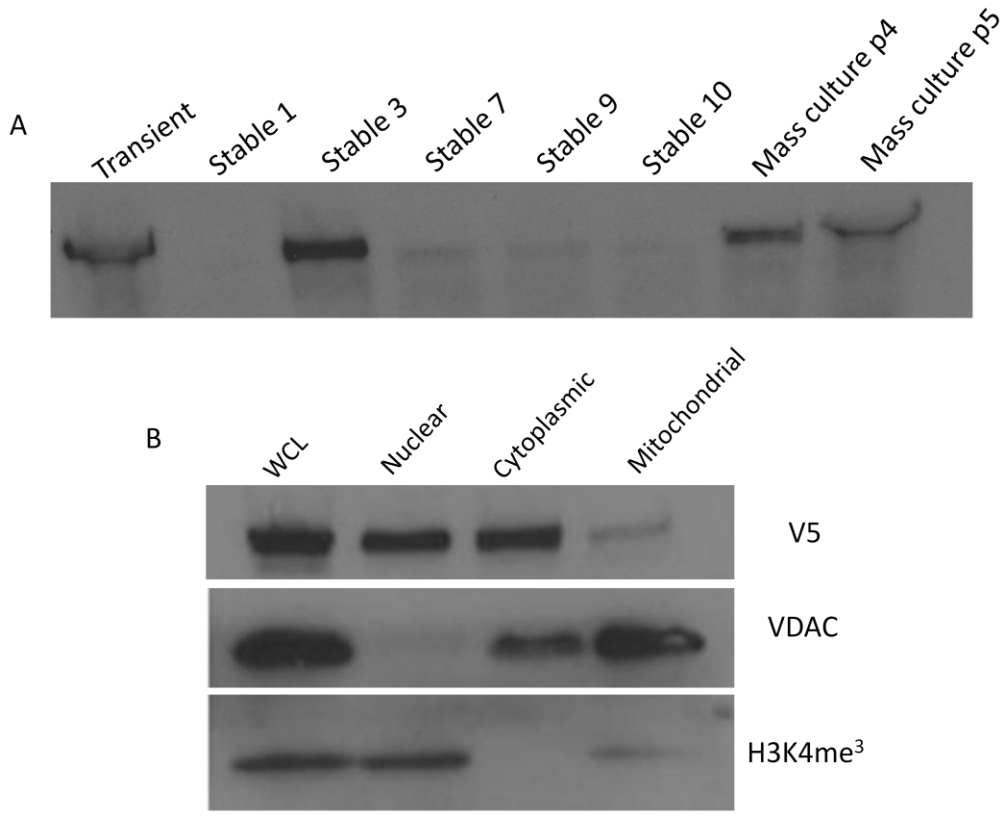

Fig 2-9. Δ166mtDNMT1 is not well expressed in mitochondria in stable clones. A) V5 immunoblot of whole cell lysates from Δ166mtDNMT1 stable clones, passage 3 (n=1). Most clones are not expressing. B) Cell fractionation of clone 3 at passage 5. Most V5 signal is located in the nuclear and cytoplasmic fractions.

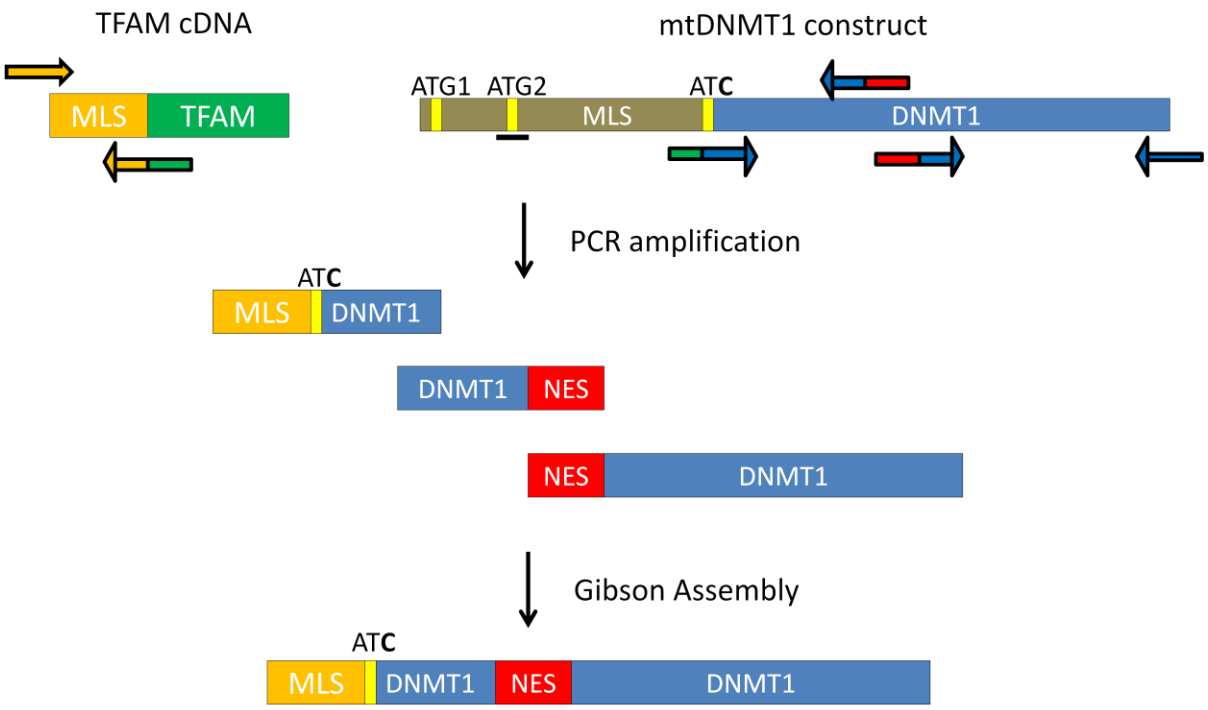

Fig 2-10. Design for a DNMT1 construct with the MLS from TFAM and a NES

messages were measured (Figure 2-2a). Polycistronic messages are quickly cleaved into the individual rRNAs, mRNAs, and tRNAs [15], and are present at a much lower level than the mature messages [70]. Changes in the smaller population of polycistronic messages could be lost when analyzing the larger pool of more stable mature mRNAs, because a larger increase would be necessary to determine a statistically significant change. The smaller amount of transcripts present in the strand-specific cDNA synthesis method may have led to the detection of differences when these differences would be harder to detect in the larger population of more stable mature messages (see Figure 2-2b for a visual representation of this effect). Overall, these results suggest an increase in transcription firing from HSP.

ND1 and Cox1 are transcribed as part of the polycistronic message generated by transcription initiated from HSP2, and are immediately downstream of the termination site for transcription initiated at HSP1 [14]. Changes in mitochondrial DNA modification due to the increased levels of mtDNMT1 observed in p53 null cells [57] could result in increased ND1 and Cox1 transcripts by altering the interaction of mitochondrial transcription factors with the DNA. Increased modification of the mTERF1 binding site could prevent mTERF1 binding and termination of transcription from HSP1. Reduced termination would allow transcription to continue through the mTERF1 binding site and into the ND1 and Cox1 coding sequences, which are immediately downstream of the termination site. This possibility is investigated in the next chapter.

Another possible mechanism by which mitochondrial DNA modification could affect ND1 and Cox1 transcription is by increasing transcription initiation from HSP2. HSP2 has been shown to be 100-fold less active than HSP1 in the presence of POLRMT, TFB2M, and TFAM *in vitro* [28]. While TFAM is required for transcription from HSP1, recent *in vitro* studies have

shown that TFAM is not required for transcription from HSP2 [28], and may even repress initiation from HSP2 [29]. If CpG modifications affect TFAM binding at the heavy strand promoters, a shift in promoter usage could result in increased polycistronic message.

Because TFAM appears to have different effects on transcription from the two heavy strand promoters, it was necessary to determine if the loss of p53 was affecting TFAM levels in the cells used in the transcription studies. Previous studies demonstrated that p53 shRNA-mediated knockdown in primary human fibroblasts results in a decrease in TFAM protein [69]. However, we observed no difference in TFAM protein levels in p53 +/+ and -/- HCT116 cells (Figure 2-4). This suggested that the observed changes in transcription were not due to the changes in the amount of TFAM present, and could be a result of changes in mitochondrial DNA modifications.

A mitochondrial DNMT1 construct can be transiently expressed in mitochondria, but stable expression is lost over time

In order to examine the effect of mtDNMT1 overexpression on mitochondrial transcription without the confounding effects of p53 loss, HEK293 cells were transfected with expression vectors containing several DNMT1 constructs. It was found that cells transiently transfected with a V5-tagged mtDNMT1 construct containing only the second ATG (mtDNMT1 Δ166) (Figure 2-5) showed the presence of V5 in the mitochondrial fraction (Figure 2-7). This indicated that the second ATG was the translational start site of the mitochondrial leader sequence, and that a tagged DNMT1 construct could be directed to the mitochondria.

A nuclear DNMT1 construct was used as a positive control for transfection and V5 expression. It was expected that these cells would only show V5 expression in the whole cell

lysate, but some V5 signal is present in the mitochondrial fraction generated from these cells (Figure 2-7). There does not appear to be any H3K4me^3 signal in the mitochondrial fraction generated from these cells, indicating no detectable nuclear contamination. It is possible that some protein adhered to the outside of the mitochondria and was not digested during the trypsin treatment, but some H3K4me^3 signal would still be expected in that situation. This leaves the possibility that some V5-tagged DNMT1 was imported into the mitochondria without a MLS. In other studies in the lab, the MLS of DNMT1 was disrupted by Cas/CRISPR genome editing, but DNMT1 was still detected in the mitochondria (Jason Robinson, unpublished data). This suggests that DNMT1 may be transported into the mitochondria without a MLS.

After it was determined that a DNMT1 construct could be transiently expressed in the mitochondria, I attempted to derive stably-expressing cell lines. These lines would allow the analysis of changes in mitochondrial DNA modification and transcription over time in the presence of increased mtDNMT1. However, many of the clones selected did not express the V5 tag (Figure 2-9a), and passaging a clone that did initially express mtDNMT1 resulted in nearly complete loss of expression by passage 5. Furthermore, mass cell cultures grown under selection lost mitochondrial expression over time (Figure 2-8). This suggests that overexpression of mtDNMT1 may be detrimental to cell growth or survival. The passaging of cells in culture over time selects for cells that grow well, so it is possible that cells expressing the V5-tagged construct in the mitochondria may have grown more slowly and been competed out by cells that did not have mitochondrial expression.

The V5 epitope of Δ166mtDNMT1was detected in nuclear extracts, increasing as cells were passaged, indicating that some of the mtDNMT1 construct was being transported to the nucleus (Figure 2-8, 9b). To prevent nuclear localization of the protein and generate more robust

mitochondrial localization, a mtDNMT1 construct was designed in which the MLS from DNMT1 was replaced with the TFAM MLS, and the NLS was replaced by a nuclear export signal (NES) (Figure 2-10). However, plasmid recombination during bacterial growth prevented these constructs from being successfully generated. The difficulty maintaining mtDNMT1 overexpression suggests that increased methyltransferase activity in the mitochondria negatively effects cell growth. Dr. Taylor has therefore designed an inducible expression construct in which the TFAM MLS has been added to a human codon-optimized bacterial CpG methyltransferase, M.SssI. This may allow the lab to test the effect of increased methyltransferase activity on mitochondrial DNA modification, transcription, and cell growth without the loss of p53.

These data demonstrate that loss of p53 affects mitochondrial transcription on the polycistronic level, specifically resulting in increased ND1 and Cox1 transcript in MEF p53 -/- cells. This is likely due to changes in heavy strand promoter usage. It was also found that while a plasmid expressing mtDNMT1 can be transiently overexpressed, long term overexpression appears to be selected against in cell culture. These findings support the hypothesis that mitochondrial DNA modification may have an effect on transcription and mitochondrial function.

Chapter 3: Effect of mtDNA methylation on interaction of mTERF and TFAM with recognition sequences

Introduction

Previous studies have shown that loss of p53 leads to increased expression of the mitochondrial isoform of DNMT1 [57]. This increase in mtDNMT1 is associated with increased modification of mitochondrial DNA (Lisa Shock, unpublished data) (Figure 1-4) and strand-specific changes in mitochondrial transcription [57] (Prashant Thakkar, unpublished data) (Figures 2-1, 2a, 3). Specifically, an increase in ND1 and Cox1 transcripts was observed when polycistronic messages were reverse transcribed in a strand-specific manner (Prashant Thakkar, unpublished data) (Figures 2-1).

ND1 and Cox1 are the first protein coding genes transcribed as part of a polycistronic message initiated at the second heavy strand promoter, HSP2 [14]. The polycistronic messages transcribed from HSP1 do not contain these sequences, due to termination by mTERF1 binding within the Leu tRNA coding region [31]. Changes in mitochondrial DNA modification due to the increased levels of mtDNMT1 observed in p53 nulls cells [57] could result in altered interaction of mTERF1 with its binding site. If methylation of the termination site were to prevent mTERF1 from binding, HSP1 transcription might fail to terminate and continue downstream into the ND1 and Cox1 coding sequences.

The structure of mTERF1 is composed entirely of helices, consisting of 19 α-helices and 7 3_{10} helices (a more tightly coiled helix with 3 residues per turn instead of the 4 residues per

turn found in α-helices) that are arranged in a repeating motif of two α-helices followed by a 3_{10} helix [71]. The protein contains 8 repeats of this motif, which suggests a modular architecture – the individual motifs are thought to be fairly rigid, but there is relative flexibility between motifs [71]. mTERF1 binds along the major groove of DNA, resulting in a 25˚ bend in the double helix [71]. In addition to bending the DNA, mTERF1 binding disrupts the twist of the helix, unwinding and partially melting the DNA, resulting in three nucleotides being everted from the double helix [71]. Cytosine methylation has been shown to change the mechanical properties of DNA, decreasing flexibility [72] and increasing the forces necessary for strand separation [73]. Because bending and melting of the termination site are required for mTERF1 binding, methylation of this sequence could affect mTERF binding and transcriptional termination.

Another possible explanation for the observed increase in ND1 and Cox1 transcripts (Prashant Thakkar, unpublished data) (Figures 2-1) would be an increase in transcription initiation from HSP2. Increased initiation from HSP2 would result in more of the polycistronic message containing the ND1 and Cox1 sequences being synthesized. The first component of the transcription initiation complex to bind to the promoter region is TFAM [26]. TFAM binds along the minor groove of the double helix and creates two kinks in DNA, which forces it to undergo a U-turn [23]. This U-turn brings the C-terminal tail of TFAM closer to the transcription start site, where it is necessary for recruitment of POLRMT and TFB2M and the activation of transcription [24]. Methylation of the promoter sequence could alter TFAM binding and, therefore, transcription initiation.

Interestingly, TFAM has been shown to have different effects on transcription initiation at the two heavy strand promoters [28, 29]. While required for transcription from HSP1, TFAM is not necessary for transcription initiation at HSP2 *in vitro* [28], and may even be a repressor

[29]. If methylation of the promoter sequence were to disrupt TFAM binding, transcription from HSP2 might increase.

Changes in protein-DNA interactions can be observed through electrophoretic mobility shift assays (EMSA) or fluorescence polarization (FP). Both of these techniques take advantage of the increased size of a protein-DNA complex relative to the DNA alone. In an EMSA, one of the complex components (typically the DNA) is labeled with a radioactive nucleotide or fluorophore. The components are then allowed to interact. The reactions are then run on a native gel, through which the larger complexes travel more slowly than the individual components. This is visualized as an upwards shift on the gel.

FP also takes advantage of relative changes in complex size, but these interactions are measured in solution. Molecules in solution tumble randomly, a phenomenon referred to as Brownian motion [74]. If a small molecule in solution labeled with a fluorophore is excited, it will randomly and rapidly reorient itself before emission, due to this motion [74]. This will result in largely depolarized light. If another molecule binds to the fluorescent probe, the resulting complex will be larger and tumble more slowly. This will result in slower reorientation of the molecule, and the emission from the fluorophore will be along the same axis as the excitation, resulting in polarization. FP uses this principle to determine the degree of polarization when complexes are allowed to form, which is indicative of the amount of binding occurring [74]. The relative polarization of samples can be quantified and used to determine affinity of a protein for a substrate [74].

While EMSA and FP can identify changes in protein-DNA interactions, they cannot provide data on the molecular basis for those changes. One way to analyze molecular interaction in detail is through the use of unnatural amino acids. Unnatural amino acids can serve as sites

for photocrosslinking or as resonance probes in Resonance Raman spectroscopy [75]. Unnatural amino acids can be incorporated into recombinant proteins produced in *E. coli* by reassigning the amber stop codon (TAG) to encode the desired unnatural amino acid [75]. First, an expression vector is generated for the protein of interest in which the coding sequence for the amino acid to be replaced has been mutated to TAG. This expression vector is used to co-transform *E. coli* cells with a pEVOL vector for the desired unnatural amino acid [75]. The pEVOL vectors contain coding sequences for an optimized CUA tRNA and a modified tRNA synthetase that can charge the CUA tRNA with the unnatural amino acid [75]. This allows for unnatural amino acid incorporation to occur during protein production, without the need for modifications after protein purification.

The two unnatural amino acids used in this work are p-benzoyl-L-phenylalanine (BpA) and cyanophenylalanine (CNF). BpA is photo reactive and can be used to form covalent adducts between the amino acid residue and nearby molecules [76]. Through crosslinking, transient interactions can be captured and analyzed. Both BpA and CNF may be used as vibrational probes for Raman Resonance spectroscopy. These unnatural amino acids can be excited at known wavelengths, and the wavenumber generated is sensitive to the polarity of the environment [77]. This allows for slight changes in the molecular environment of the residue to be detected, and this data can be used to generate models of the interactions.

It was hypothesized that methylation of the termination and HSP1 sequences would alter mTERF1 and TFAM binding, respectively. To test this hypothesis, mTERF1 and TFAM binding to methylated and unmethylated probes was analyzed using EMSA and FP. It was found that methylation did not affect mTERF1 binding. TFAM was observed to have higher affinity for methylated nonspecific DNA than unmethylated nonspecific DNA, and appeared to form

higher order complexes at lower protein concentrations with methylated HSP1 probes. The effect of methylation on transcription initiation from HSP1 was analyzed by Dr. Lisa Shock, and methylation was shown to increase transcription from HSP1. Finally, unnatural amino acids were incorporated into recombinant TFAM and mTERF1 proteins. TFAM was expressed with incorporated unnatural amino acids, while mTERF1 was not.

Methods

Cloning mTERF into pET32XT

The mTERF cDNA sequence in the pLX304 vector was obtained from ASU. Primers were designed to amplify the coding sequence without the mitochondrial leader sequence. The forward primer contained a BamHI restriction site, and the reverse primer contained a XhoI restriction site. Following PCR amplification (see Chapter 1 for conditions), the PCR product was purified using a QIAquick PCR purification kit (Qiagen), according to the manufacturer's instructions. The purified PCR product and PET32XT vector (a gift from Dr. David Williams) were digested with BamHI and XhoI in NEBuffer 3. The reactions were resolved on a 1% agarose gel with TAE (see Chapter 1), then excised and purified using an E.Z.N.A gel extraction kit (Omega), according to the manufacturer's instructions. The ligation reaction was prepared using a molar ration of 1:3 vector to insert, and the vector and insert were ligated using T4 Ligase (NEB). 1 µL of the ligation reaction was added to 25 µL of Top10 competent cells (Invitrogen), which were then incubated on ice for 30 minutes. The cells were then incubated at 42°C for 30 seconds and placed back on ice. 125 µL of S.O.C. media was added to the cells, which were then placed in a shaking incubator at 37°C for 1 hour at 225 rpm. Following the 1 hour incubation, the cells were plated onto selective LB agar plates and placed in a 37°C

incubator overnight. 5 mL of selective LB were inoculated with resulting colonies and grown at 37°C overnight in a shaking incubator. Plasmid DNA was isolated from these cultures using the E.Z.N.A Plasmid Mini Kit (Omega), according to the manufacturer's instructions. The plasmids were then analyzed by sequencing performed by Eurofins.

Expression and purification of mTERF

HMS174 competent cells obtained from Dr. Hackett's laboratory were transformed with the mTERF-pET32XT expression vector by incubating the cells on ice with the plasmid for 5 minutes, then heating the cells to 42°C for 30 seconds and returning them to ice for 2 minutes. 125 µL of S.O.C. media was added to the cells, which were then placed in a shaking incubator at 37°C for 1 hour at 250 rpm. Following the 1 hour incubation, the cells were plated onto selective LB agar plates containing 50 ug/mL Carbenicillin and placed in a 37°C incubator overnight. A colony was selected and used to inoculated 5 mL of LB containing 50 ug/mL Carbenicillin. This culture was grown overnight in a shaking incubator at 37°C at 250 rpm. The 5 mL overnight culture was then added to 95 mL of LB containing 50 ug/mL Carbenicillin. The 100 mL culture was grown at 37°C with 250 rpm shaking until it reached an OD_{600} of 0.5 relative to a blank consisting of the growth media alone, when it was split into two 50 mL cultures. To one of these cultures was added IPTG to a final concentration of 1mM, and then the cultures were incubated at 20°C for 18 hours.

After 18 hours, the cells were pelleted by centrifugation at 4000 x g for 10 minutes at 4°C. The growth media was discarded and the pellets were weighed and resuspended in NiNTA lysis buffer (50 mM sodium phosphate, 300 mM NaCl), using 5 mL for every gram of pellet wet weight. Lysozyme (Sigma) was added to a final concentration of 1 mg/mL and the resuspended

cells were incubated on ice for 30 minutes. The cells were then lysed on ice using a microtip sonicator on high for 3 minutes total sonication time, alternating between 45 seconds on and 3 minutes off to prevent the sample from overheating. The soluble and insoluble fractions were separated by centrifugation at 30,000 x g for 30 minutes at 4°C. The soluble fraction was then moved to a new tube and the pellet was resuspended in an amount of 6M urea equal to the volume of the soluble fraction. The soluble and insoluble lysates for both the induced and uninduced cultures were then evaluated using SDS-PAGE. 20 µL of each fraction were mixed with an equal volume of 2x Laemmli buffer (Bio-Rad) with 5% 2-mercaptoethanol, boiled for 5 minutes, and loaded onto an SDS-PAGE gel. 5 µL of Precision Plus Dual Color pre-stained protein ladder (BioRad) were also loaded. The gels were run in 1L of 1x running buffer (25mM Tris base, 250mM glycine, 0.1% SDS) at 150V for approximately one hour. After running, the gels were washed for 2 minutes with MilliQ H_2O, then stained with R-250 Coomassie staining solution (0.1% Coomassie Brilliant Blue, 40% methanol, 10% acetic acid).

For every 4 mL of soluble fraction obtained from the induced culture, 1 mL of 50% NiNTA resin slurry (Qiagen) was added and the lysate/resin solution was incubated for 1 hour at 4°C with rotation. The mixture was then added to an empty 10 mL column and the flowthrough was collected. The resin was then washed with twice the original resin slurry volume of lysis buffer containing 20 mM imidazole. Two washes were performed, and each was collected separately. Bound protein was then eluted with a volume of lysis buffer containing 250 mM imidazole equal to the volume of resin slurry initially added. The fractions were then evaluated by SDS-PAGE (see above).

mTERF EMSA

An oligonucleotide representing the mTERF binding site [82] (see Table 2-1) was methylated with MsssI (NEB). 1 μg of the oligo was mixed with NEBuffer 2, 80 μM SAM (stock solution stored at -20˚C and diluted with HPLC), and 4 units of M.SssI. The reaction was incubated at 37°C for 1 hour, then the enzyme was inactivated by a 20 minute, 65°C incubation. To prepare an unmethylated oligo, the same reaction was performed without SAM. The methylated and unmethylated oligos were labeled with γ-32P ATP (3000Ci/mmol, 10mCi/ml) (Perkin Elmer) with T4 Polynucleotide Kinase (NEB) according to the protocol provided by the manufacturer. Unincorporated ATP was removed using illustra ProbeQuant G-50 Micro Columns (GE Healtcare) according to the manufacturer's instructions, and labeling efficiency was checked by taking readings with a scintillation counter.

4 μg of NiNTA purified mTERF and 10 nM of termination probe were mixed in reaction buffer (25 mM HEPES, pH 7, 50 mM KCl, 12.5 mM $MgCl_2$, 1 mM DTT, 20% glycerol, 0.1% Tween 20) with 0.5 μg polydIdC, and 5 μg BSA in a volume of 25 μL. For reactions containing cold competitor, 10, 100 or 1000 nM of unlabelled probe were also added. The reactions were incubated at 22°C for 20 minutes. Following the incubation, the samples were mixed with 6x loading buffer (15% Ficoll 400) without dye and loaded onto a pre-run native 10% gel containing 28.25:1 acrylamide/bis-acrylamide, 0.5x TBE, and 0.1% ammonium persulfate. The gel was run in 0.5x TBE at 200 V for approximated 30 minutes on ice at 4°C. The gel was then vacuum dried at 60˚C for 2 hours and developed using a phosphorscreen and Typhoon scanner. Exposure times ranged from 20 minutes to overnight.

Expression and purification of TFAM

TFAM was cloned without the MLS in the same manner as mTERF and ligated into the pET28 expression vector by the VCU Molecular Biology Core Facility. HMS174 competent cells obtained from Dr. Hackett's laboratory were transformed with the TFAM expression vector by incubating the cells on ice with the plasmid for 5 minutes, then heating the cells to 42°C for 30 seconds and returning them to ice for 2 minutes. 125 µL of S.O.C. media was added to the cells, which were then placed in a shaking incubator at 37°C for 1 hour at 250 rpm. Following the 1 hour incubation, the cells were plated onto selective LB agar plates containing 50 ug/mL Kanamycin and placed in a 37°C incubator overnight. A colony was selected and used to inoculated 5 mL of LB containing 50 ug/mL Kanamycin. This culture was grown overnight in a shaking incubator at 37°C at 250 rpm. The 5 mL overnight culture was then added to 95 mL of LB containing 50 ug/mL Kanamycin. The 100 mL culture was grown at 37°C with 250 rpm shaking until it reached an OD_{600} of 0.5 relative to a blank consisting of the growth media alone, when it was split into two 50 mL cultures. To one of these cultures was added IPTG to a final concentration of 1mM, and then the cultures were incubated at 20°C for 18 hours.

After 18 hours, the cells were pelleted by centrifugation at 4000 x g for 10 minutes at 4°C. The growth media was discarded and the pellets were weighed and resuspended in NiNTA lysis buffer (50 mM sodium phosphate, 300 mM NaCl), using 5 mL for every gram of pellet wet weight. Lysozyme (Sigma) was added to a final concentration of 1 mg/mL and the resuspended cells were incubated on ice for 30 minutes. The cells were then lysed on ice using a microtip sonicator on high for 3 minutes total sonication time, alternating between 45 seconds on and 3 minutes off to prevent the sample from overheating. The soluble and insoluble fractions were separated by centrifugation at 30,000 x g for 30 minutes at 4°C. The soluble fraction was then moved to a new tube and the pellet was resuspended in an amount of 6M urea equal to the

volume of the soluble fraction. The soluble and insoluble lysates for both the induced and uninduced cultures were then evaluated using SDS-PAGE. 5 μL of each fraction were mixed with an equal volume of 2x Laemmli buffer (Bio-Rad) with 5% 2-mercaptoethanol, boiled for 5 minutes, and loaded onto an SDS-PAGE gel. 5 μL of Precision Plus Dual Color pre-stained protein ladder (BioRad) were also loaded. The gels were run in 1L of 1x running buffer (25mM Tris base, 250mM glycine, 0.1% SDS) at 150V for approximately one hour. After running, the gels were washes for 2 minutes with MilliQ H_2O, then stained with R-250 Coomassie staining solution (0.1% Coomassie Brilliant Blue, 40% methanol, 10% acetic acid).

For every 4 mL of soluble fraction obtained from the induced culture, 1 mL of 50% NiNTA resin slurry (Qiagen) was added and the lysate/resin solution was incubated for 1 hour at 4°C with rotation. The mixture was then added to an empty column and the flowthrough was collected. The resin was then washed with twice the original resin slurry volume of lysis buffer containing 20 mM imidazole. Two washes were performed, and each was collected separately. Bound protein was then eluted with a volume of lysis buffer containing 250 mM imidazole equal to the volume of resin slurry initially added. The fractions were then evaluated by SDS-PAGE (see Expression and Purification of mTERF).

The NiNTA elution fraction from was dialyzed overnight at 4°C into ion exchange buffer (50 mM Hepes, pH 7.0, 50 mM NaCl, 1 mM DTT) using dialysis tubing with a 10 kDa pore size. An ENrich S 5 x 50 mm column (Bio-Rad) was connected to an NGC system (Bio-Rad) and equilibrated with 5 mL of ion exchange buffer (50 mM Hepes, pH 7.0, 50 mM NaCl, 1 mM DTT). The dialyzed NiNTA elution was then loaded onto the column and washed with 3 mL of ion exchange buffer. The flowthrough and wash were collected. A 15 mL gradient was then run from the starting 50 mM NaCl concentration to 0.5 M NaCl, and 1 mL fractions were collected.

To elute any protein remaining on the column after the gradient, 3 mL of ion exchange buffer contain 1 M NaCl were run over the column and collected. The fractions were evaluated by SDS-PAGE (see Expression and Purification of mTERF).

Methylation reaction and analysis for EMSA and FP probes

EMSA and FP probes were methylated with M.SssI (NEB). To assess the methylation efficiency, 1 μg of HSP1 transcription template was mixed with NEBuffer 2, 320 μM SAM (stock solution stored at -20˚C and diluted with HPLC), and 4 units of M.SssI. The reaction was incubated at 37°C overnight, then the enzyme was inactivated by a 20 minute, 65°C incubation. The reaction was purified by phenol/chloroform extraction and precipitated with ethanol. 200 μg of the methylated DNA was digested with the methylation sensitive restriction enzyme AciI (NEB) in CutSmart buffer for 1 hour and 37°C. Percent protection was then determined by qPCR (See Chapter 1 for reaction conditions). 40 cycles were performed, with a 55˚C annealing step. A set of primers amplifying the entire sequence was used to determine the amount of protection, as only methylated sequences would remain intact and be able to be amplified. Another primer specific for the region of the sequence between the restriction site and the end of the sequence was used as an input control.

TFAM EMSA

EMSAs were performed with rmtTFA purchased from Enzymax, LLC. Binding probes (see Table 2-1) were labeled with γ-32P ATP (3000Ci/mmol, 10mCi/ml) (Perkin Elmer) with T4 Polynucleotide Kinase (NEB) according to the protocol provided by the manufacturer. Unincorporated ATP was removed using illustra ProbeQuant G-50 Micro Columns (GE

Healtcare) according to the manufacturer's instructions, and labeling efficiency was checked by taking readings with a scintillation counter.

200 nM rmtTFA and 10 nM probe were mixed with reaction buffer (50 mM HEPES, pH 7.5, 50 mM KCl, 2 mM $MgCl_2$ and 2 μg/mL BSA for Figures 16 and 18 or 20 mM Tris HCL, pH 8, 10 mM $MgCl_2$, 60 mM NaCl, 15% glycerol, 1 mM EDTA, 1mM DTT, and 0.1mg/mL in Figures 20 and 21) in a 10 μL reaction. For experiments using cold competitor, 10 or 100 nM of unlabelled probe were also added. The reactions were incubated at 22°C for 30 minutes. Following the incubation, the samples were mixed with 6x loading buffer (15% Ficoll 400) and loaded onto a pre-run native 12% gel containing 28.25:1 acrylamide/bis-acrylamide, 0.33x TBE (in Figures 16 and 18) or 0.5x TBE (in Figures 20 and 21), and 0.1% ammonium persulfate. The gel was run in 0.33x or 0.5x TBE (the same as the concentration of TBE present in the gel) at 100 V for approximated 2.5 hours on ice at 4°C. The gel was then vacuum dried and developed using autoradiography film (ISC Bioexpress) and a Konica SRX-101A developer or a phosphorscreen and Typhoon scanner. Exposure times ranged from 20 minutes to overnight.

Native gel immunoblotting

1200 nM rmtTFA and 60 nM cold probe or 1800 nM rmtTFA and 90 nM probe were mixed with reaction buffer (50 mM HEPES, pH 7.5, 50 mM KCl, 2 mM $MgCl_2$ and 2 μg/mL BSA) in a 10 μL reaction. The reaction was incubated and run on a 12% native gel as for an EMSA (described above). After running, the gel was washed with MilliQ H_2O and incubated in 1x transfer buffer with 1% SDS for 1 hour at 4°C. Following this incubation, the gel was transferred to a PVDF membrane, probed with an antibody specific for TFAM, and developed as described in Chapter 2.

TFAM Fluorescence Polarization

FAM-labeled probes for fluorescence polarization (FP) studies were methylated as described above. 10 μg of methylated or unmethylated probe was diluted into 500 μL of 20 mM Tris, pH 8, and loaded onto an Enrich Q column (Bio-Rad) connected to an NGC system (Bio-Rad) that had been equilibrated with 5 mL of the buffer. The column was washed with 5 mL of 20 mM Tris, pH 8, and the wash was collected. A gradient from 20 mM Tris, pH 8 containing no NaCl to 20 mM Tris, pH 8 plus 1 M NaCl was run over the column over 15 mL. 1 mL fractions were collected. 5 mL of 20 mM Tris, pH 8 plus 1 M NaCl were then run over column, and 1 mL fractions were collected. The fractions containing DNA were identified using a NanoDrop spectrophotometer and the DNA was precipitated by adding 3 volumes of 100% ethanol to the fractions and incubating them for at least 1hour at -80°C or overnight at -20°C. The DNA was then pelleted by centrifugation at 16100 x g for 45 minutes at 4°C. The pellet was washed with 75% ethanol and resuspended in HPLC H_2O.

Varing concentrations of rmtTFA and 0.5 nM probe were mixed with reaction buffer (50 mM HEPES, pH 7.5, 50 mM KCl, 2 mM $MgCl_2$ and 2 μg/mL BSA for Figure 17 or mM Tris HCL, pH 8, 10 mM $MgCl_2$, 60 mM NaCl, 15% glycerol, 1 mM EDTA, and 1mM DTT in Figures 22) in a 100 μL reaction volume. The reactions were performed in triplicate. The reactions were incubated at 22˚C for 30 minutes, then transferred to a 96 well black Optiplate F. The reactions were read using a PHERAstar FS fitted with a FP optic module. The data were fit to the Hill equation in Prism GraphPad to determine Kd.

Transcription assays

Transcription assays were performed by Dr. Lisa Shock as described by Morozov YI, et al. (2014). Transcription templates were designed so that the respective promoter sequences were placed upstream of a common transcribed sequence, based on the sequence transcribed from LSP. Reactions were performed using varied amounts of template, mtRNAP (50 nM), TFAM (50 nM), TFB2M (50 nM) in a transcription buffer containing 40 mM Tris (pH = 7.9), 10 mM MgCl2 and 10 mM dithiothreitol (DTT) in the presence of ATP (0.3 mM), GTP (0.3 mM), UTP (0.01 mM) and 0.3 μCi[α-32P] UTP (800 Ci/mmol). The reactions were incubated at 35°C for 30 minutes and stopped by addition of an equal volume of stop buffer (95% formamide, 0.05M EDTA, 0.25% bromophenol blue). The reactions were resolved on a 20% polyacrylamide gel electrophoresis (PAGE) gel containing 6 M urea and developed using a phosphorscreen and Typhoon scanner.

Results

mTERF can be expressed in and purified from *E. coli*

An expression construct containing the mTERF coding sequence without the MLS was generated by PCR amplification, restriction digest, and ligation (Fig. 3-1a). HMS174 competent cells were transformed with this expression construct and induced with IPTG (Fig. 3-1b). The cells were lysed and the soluble lysate was purified using a NiNTA column (Fig. 3-1b). A band of the appropriate size for mTERF was found in the soluble lysate (Fig. 3-2a) and the elution fraction of the NiNTA column purification (Fig. 3-2b). Additional bands were observed in the elution fraction, but the expected band was the dominant species.

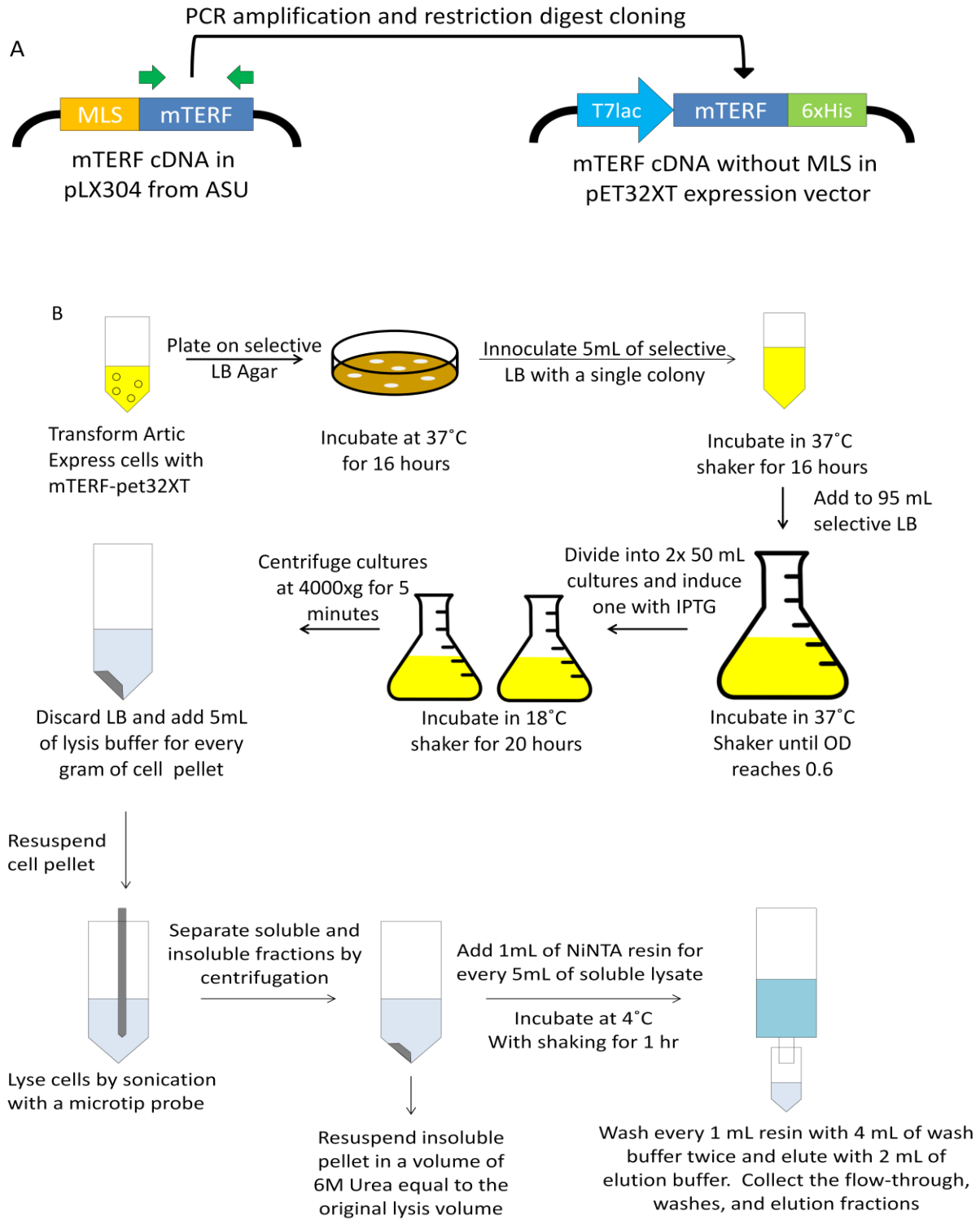

Fig 3-1. Schematic for the expression and purification of mTERF. mTERF sequence was confirmed by sequencing.

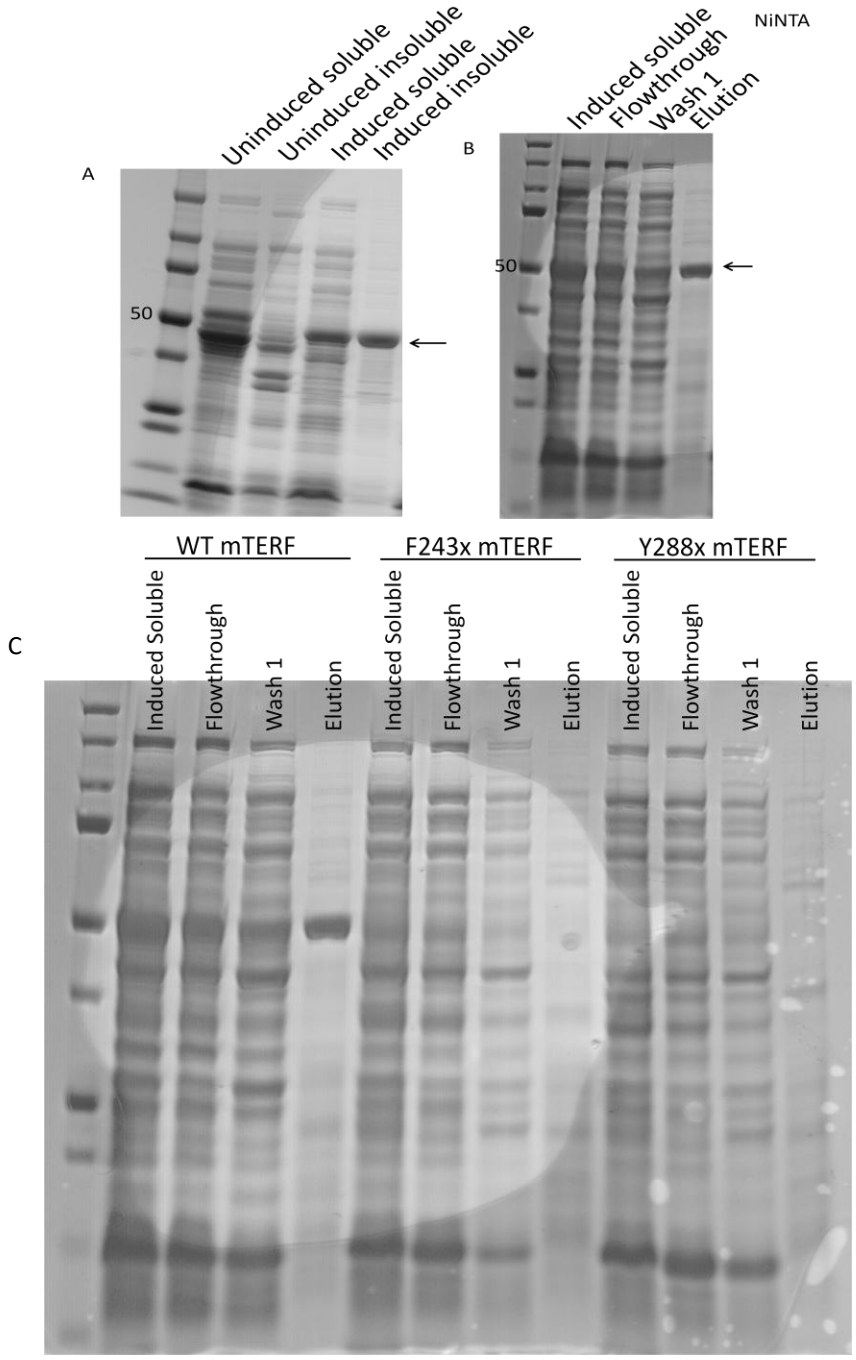

Fig 3-2. Wild-type mTERF can be expressed and purified from bacterial cells, but incorporation of unnatural amino acids resulted in no detectable protein production. SDS-PAGE gels showing mTERF (A) is present in both the soluble and insoluble fraction of induced cells and (B) can be purified using a NiNTA column. (C) An SDS-PAGE gel comparing wild-type and mutant mTERF expression after NiNTA purification. No bands of the appropriate size are visible in the elution fractions of the F243x or Y288x purifications.

Expression constructs of mTERF in which key residues had been mutated to allow the incorporation of an unnatural amino acid were generated by the VCU Molecular Biology Core Facility. Unnatural amino acids can be used as vibrational probes and crosslinking sites to evaluate changing in molecular interactions in further detail. However, when expression of mTERF with incorporated unnatural amino acids was attempted, no expressed proteins were detected (Figure 3-2c).

Methylation does not affect mTERF binding to the termination site

The mTERF purified from HMS174 cells was used in an EMSA with a probe containing the termination site. mTERF was found to bind to both unmethylated and methylated probe, and was able to be competed off using unlabeled unmethylated probe (Fig. 3-3). No differences were observed in the shift of the unmethylated and methylated DNA.

TFAM can be expressed in and purified from *E. coli*

An expression construct containing the TFAM coding sequence without the MLS was generated by PCR amplification, restriction digest, and ligation by the VCU Molecular Biology Core Facility (Fig. 3-4a). HMS174 competent cells were transformed with this expression construct and induced with IPTG (Fig. 3-4b). The cells were lysed and purified using a NiNTA column and an ENrich S column (Fig. 3-4b). A band of the expected size was present in the induced soluble lysate and the NiNTA elution fraction (Fig. 3-5). There were other bands present, so the elution fraction was further purified over an ENrich S column (Fig. 3-5). The NiNTA column yielded approximately 50% purified TFAM, and the EnRICH S column yielded

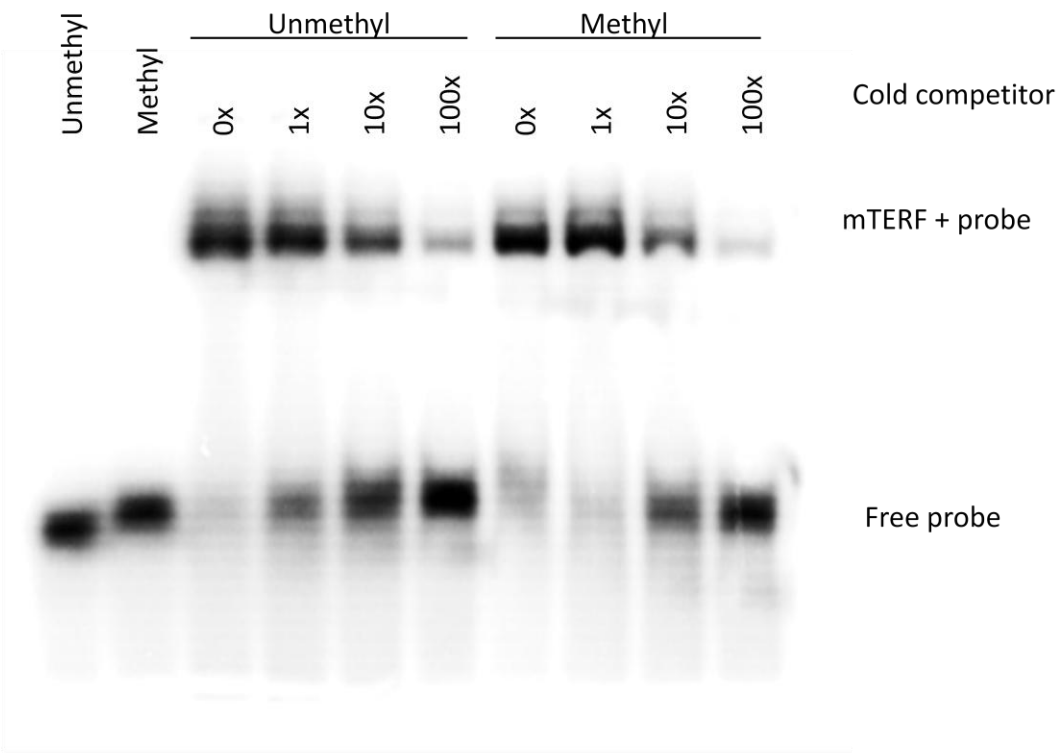

Fig 3-3. Methylation does not affect mTERF binding to the termination site. Shown is an EMSA in which mTERF was incubated with methylated or unmethylated radiolabeled DNA containing its binding site (n=1). Unlabeled, unmethylated DNA was used as a cold competitor.

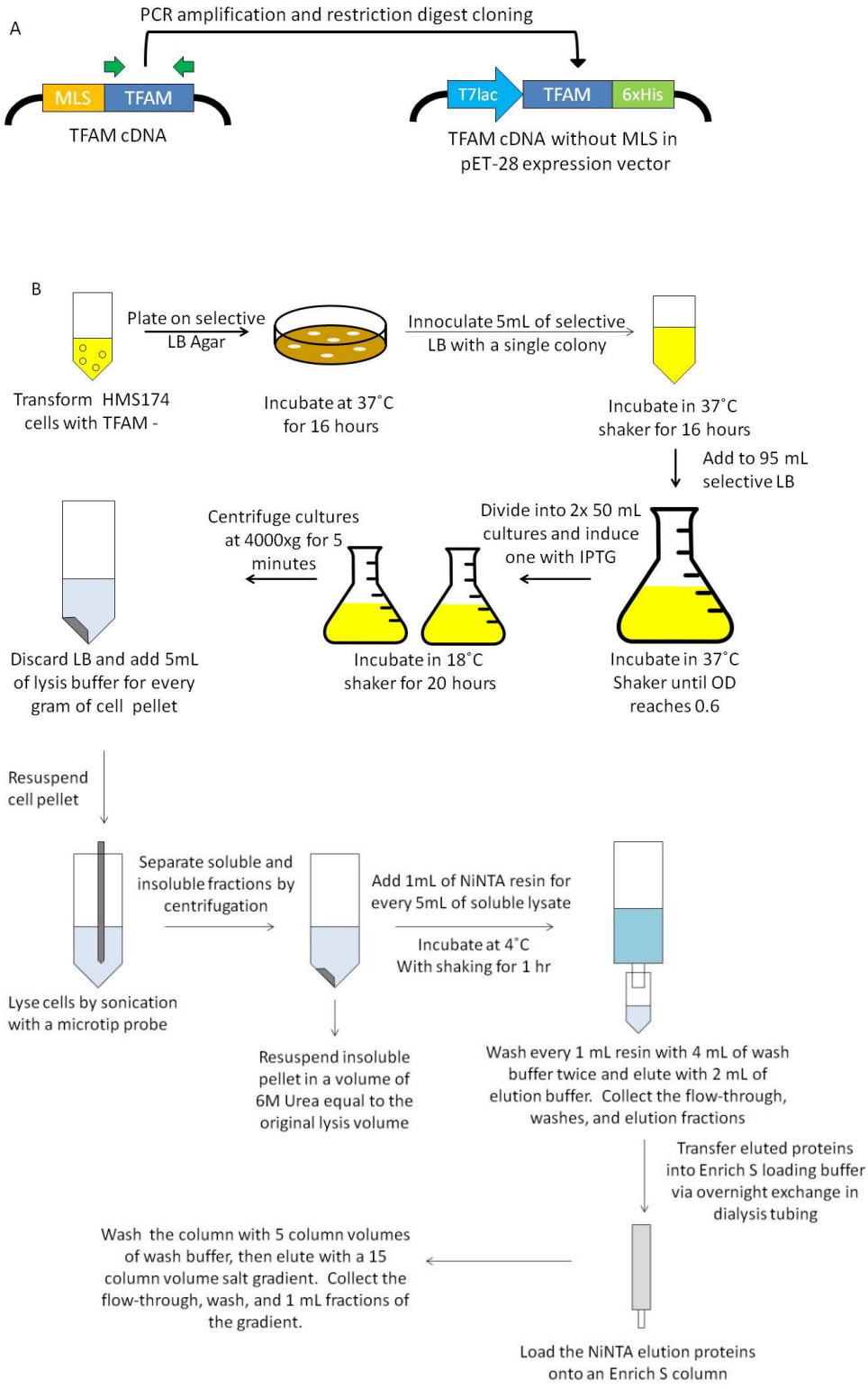

Fig 3-4. Schematic for the expression and purification of TFAM. TFAM sequence was confirmed by sequencing.

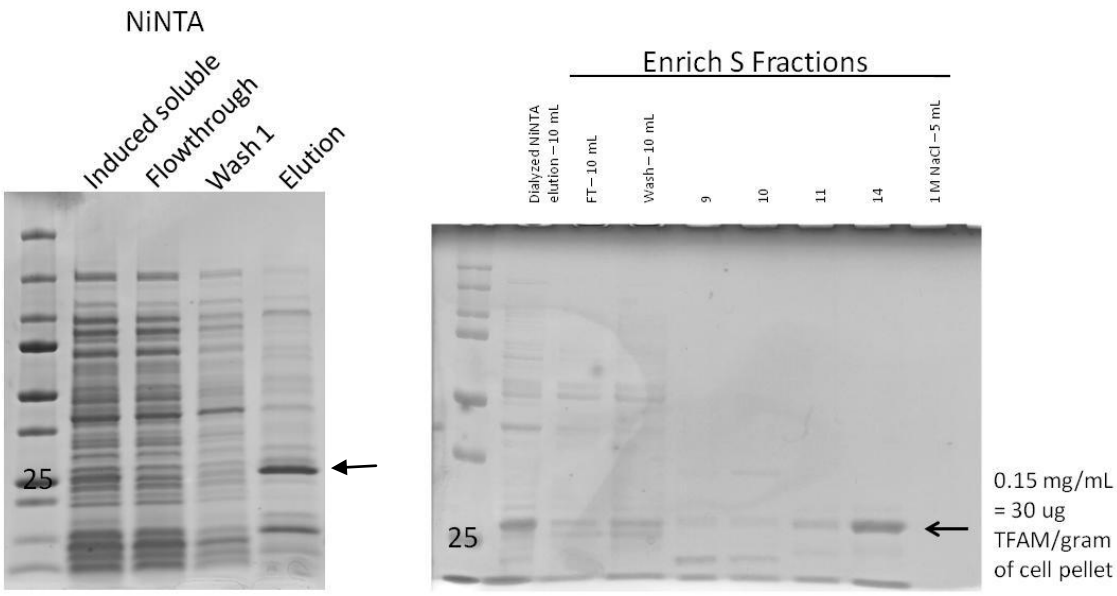

Fig 3-5. TFAM can be expressed in and purified from *E. coli.* SDS-PAGE gels showing TFAM is present in the soluble lysate of induced cells, the elution fraction of an NiNTA column purification and in fraction 14 of an Enrich S column purification.

approximately 80% purified TFAM (Figure 3-5). After both purification steps, approximately 30 μg/gram of cell pellet were recovered.

Unnatural amino acids can be incorporated into bacterially expressed TFAM

Expression constructs of TFAM in which key residues have been mutated to allow the incorporation of an unnatural amino acid were generated by the VCU Molecular Biology Core Facility. The sequences encoding tyrosines 15 and 120 were mutated to match the amber stop codon, TAG, which allows an optimized CUA tRNA charged with an unnatural amino acid to used during translation [75]. These residues were selected based on X-ray crystallography data [23] and binding simulations performed by Dr. John Hackett. Unnatural amino acids can be used as vibrational probes and crosslinking sites to evaluate changes in molecular interactions in further detail. BpA and CNF residues were individually incorporated into TFAM, replacing residues Y15 and Y120. The proteins with BpA substituted were expressed less robustly than the wild-type TFAM (Fig. 3-6), but more robustly than CNF substituted proteins (Fig 3-8). Incorporation of the unnatural amino acids was verified by mass spec analysis performed by Charles Lyons (Fig. 3-7).

Methylation affects TFAM binding to DNA

Purchased recombinant TFAM was used in EMSAs to determine if methylation affects TFAM binding to DNA. Figure 3-8 shows HSPxTFAM, the DNA probe used in the initial binding studies. The underlined sequence shows the published TFAM binding site at HSP1, while the CpG residues near the binding site are shown in red. HSPxTFAM was methylated, labeled with P^{32}, and incubated with purchased recombinant TFAM. EMSA data showed that

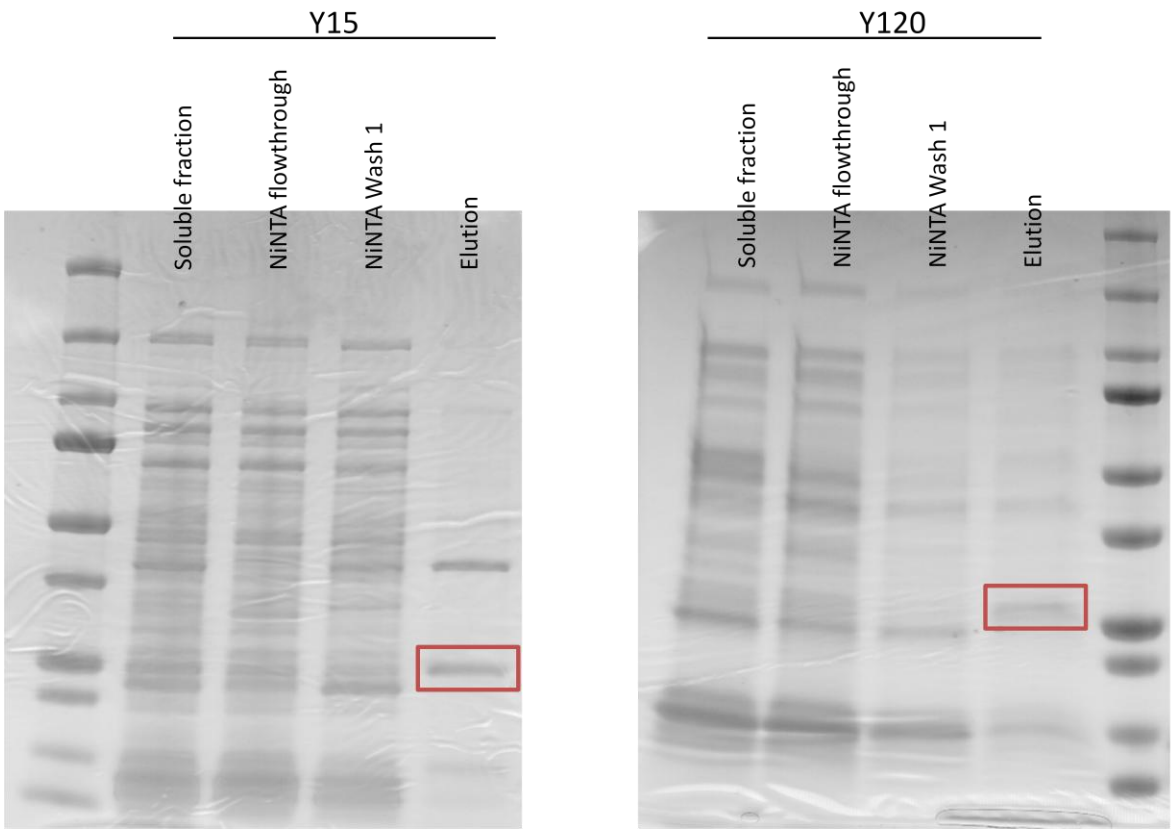

Fig 3-6. TFAM can be expressed with unnatural amino acid BpA substituted positions Y15 and Y120. SDS-PAGE of induced soluble and NiNTA column fractions showng a band at 25 kDa.

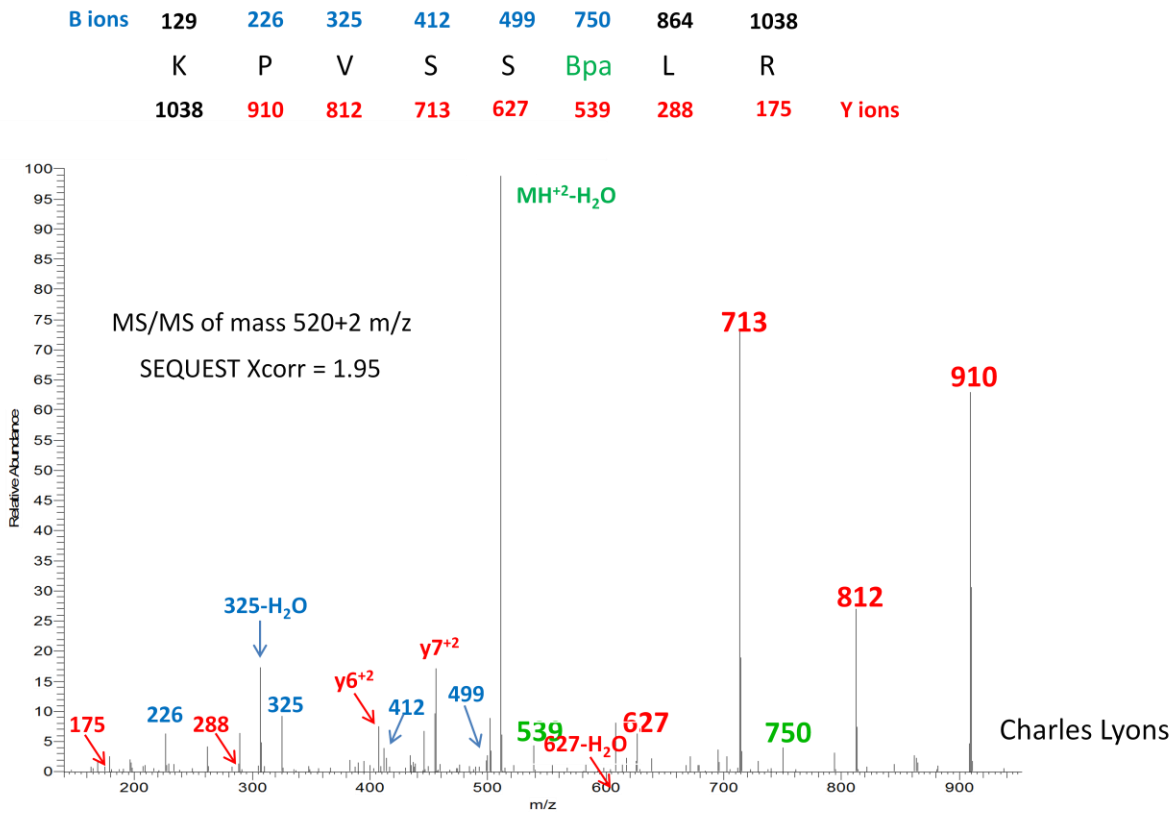

Fig 3-7. TFAM mutants contain unnatural amino acids. A representative mass spectrometry scan showing the peptide with the appropriate substituation. Experiment and figure done by Charles Lyons.

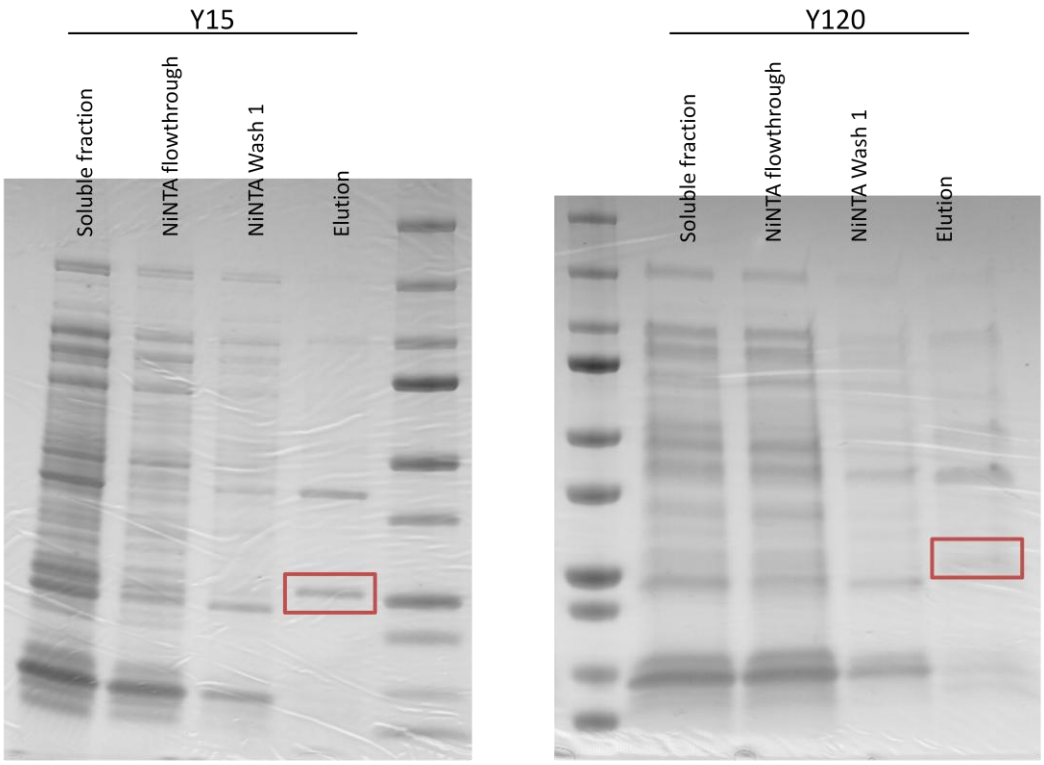

Fig 3-8. TFAM can be expressed with unnatural amino acid BpA substituted positions Y15 and Y120. SDS-PAGE of induced soluble and NiNTA column fractions showng a band at 25 kDa.

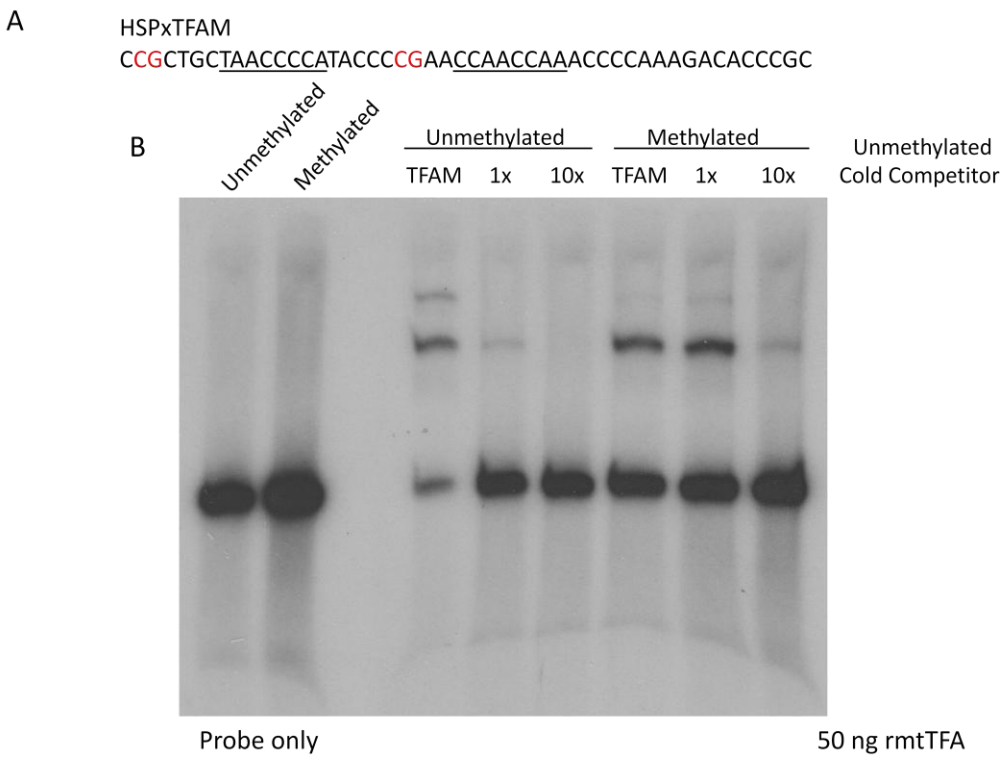

Fig 3-9. Methylation affects binding at HSP1 binding site described by Ngo et al [78]. (A) The sequence of the HSP1 probe. The TFAM binding half-sites are underlined. (B) EMSA with methylated and unmethylated probe and unmethylated cold competitor. Image shown is representative of 3 experiments. More probe is shifted up when the probe is methylated.

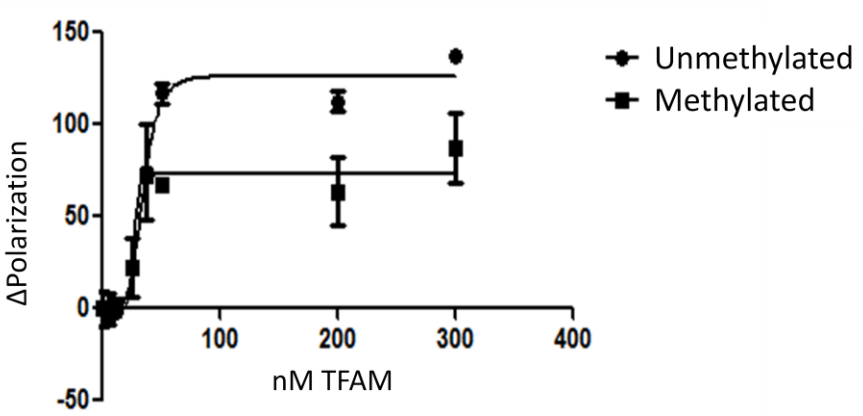

	Unmethylated	Methylated
Kd	34.37	26.69

Fig 3-10. Fluorescence polarization shows an increased affinity for methylated HSPxTFAM. Polarization values for reactions containing methylated and unmethylated HSPxTFAM-fam were fit to the Hill Equation and the Kd values for each trend line were calculated using Prism Graphpad. Each data point represents 3 replicate reactions.

TFAM binds to methylated and unmethylated HSPxTFAM, but more unmethylated cold competitor is required to compete TFAM off methylated HSPxTFAM (Fig. 3-9b). This suggested that TFAM has a higher affinity for methylated HSPxTFAM than unmethylated HSPxTFAM. Fluoresence polarization data supported this (Fig 3-10). Reactions containing methylated probe reached the maximum polarization value at a lower concentration of TFAM than reactions containing unmethylated probe.

In order to determine if the individual CpG residues near the published TFAM binding site contributed differently to this change in binding, the CpG residues were changed to CpC residues separately and simultaneously. These probes were methylated and used in an EMSA (Fig. 3-11). Loss of the second CpG residue (ΔCpG2) resulted in less signal being shifted upward proportionately than loss of the first CpG residue (ΔCpG1). This suggests that methylation of CpG2 contributed more to the increase in affinity than methylation of CpG1.

Multiple bands were observed on the EMSAs, so in order to determine if TFAM was present in the higher order complexes, the protein was allowed to bind to unlabelled probe and run on a native gel. This gel was then transferred to a membrane and probed with antibody specific to TFAM (Fig. 3-12). This demonstrated that TFAM was present in all the shifted bands.

During the course of these studies, the Temiakov laboratory demonstrated that the published TFAM binding site for HSP1 was incorrect. The previous (underlined) and new (bolded) binding sites are shown in Figure 3-13a. Because the HSP1 transcription template used in transcription assays contained the new binding site, it was used for further studies. It was found that increasing levels of TFAM relative to the HSP1 transcription probe resulted in larger complexes being formed (Fig. 3-13b), as expected. Methylation was found to cause the

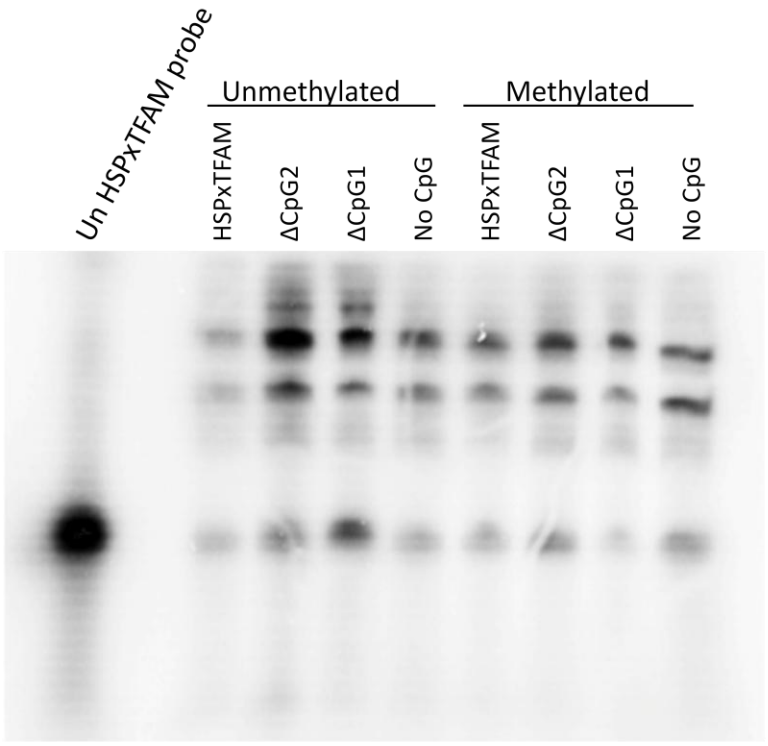

Fig 3-11. Loss of methylation at CpG2 results in loss of increased binding. The CpG residues in the HSPxTFAM probe were changed to CpC to prevent methylation. TFAM binding to methylated and unmethylated forms of the mutated and original probe was compared using EMSA (n=2, representative image).

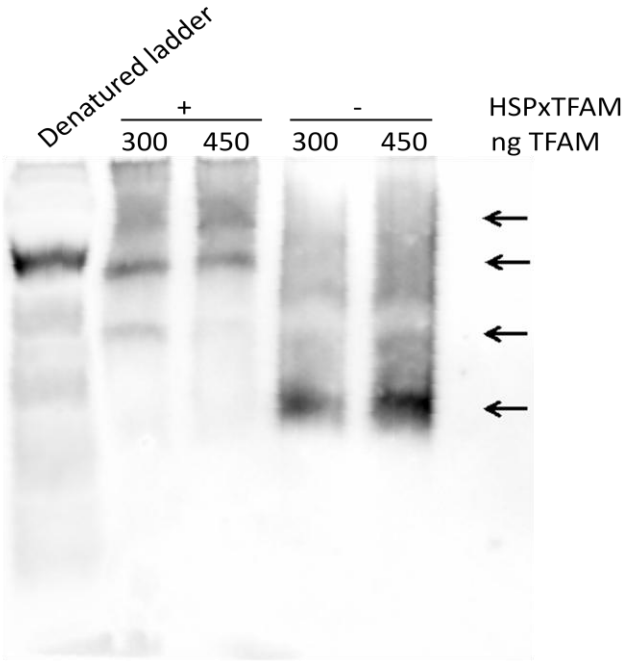

Fig 3-12. Shifted bands contain TFAM. TFAM was incubated with unlabeled, unmethylated probe and the reaction was run on a 12% native gel. This was then transferred to a membrane and immunoblotted with a TFAM-specific antibody (n=1). The arrows indicate bands of different sizes containing TFAM. The reactions labeled with "+" include the binding oligo, while the reactions labeled with "-" do not.

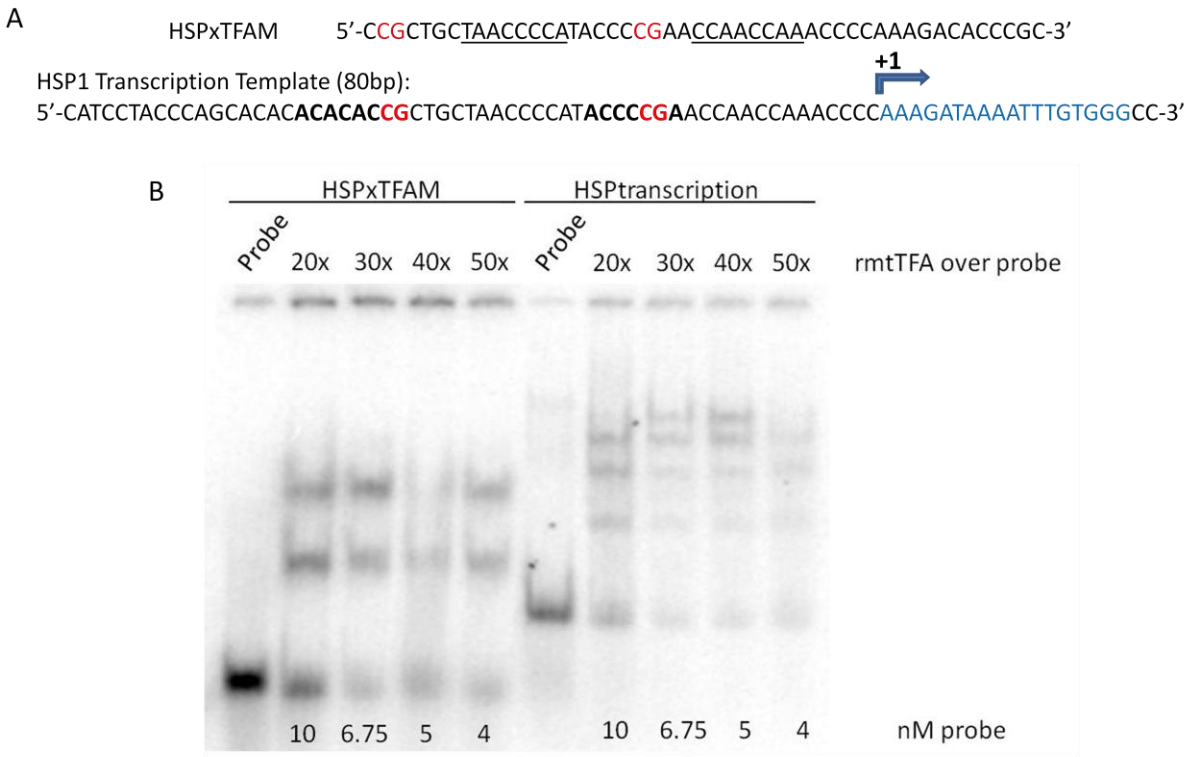

Fig 3-13. Increase in the relative amount of TFAM results in larger complexes being formed with a larger probe [26]. EMSA comparing the shorter HSPxTFAM probe and the longer HSPtranscription oligo used as a template for transcription assays (n=1). Increases in relative TFAM concentration result in more probe being shifted upward.

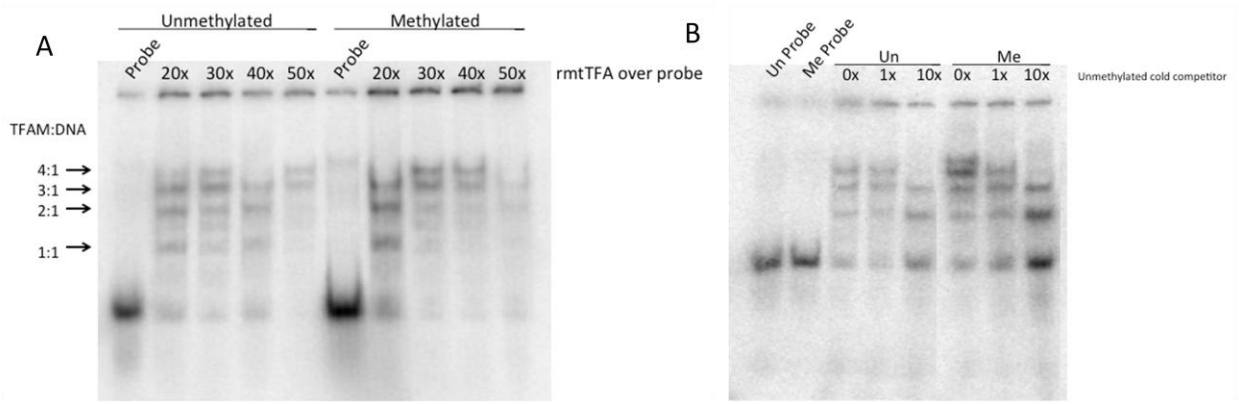

Fig 3-14. Methylation results in larger complexes being formed. EMSAs using (A) increasing relative amounts of TFAM (n=2) and (B) unmethylated cold competitor (n=2). Reactions with the methylated probe results in larger complexes being formed at lower concentrations of TFAM.

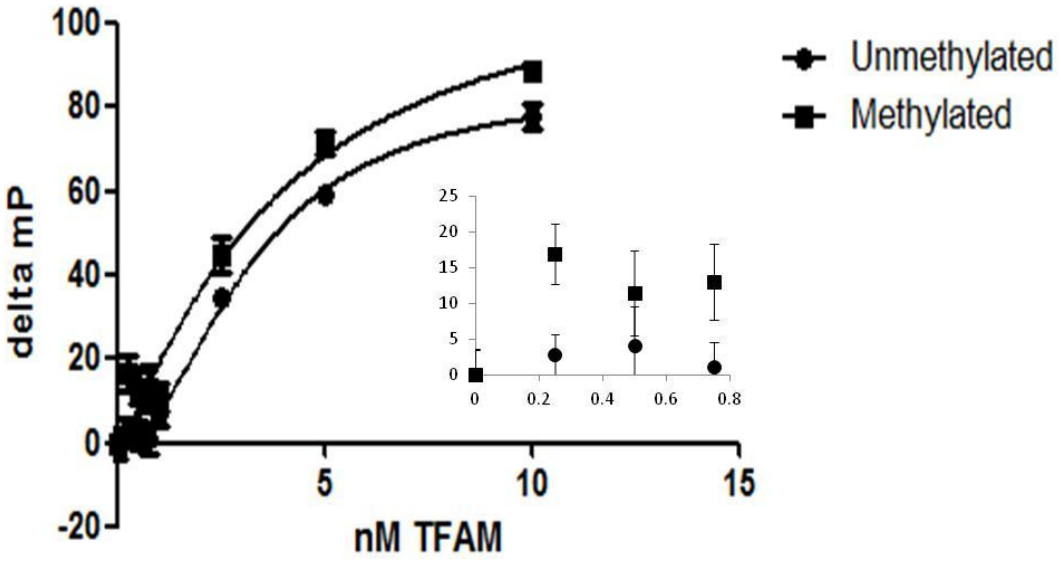

Fig 3-15. Fluorescence polarization using the HSP1 transcription template shows higher polarization of methylated probe at low levels of TFAM, but no change in Kd. Polarization values for TFAM concentrations below 1 nM are higher using the methylated probe, but the trendlines for the data are not significantly different. Each data point represents 3 replicate reactions.

formation of larger complexes at lower relative levels of TFAM to probe (Fig. 3-14a). Unmethylated cold competitor was able to compete TFAM off of the methylated probe at similar levels as the unmethylated probe (Fig. 3-14b). This was different than what was seen in the previous studies with HSPxTFAM, which is representative of nonspecific DNA. Fluorescence polarization showed no significant difference in Kd for methylated and unmethylated HSP1 transcription probe (Fig. 3-15). Interestingly, higher polarization was observed at lower concentrations of TFAM when methylated probe was used in the reaction, indicating there may be some differences in how TFAM interacts with methylated and unmethylated promoter DNA.

Methylation results in increased transcription from HSP1

In order to determine if the changes seen in TFAM binding affect transcription, transcription assays were performed by Dr. Lisa Shock. These assays demonstrated that methylation of HSP1 results in increased transcription (Fig. 3-16). At 10 nM template, more product is produced from a methylated template (Fig. 3-16b). The increase is about 3-fold (Fig. 3-16c). This change at 10 nM template is interesting, because there is a TFAM molecule for every 16.6 bp in the mitochondrial genome in human fibroblasts [80]. This is very similar to the ratio present when 10 nM of tenplate are used in the transcription assay, suggesting that the results obtained at that ratio are the most biologically relevant.

In order to determine if the individual CpG residues in the HSP1 promoter contributed differently to this change in transcription inititation, the CpG residues were changed to CpC residues separately and simultaneously. These probes were methylated and used in transcription assays at 10 nM (Fig. 3-17). The changes of the CpG residues to CpC residues alone were found to have an extreme effect on transcription (Fig. 3-17b). Loss of methylation at either CpG

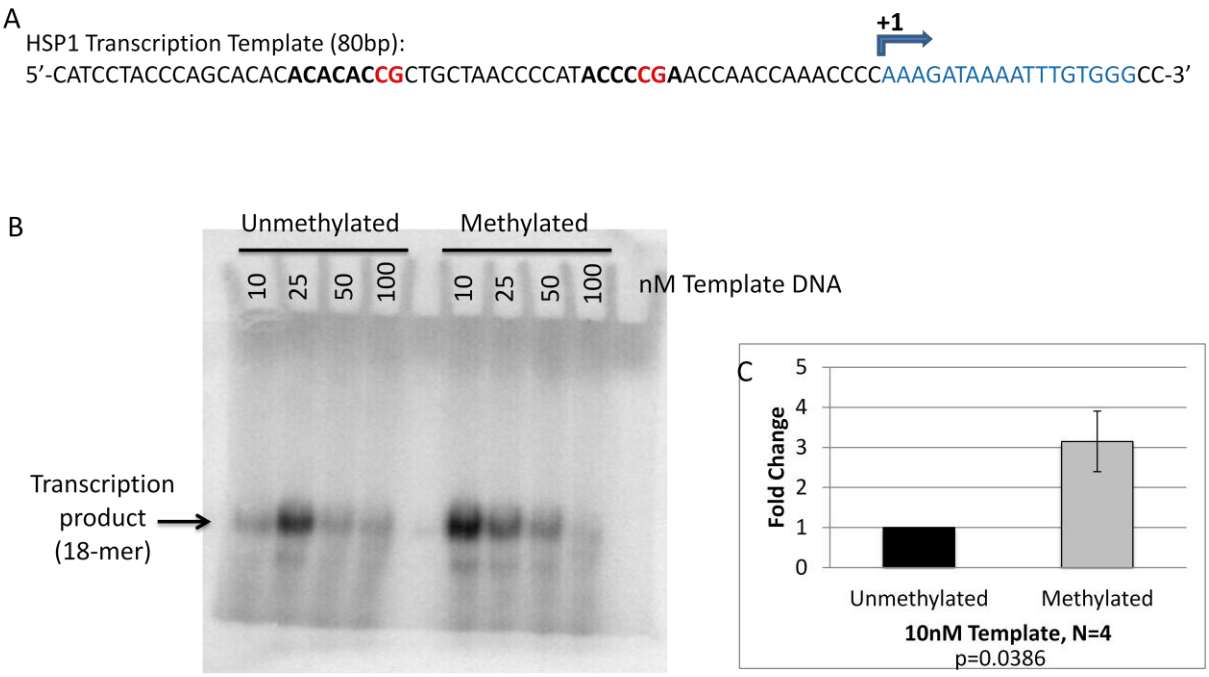

Fig 3-16. Methylation increases transcription from the Heavy Strand Promoter. Assays designed and analyzed by Lisa Shock. (A) Transcription template used in assays. Methylation targets are in red, and the blue sequence indicates the transcribed sequence. (B) Representative image of assay. (C) Quantitation of 10 nM reactions performed using ProbeQuant software.

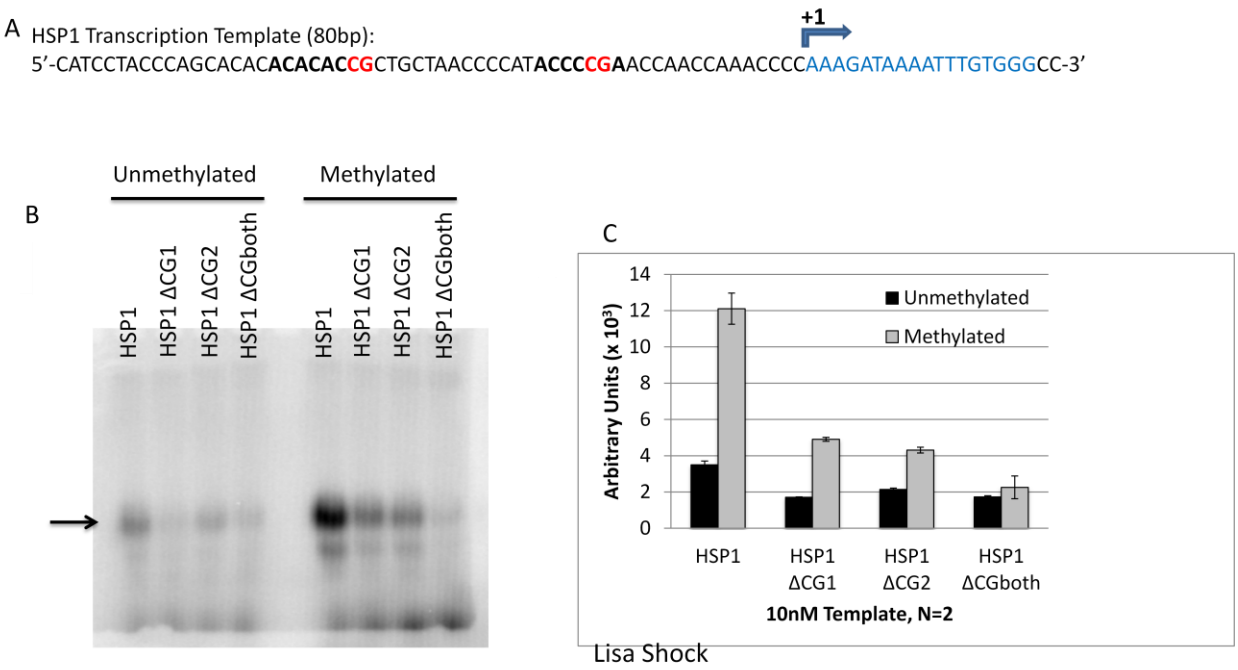

Fig 3-17. Methylation of individual CpG residues contributes differently to increases in transcription from the Heavy Strand Promoter. Assays designed and analyzed by Lisa Shock. (A) Transcription template used in assays. Methylation targets that were mutated to CC are in red, and the blue sequence indicates the transcribed sequence. (B) Representative image of assay. (C) Quantitation of assays performed using ProbeQuant software.

residue impacted transcription, but loss of methylation at CpG2 seemed to have a greater impact (Fig. 17c). These findings support the observation above that methylation has an effect on TFAM binding, and may partially explain the transcriptional differences observed in Chapter 1.

Discussion

Expression of recombinant mTERF1 and TFAM in *E. coli*

Both wild-type mTERF1 and TFAM were expressed in and purified from *E. coli*. However, unnatural amino acids were only successfully incorporated into TFAM. Attempts to incorporate unnatural amino acids into mTERF1 resulted in no protein being expressed. This could be due to the helical structure and rigid motifs of mTERF1 [71], resulting in co-translational protein degradation.

It has been shown that elongation factor thermal unstable (EF-Tu) binds less efficiently to tRNAs charged with unnatural amino acids [81], which can lead to translational pausing, inefficient incorporation and translation, and co-translational protein degradation. Overexpression of this elongation factor has been shown, in many cases, to minimize these effects and allow more efficient production of proteins carrying unnatural amino acids (REF). In an attempt to improve expression of mutant mTERF, HMS174 were transformed with an expression vector encoding EF-Tu, then made competent and transformed with the mutated mTERF1 expression vector and pEVOL. Protein expression was then induced. However, the recombinant EF-Tu is close in size to the recombinant mTERF and also contained a 6x His tag, resulting in its co-purification by NiNTA resin. This made visualization of the unnatural amino acid-substituted mTERF1 protein difficult. Attempts were made to remove the 6x his tag from

the EF-Tu expression vector by mutagenesis, but these were unsuccessful. If the tag were to be removed, increased expression of EF-Tu could be used in an attempt increase the levels of mutant TFAM produced, as well.

Methylation does not affect mTERF1 interaction with the termination sequence

Methylation of the termination sequence did not appear to affect mTERF binding to its recognition sequence (Figure 3-3). This observation led us to focus our analysis on the impact of methylation on TFAM binding to promoter DNA. However, mTERF1 has been shown to also bind upstream of HSP1, forming a loop in the DNA that is thought to facilitate recycling of the transcription machinery [82]. Given the recent suggestion that the primary termination role of mTERF1 may be on transcription of the light strand [32], the effect of methylation on mTERF1 promoter binding transcription loop formation may be worth investigating.

Methylation affects the interaction of TFAM with nonspecific and promoter DNA differently

The HSPxTFAM binding probe was designed based on the published TFAM binding site at HSP described by Ngo, et al [78]. The probe was reported to contain the TFAM binding site and the transcription start site. TFAM was found to have a higher affinity for methylated HSPxTFAM probe than unmethylated probe (Figures 3-9, 3-10), and was observed to form complexes of an appropriate size to contain multiple TFAM molecules. These larger complexes were shown to contain TFAM through immunoblotting with an antibody specific for TFAM (Figure 3-11). However, there was some concern over the apparent loss of probe observed (see Figure 3-9, Unmethylated/TFAM only lane). It was possible that some of the complexes being

formed were remaining in the reaction tube and therefore were not represented on the gel. Reaction conditions were changed from those described by Gangelhoff et al [79] to those used by Kukat et al [25]. The primary difference between the two sets of reaction conditions was the addition of 15% glycerol and a 50-fold increase in the amount of BSA present. After changing reaction conditions, recovery of probe was consistent between experimental samples and close to complete (Figure 3-13a).

While the experiments with the HSPxTFAM probe were being conducted, it was demonstrated that the TFAM binding site published by Ngo, et al. was incorrect (Temiakov, personal communication), using DNA-protein crosslinking studies. The binding site is further upstream from the transcription start site (shown in bold in Figure 3-12a), placing it at a similar position relative to the transcription start site as the TFAM binding site at LSP (Temiakov, personal communication). The complete binding site was not present in the HSPxTFAM probe, meaning that the changes in TFAM binding due to methylation observed using the HSPxTFAM probe are representative of the effect of methylation on TFAM binding to non-specific, rather than promoter DNA.

A longer oligo had been developed for use in transcription assays, HSPtranscription (Figure 3-12a). This oligo contained the entire TFAM binding site at HSP1, so was used in further studies to evaluate the effect of methylation on the binding of TFAM at HSP1. In EMSAs with the HSPtranscription oligo, TFAM was observed to form higher order complexes at lower concentrations when the probe was methylated (Figure 3-13). However, FP with fluorophor-labeled HSPtranscription probe did not reveal any differences in the affinity of TFAM for methylated and unmethylated promoter DNA (Figure 3-14). This could be due to the formation of larger complexes than was observed with EMSA (Figure 3-13). If a 1:1 binding

ratio of TFAM:DNA forms a large enough complex to polarize the fluorescence emitted from the probe, still larger complexes will not result in increased polarization. The formation of the larger complexes at lower relative levels of TFAM when the DNA is methylated would not be observed with this technique.

Methylation results in increased transcription from HSP1

Transcription assays performed by Dr. Lisa Shock demonstrated that transcription from a methylated template is increased relative to transcription from an unmethylated template in reactions containing 10 nM of the HSP1 transcription template and 50 nM TFAM, POLRMT, and TFB2M (Figure 3-15b). These relative concentrations are biologically relevant, because the amount of TFAM present in mitochondria has been calculated to be 1 TFAM molecule for every 16.6 bp of mtDNA [80]. Because the HSP1 transcription template is 80 bp, the 1:5 ratio of TFAM:DNA molecules almost perfectly replicates the relative levels of TFAM and mtDNA observed *in vivo*.

This increase in transcription from HSP1 could be easily explained if TFAM had been shown to bind with higher affinity to methylated promoter DNA, but this was not found (Figures 3-13, 3-14). However, the formation of larger complexes at lower relative levels of TFAM observed when the promoter sequence was methylated provides a potential alternate hypothesis. The formation of larger complexes suggests that TFAM may be able to more effectively recruit additional proteins to the promoter when it is methylated. In the EMSA and FP experiments, the only available proteins were other TFAM molecules. It is possible that this increase in recruitment efficiency may apply to the other components of the mitochondrial transcription

machinery, as well. If POLRMT and TFB2M are recruited to the promoter more efficiently when the promoter is methylated, an increase in transcription would be expected.

This could be tested using the protein-DNA and protein-protein photocrosslinking protocol described by Morozov, et al [26]. Photo-reactive molecules incorporated into TFAM and promoter oligos allow TFAM to be crosslinked with POLRMT and POLRMT to be crosslinked with the DNA [26]. If TFAM is able to more efficiently recruit POLRMT to a methylated promoter, more crosslinked complexes should be observed when methylated oligo is used in the reaction.

Chapter 4: Conclusions and Perspectives

The effects of cytosine modifications in DNA are fairly well understood in the nuclear genome. Cytosines in CpG dinucleotides can be modified with methyl groups, which is associated with chromatic compaction and transcriptional silencing [1], or hydroxymethyl groups, which is associated with active demethylation and gene expression [3]. However, the effects of these modifications in the mitochondrial genome are not yet understood.

Methylated cytosine residues were identified in the mitochondrial genome several decades ago [45], but a methyltransferase was not identified in the organelle until the Taylor laboratory demonstrated an isoform of DNMT1 which is translocated to the mitochondria [57]. It was found that expression of mtDNMT1 is increased in the absence of p53 [57], and this increase is correlated to increased methylation at the mitochondrial promoters (Figure 1-1) and strand-specific changes in mitochondrial transcription [57]. Specifically, loss of p53 results in an increase in the polycistronic transcript encoding the ND1 and Cox1 sequences (Prashant Thakkar, unpublished data and Figure 2-1). Thus, it appears that cytosine methylation has a different effect on transcription in the mitochondria than in the nucleus.

ND1 and Cox1 encode the core subunits of Complex I and IV of the electron transport chain, respectively. Changes in the expression levels of these proteins could affect oxidative phosphorylation and ATP synthesis by altering the flow of electrons from the mitochondrial matrix to the intermembrane space. An increase in the amounts of ND1 and Cox1 proteins may

be detectable by immunoblotting with specific antibodies. It is also possible to measure mitochondrial respiration in cell cultures by determining the oxygen consumption and extracellular acidification rates using an instrument such as the Seahorse XF (Agilent Technologies). These analyses would allow us to determine what effect changes in mitochondrial DNA methylation might have on cellular energy levels.

The observed changes may be due to the impact of methylation on TFAM binding to promoter DNA (Figure 3-14), as methylation of the promoter sequence increases transcription from HSP1 (Lisa Shock, unpublished data) (Figure 3-16). Methylation of the promoter sequence results in larger TFAM:DNA complexes forming at lower protein concentrations (Figure 3-14), which suggests an increase in cooperativity. This increase in cooperativity may result in increased efficiency in the compaction of mtDNA into nucleoids [25]. The compaction of the mitochondrial genome by different relative amounts of TFAM has been visualized by electron microscopy [25]. Using this method, the degree of compaction achieved by different relative concentrations of TFAM and DNA, methylated and unmethylated, could be compared. Methylation may impact binding in such a way that TFAM is more able to recruit other proteins, which may allow TFAM to more efficiently bring POLRMT and TFB2M to the promoter and initiate transcription. This could be investigated through crosslinking studies described by Morozov et al [26]. TFAM and POLRMT would be allowed to bind to methylated and unmethylated promoter sequences, then crosslinked via photoreactive sites incorporated into the proteins and DNA. The relative efficiency of complex formation could then be analyzed by running the complexes on a gel to visualize differences in size. Crosslinking at different incubation times could provide information regarding how quickly the complexes are formed, and the relative amounts of shifted probe could be used to determine changes in total complexes

formed. Formaldehyde-mediated DNA:protein crosslinking could also be performed in cell culture, and chromatin immunoprecipitation with antibodies specific for components of the mitochondrial transcription initiation complex could be used to test for increased presence of POLRMT and TFB2M at the promoter regions. Based on the *in vitro* data presented in this thesis, increased methylation at the promoter region through increased methyltransferase expression is expected to result in enrichment of the promoter regions in qPCR analysis of POLRMT and TFB2M IPs.

In order to better understand the molecular basis for the effect promoter methylation has on TFAM binding and transcription initiation, recombinant TFAM proteins were expressed in which key residues were replaced with unnatural amino acids (Figures 3-6, 3-8). These unnatural amino acids will be used as vibrational probes for Raman Resonance spectroscopy and crosslinking sites to determine if methylation of DNA results in changes in the protein:DNA interactions.

It is important to try to understand the impact cytosine modification has on mitochondrial transcription because of its critical role in oxidative phosphorylation and normal cellular function. The fact that mtDNMT1 could not be stably overexpressed suggests that regulation of methylation in the mitochondria is important for cell growth and survival (Figure 2-8, 2-9). It appears that cytosine methylation has a different effect on transcription in the mitochondria than in the nucleus, enhancing, rather than reducing gene expression, so further studies will be necessary to better understand the role of DNA modifications in this organelle. Cells expressing a M.SssI construct containing the MLS from TFAM in cell culture will be generated to investigate the effect of increased mitochondrial methyltransferase activity without the loss of p53 through strand-specific transcription assays and analysis of cellular respiration. The effect

of increased TFAM cooperativity on initiation complex assembly will be studied through crosslinking studies, and the molecular basis for the changes observed will be analyzed using proteins containing unnatural amino acids through crosslinking and Raman Resonance spectroscopy.

Literature Cited

Literature Cited

1. Felsenfeld, G; Groudine, M. Controlling the double helix. *Nature* **2003**, *421,* 448-453.

2. Kornberg, RD. Chromatin structure: a repeating unit of histones and DNA. *Science* **1974,** *184,* 868-871.

3. Pfeofer, GP; Szabo, PE. 5-hydroxymethyl cytosine, a modified mammalian DNA base with a potential regulatory role. *Epigenomics* **2009,** *1,* 21-23.

4. Okano, M; Bell, DW; Haber, DA; Li, E. DNA Methyltransferases Dnmt3a and Dnmt3b Are Essential for De Novo Methylation and Mammalian Development. *Cell,* **1999,** *99,* 247-257.

5. Jones, PA; Liang G. Rethinking how DNA methylation patterns are maintained. *Nat Rev Genet.* **2009,** *10,* 805-811.

6. Tahiliani, M; Koh, KP; Shen, Y; Pastor, WA; Bandukwala, H; Brudno, Y; Agarwal, S; Iyer, LM; Liu, DR; Aravind, L; Rao, A. Conversion of 5-methylcytosine to 5-hydroxymethylcytosine in mammalian DNA by MLL partner TET1. *Science* **2009,** *324,* 930-935.

7. Richards, EJ; Elgin, SC. Epigenetic codes for heterochromatin formation and silencing: rounding up the usual suspects. *Cell* **2002,** *108,* 489-500.

8. Satoh, M.; Kuroiwa, T. Organization of multiple nucleoids and DNA molecules in mitochondria of a human cell. *Exp. Cell Res.* **1991**, *196*, 137–140.

9. Iborra, F.J.; Kimura, H.; Cook, P.R. The functional organization of mitochondrial genomes in human cells. *BMC Biol.* **2004**, *2*, 9.

10. Iacobazzi, V; Castegna, A; Infantino, V; Andria, G. Mitochondrial DNA methylation as a next generation biomarker and diagnostic tool. *Molecular Genetics and Metabolism* **2013**, *110*, 25-34.

11. Kasamatsu, H; Vinograd, J. Replication of circular DNA in eukaryotic cells. *Annu. Rev. Biochem.* **1974,** *43,* 695-719.

12. Taanman, JW. The mitochondrial genome: structure, transcription, translation, and replication. *Biochemica et Biophysica Acta* **1999**, *1410,* 103-123.

13. Shadel, GS; Clayton, DA. Mitochondrial DNA maintenance in vertebrates. *Annu. Rev. Biochem.* **1997,** *66,* 409-435.

14. Bonawitz, ND; Clayton, DA; Shadel, GS. Initiation and beyond: multiple functions of the human mitochondrial transcription machinery. *Mol Cell,* **2006,** *24,* 813-825.

15. Ojala, D; Montoya, J; Attardi, G. tRNA punctuation model of RNA processing in human mitochondria. *Nature* **1981,** *290,* 470-474.

16. Cermakian, N; Ikeda, TM; Cedergren, R; Gray, MW. Sequences Homologous to Yeast Mitochondrial and Bacteriophage T3 and T7 RNA Polymerases Are Widespread Throughout the Eukaryotic Lineage. *NAR* **1996,** *24,* 648-654.

17. Shutt, TE; Gray, MW. Homologs of Mitochondrial Transcription Factor B, Sparsely Distributed Within the Eukaryotic Radiation, Are Likely Derived from the Dimethyladenosine Methyltransferase of the Mitochondrial Endosymbiont. *Mol Bio Evol* **2006,** *23,* 1169-1179.

18. Falkenberg, M; Gaspari, M; Rantanen, A; Trifunovic, A; Larsson, NG; Gustafsson, CM. Mitochondrial transcription factors B1 and B2 activate transcription of human mtDNA. *Nature Genetics* **2002,** *31*, 289–294.

19. Seidel-Rogol, BL; McCulloch, V; Shadel, GS. Human mitochondrial transcription factor B1 methylates ribosomal RNA at a conserved stem-loop. *Nat. Genet.* ***2003,*** *33,* 23–24.

20. Cotney, J; Shadel, GS. Evidence for an Early Gene Duplication Event in the Evolution of the Mitochondrial Transcription Factor B Family and Maintenance of rRNA Methyltransferase Activity in Human mtTFB1 and mtTFB2. *J Mol Evol* **2006,** *62,* 707-717.

21. Matsushima, Y; Garesse, R; Kaguni, LS. Drosophila Mitochondrial Transcription Factor B2 Regulates Mitochondrial DNA Copy Number and Transcription in Schneider Cells. *J. Biol. Chem* **2004,** *279*, 26900–5

22. Matsushima, Y; Adan, C; Garesse, R; Kaguni, LS. Drosophila Mitochondrial Transcription Factor B1 Modulates Mitochondrial Translation but Not Transcription or DNA Copy Number in Schneider Cells. *J Biol Chem* **2005,** *280,* 16815–20

23. Ngo, HB; Kaiser, JT; Chan, DC. The mitochondrial transcription and packaging factor Tfam imposes a U-turn on mitochondrial DNA. *Nature Structural and Molecular Biology* **2011,** *18,* 1290-1296.

24. Dairaghi, DJ; Shadel, GS; Clayton, DA. Addition of a 29 Residue Carboxyl-terminal Tail Converts a Simple HMG Box-containing Protein into a Transcriptional Activator. *J Mol Biol* **1995,** *249,* 11-28.

25. Kukat, C; Davies, KM; Wurm, CA; Spåhr, H; Bonekamp, NA; Kühl, I; Joos, F; Polosa, PL; Park, CB; Posse, V; Falkenberg, M; Jakobs, S; Kühlbrandt, W; Larsson, NG. Cross-strand binding of TFAM to a single mtDNA molecule forms the mitochondrial nucleoid. *PNAS* **2015,** *112,* 11288–11293.

26. Morozov, YI; Agaronyan, K; Cheung, AC; Anikin, M; Cramer, P; Temiakov, D. A novel intermediate in transcription initiation by human mitochondrial RNA polymerase. *NAR* **2014,** *42,* 3884-3893.

27. Morozov, YI; Parshin, AV; Agaronyan, K; Cheung, AC; Anikin, M; Cramer, P; Temiakov, D. A model for transcription initiation in human mitochondria. *NAR* **2015,** *43*, 3726-3735.

28. Zollo, O; Tiranti, V; Sondheimer, N. Transcriptional requirements of the distal heavy-strand promoter of mtDNA. *PNAS* **2012,** *109*, 6508-6512.

29. Lodeiro, MF; Uchinda, A; Bestwick, M; Moustafa, IM; Arnold, JJ; Shadel, GS; Cameron, CE. Transcription from the second heavy-strand promoter of human mtDNA is repressed by transcription factor A in vitro. *PNAS* **2012**, *109*, 6513-6518.

30. Kukat, C; Larsson, NG. mtDNA makes a U-turn for the mitochondrial nucleoid. *Trends Cell Bio* **2013,** *23*, 457-463.

31. 5. Kruse, B; Narasimhan, N; Attardi, G. Termination of transcription in human mitochondria: Identification and purification of a DNA binding protein factor that promotes termination. *Cell* **1989,** *58*, 391-397.

32. Terzioglu, M; Ruzzenente, B; Harmel, J; et al. MTERF1 binds mtDNA to prevent transcriptional interference at the light-strand promoter but is dispensable for rRNA gene transcription regulation. *Cell Metab* **2013**, *17*, 618–626.

33. Fuste, JM; Wanrooij, S; Jemt, E; Granycome, CE; Cluett, TJ; Shi, Y; Atanassova, N; Holt, IJ; Gustafsson, CM; Falkenberg, M. Mitochondrial RNA polymerase is needed for activation of the origin of light-strand DNA replication. *Mol Cell* **2010,** *37*, 67-78.

34. McKinney, EA; Oliveira, MT. Replicating animal mitochondrial DNA. *Genetics and Molecular Biology* **2013,** *36*, 308-315.

35. Robberson, DL; Kasamatsu, H; Vinograd, J. Replication of mitochondrial DNA. Circular replicative intermediates in mouse L cells. *Proc Natl Acad Sci USA* **1972**, *69*, 737-741.

36. Bogenhagen, D; Gillum, AM; Martens, PA; Clayton, DA. Replication of mouse L-cell mitochondrial DNA. *Cold Spring Harb Symp Quant Biol* **1979**, *43*, 253-262.

37. Bogenhagen, DF; Clayton, DA. The mitochondrial DNA replication bubble has not burst. *Trends Biochem Sci* **2003**, *28*, 357-360.

38. Yang, MY; Bowmaker, M; Reyes, A; Vergani, L; Angeli, P; Gringeri, E; Jacobs, HT; Holt, IJ. Biased incorporation of ribonucleotides on the mitochondrial L-strand accounts for apparent strand-asymmetric DNA replication. *Cell* **2002**, *111*, 495-505.

39. Yasukawa, T; Reyes, A; Cluett, TJ; Yang, MY; Bowmaker, M; Jacobs, HT; Holt, IJ. Replication of vertebrate mitochondrial DNA entails transient ribonucleotide incorporation throughout the lagging strand. *EMBO J* **2006**, *25*, 5358-5371.

40. Holt, IJ; Lorimer, HE; Jacobs, HT. Coupled leading- and lagging-strand synthesis of mammalian mitochondrial DNA. *Cell* **2000**, *100*, 515-524.

41. Ekstrand, MI; Falkenberg, M; Rantanen, A; Park, CB; Gaspari, M; Hultenby, K; Rustin, P; Gustafsson, CM; Larsson, NG. Mitochondrial transcription factor A regulates mtDNA copy number in mammals. *Hum Mol Genet* **2004**, *13*, 935–944.

42. Pohjoismäki, JL; Wanrooij, S; Hyvärinen, AK; Goffart, S; Holt, IJ; Spelbrink, JN; Jacobs, HT. Alterations to the expression level of mitochondrial transcription factor A, TFAM, modify the mode of mitochondrial DNA replication in cultured human cells. *Nucleic Acids Res* **2006**, *34*, 5815–5828.

43. Farge, G; Mehmedovic, M; Malayon, M; Wildenberg, SMJL; Roos, WH; Gustafsson, CM; Wuite, GJL; Falkenberg, M. In vitro-reconstituted nucleoids can block mitochondrial DNA replication and transcription. *Cell Reports* **2014**, *8*, 66-74.

44. Vanyushin, BF; Kiryanov, GI; Kudryashova, IB; Belozersky, AN. DNA-methylase in loach embryos (Misgurnus fossilis). *FEBS Lett,* **1971,** *15,* 313-316.

45. Nass, MMK. Differential methylation of mitochondrial and nuclear DNA in cultered mouse, hamster, and virus-transformed hamster cells *in vivo* and *in vitro* methylation. *J. Mol. Biol.* **1973,** *80,* 155-175.

46. Vanyushin, BF; Kirnos, MD. The nucleotide composition and pyrimidine clusters in DNA from beef heart mitochondria. *FEBS Lett,* **1974,** *39,* 195-199.

47. Dawid, IB. 5-methylcytidylic acid: absence from mitochondrial DNA of frogs and HeLa cells. *Science,* **1974,** *184,* 80-81.

48. Bummings, DJ; Tait, A; Goddard, JM. Methylated bases in DNA from *Paramecium aurelia. Biochimica et Biophysica Acta,* **1974,** *374,* 1-11.

49. Pollack, Y; Kasir, J; Shemer, R; Metzger, S; Szyf, M. Methylation pattern of mouse mitochondrial DNA. *Nucleic Acids Research,* **1984,** *12,* 4811-4824.

50. Cardon, LR; Burge, C; Clayton, DA; Karlin, S. Pervasive CpG suppression in animal mitochondrial genomes. *Proc. Natl. Acad. Sci. USA,* **1994,** *91,* 3799-3803.

51. Bestor, TH. The DNA methyltransferases of mammals. *Hum. Mol. Genet.* **2000,** *9,* 2395-2402.

52. Yoder, JA; Soman, N; Verdine, GV; Bestor, TH. DNA methyltransferases in mouse tissues and cells. Studies with a mechanism-based probe. *J. Mol. Biol.* **1997**, *270*, 385–395.

53. Okano, M; Bell, DW; Haber, DA; Li, E. DNA methyltransferases Dnmt3a and Dnmt3b are essential for de novo methylation and mammalian development. *Cell* **1999,** *99,* 247–257.

54. Egger, G; Jeong, S; Escobar, SG; Cortez, CC; Li, TW; Saito, Y; Yoo, CB, Jones, PA, Liang, G. Identification of DNMT1 (DNA methyltransferase 1) hypomorphs in somatic knockouts suggests an essential role for DNMT1 in cell survival. *PNAS* **2006,** *103,* 14080-14085.

55. Li, E; Bestor, TH; Jaenisch, R. Targeted mutation of the DNA methyltransferase gene results in embryonic lethality. *Cell* **1992**, *69*, 915–926.

56. T. Chen, S. Hevi, F. Gay, N. Tsujimoto, T. He, B. Zhang, Y. Ueda, E. Li. Complete inactivation of DNMT1 leads to mitotic catastrophe in human cancer cells. *Nat. Genet.* **2007**, *39*, 391–396.

57. Shock, LS; Thakkar, PV; Peterson, EJ; Moran, RG; Taylor, SM. DNA methyltransferase 1, cytosine methylation, and cytosine hydroxymethylation in mammalian mitochondria. *PNAS*, **2011,** *108*, 3630-3635.

58. Peterson, EJ; Bögler, O; Taylor, SM. p53-mediated repression of DNA methyltransferase 1 expression by specific DNA binding. *Cancer Res* **2003,** *63*, 6579-6582.

59. Tahiliani, M; Koh, KP; Shen, Y; Pastor, WA; Bandukwala, H; Brudno, Y; Agarwal, S; Iyer, LM; Liu, DR; Aravind, L; Rao, A. Coversion of 5-Methylcytosine to 5-Hydroxymethylcytosine in mammalian DNA by MLL partner TET1. *Science*, **2009,** *324*, 930-935.

60. Bellizzi, D; D'Aquila, P; Scafone, T; Giordano, M; Riso, V; Riccio, A; Passarino, G. The control region of mitochondrial DNA shows an unusual CpG and non-CpG methylation pattern. *DNA Research*, **2013,** *20*, 537-547.

61. Dzitoyeva, S; Chen, H; Manev, H. Effect of aging on 5-hydroxymethylcytosine in brain mitochondria. *Neurobiol Aging*, **2012,** *33*, 2881-2891.

62. Chestnut, BA; Chang, Q; Price, A; Lesuisse, C; Wong, M; Martin, LJ. Epigenetic regulation of motor neuron cell death through DNA methylation. *J Neurosci.* **2011,** *31*, 16619-16636.

63. Nan, X; Ng, HH; Johnson, CA; Laherty, CD; Turner, BM; Eisenman, RN; Bird, A. Transcriptional repression by the methyl-CpG-binding protein MeCP2 involves a histone deacetylase complex. *Nature* **1998,** *393*, 386-389.

64. Lei, H; Oh, SP; Okano, M; Juttermann, R; Goss, KA; Jaenisch, R; Li, E. De novo DNA cytosine methyltransferase activities in mouse embryonic stem cells. *Development* **1996,** *122*, 3195-3205.

65. Okano, M; Bell, DW; Haber, DA; Li, E. DNA Methyltransferases Dnmt3a and Dnmt3b

Are Essential for De Novo Methylation and Mammalian Development. *Cell* **1999,** *99*, 247-257.

66. Hazkani-Covo, E; Covo, S. Numt-Mediated Double-Strand Break Repair Mitigates

Deletions during Primate Genome Evolution. *PLoS Genetics* **2008,** *4*, e1000237

67. Ramos, A; et al. Nuclear insertions of mitochondrial origin: Database updating and usefulness in cancer studies. *Mitochondrion* **2011,** *11*, 946-953.

68. Tucker, KL. Methylated Cytosine and the Brain: A New Base for Neuroscience. *Neuron* **2001**, *30*, 649–652.

69. Lebedeva, MA; Eaton, JS; Shadel, GS. Loss of p53 causes mitochondrial DNA depletion and altered mitochondrial reactive oxygen species homeostasis. *BBA Bioenergetics* **2009,** *1787*, 328-334.

70. Chatfield, KC et al. Mitochondrial energy failure in HSD10 disease is due to defective mtDNA transcript processing. *Mitochondrion* **2015,** *21,* 1-10.

71. Yakubovskaya, E; Mejia, E; Byrnes, J; Hambardjieva, E; Garcia-Diaz, M. Helix unwinding and base flipping enable human MTERF1 to terminate mitochondrial transcription. *Cell* **141,** *2010,* 982-993.

72. Nathan, D; Crothers, DM. Bending and flexibility of methylated and unmethylated EcoRI DNA. *Journal of Molecular Biology* **2002,** *316,* 7-17.

73. Severin, PMD; Zou, X; Gaub, HE; Schulten, K. Cytosine methylation alters DNA mechanical properties. *NAR* **2011,** *39,* 8740-8751.

74. Moerke, NJ. Fluorescence Polarization (FP) Assays for Monitoring Peptide-Protein or Nucleic Acid-Protein Binding. *Current protocols in Chemical Biology* **2009,** *1,* 1-15.

75. Young, TS; Ahmad , I; Yin, JA; Schultz, PG. An Enhanced System for Unnatural Amino Acid Mutagenesis in E. coli. *Journal of Molecular Biology* **2010**, *395,* 361-374.

76. Kauer, JC; Erickson-Viitanen, S; Wolfe, HR; DeGrado, WF. Benzoyl-L-phenylalanine: A New Photoreactive Amino Acid. *Journal of Biological Chemistry* **1986,** *261,* 10695-1070.

77. Weeks, CL; Polishchuk, A; Getahun, Z; Degrado, WF; Spiro, TG. Investigation of an unnatural amino acid for use as a resonance Raman probe: Detection limits, solvent and temperature dependence of the νC≡N band of 4-cyanophenylalanine. *J Raman Spectrosc* **2008,** *39,* 1606-1613.

78. Ngo, HB; Lovely, GA; Phillips, R; Chan, DC. Distinct structural features of TFAM drive mitochondrial DNA packaging versus transcriptional activation. *Nat Commun* **2014,** *5,* DOI: 10.1038/ncomms4077.

79. Gangelhoff, TA; Mungalachetty, PS; Nix, JC; Churchill, ME. Structural analysis and DNA binding of the HMG domains of the human mitochondrial transcription factor A. *NAR* **2009,** *37,* 3153-3164.

80. Kukat, C; Wurm, CA; Spåhr, H; Falkenburg, M; Larsson, N; Jakobs, S. Super-resolution microscopy reveals that mammalian mitochondrial nucleoids have a uniform size and frequently contain a single copy of mtDNA. *PNAS* **2011,** *108,* 13534-13539.

81. Mittelstaet, J; Konevega, AL; Rodnina, MV. A Kinetic Safety Gate Controlling the Delivery of Unnatural Amino Acids to the Ribosome. *J. Am. Chem. Soc.* **2013,** *135,* 17031–17038.

82. Martin, M; Cho, J; Cesare, AJ; Griffith, JD; Attardi, G. Termination Factor-Mediated DNA Loop between Termination and Initiation Sites Drives Mitochondrial rRNA Synthesis. *Cell* **2005,** *123,* 1227-1240.

Appendix 1

Table 1-1: PCR primers for stand-specific polycistronic transcription analysis

Mouse			
	Forward Primer	Reverse Primer	Annealing Temp
ATP6 (cDNA synthesis)	5'-ATTCCCATCCTCAAAACGCC-3'	5'-TGTTGGAAAGAATGGAGACGGT-3'	50˚C
16S rRNA	5'-TCTCTGTTAACCCAACACCGGAATGC-3'	5'-GGACTAGCATGAACGGCTAAACGA-3'	55˚C
ND1	5'-CAGGATGAGCCTCAAACTCCA-3'	5'-CGGCTCGTAAAGCTCCGA-3'	52˚C
COX1	5'-TCGCAATTCCTACCGGTGTC-3'	5'-CGTGTAGGGTTGCAAGTCAGC-3'	53˚C
18S rRNA	5'-GTCTGTGATGCCCTTAGATG-3'	5'-AGCTTATGACCCGCACTTAC-3'	50˚C
Human			
	Forward Primer	Reverse Primer	Annealing Temp
16s rRNA	5′-ACCTTACTACCAGACAACCTTAGCC-3′	5′-TAGCTGTTCTTAGGTAGCTCGTCTGG-3′	50˚C
ND1	5′-TGCGAGCAGTAGCCAAACAAT-3′	5′-TGATGGCAGGAGTAATCAGAGG-3′	52˚C
ATP6	5′-ATTCAACCAATAGCCCTGGCCG-3′	5′-ACGTAGGCTTGGATTAAGGCGAC-3′	55˚C
GAPDH	5'-CCACGTGGTCTCCTCTGACTTC-3'	5'-TTGGAGGCCATGTGGGCCATGA-3'	55˚C
Actin	5'-TTCTCACTGGTTCTCTCTTCTGCC-3'	5'-ACCTACTTAATACACACTCCAAGGC-3'	53˚C

Table 1-2: PCR primers for gene-specific strand-specific cDNA synthesis and PCR

	cDNA synthesis	qPCR	Annealing Temp
16s rRNA	5'-AAAAGAGGGACAGCTCTTCTGGAACG-3'	5'-TCTCTGTTAACCCAACACCGGAATGC-3'	60˚C
	5'-CGGACCAAGTTACCCTAGGGATAA-3'	5'-GGACTAGCATGAACGGCTAAACGA-3'	
ND1	5'-TAATCGCCATAGCCTTGGTAACATTAG-3'	5'-GGTCCATACGGCATTTTACAACC-3'	50˚C
	5'-TTAATGGGTGTGGTATTGGTAGGG-3'	5'-CTAGTGTGAGTGATAGGGTAGGTG-3'	
Cox1	5'-TCGTAACTGCCCATGCTTT-3'	5'-CCCTTCATTTAGCTGGAGTGT-3'	57˚C
	5'-GTGTAAGCATCTGGGTAGTCTG-3'	5'-GGTTGCGGTCTGTTAGTAGTATAG-3'	
18s	Random hexamers	5'-GTCTGTGATGCCCTTAGATG-3'	50˚C
	Random hexamers	5'-AGCTTATGACCCGCACTTAC-3'	

Table 1-3: Optimal antibody conditions

Antibody	Manufacturer	Species	Blocking Buffer	Primary Dilution	Secondary Dilution	Secondary Antibody	Protein Size (kDa)
VDAC	Sigma	Rabbit	StartingBlock	1:4,000	1:10,000	Goat antirabbit	32
$H3K4me^3$	Upstate Biotechnology	Rabbit	StartingBlock	1:2,000	1:15,000	Goat antirabbit	17
TFAM	Abcam	Rabbit	StartingBlock	1:10,000	1:10,000	Goat antirabbit	25
p53	Calbiochem	Mouse	StartingBlock	1:1,000	1:2,000	Goat antimouse	53
V5	Invitrogen	Mouse	StartingBlock	1:500	1:30,000	Goat antimouse	Varies

Table 2-1: Probes used in binding studies and transcription assays. Single strand of complimentary pair shown

Termination probe	5'- AGAACAGGGTTTGTTAAGATGGCAGAGCCCGGTAATCGCATAAA-3'
HSPxTFAM	5'- CCGCTGCTAACCCCATACCCCGAACCAACCAAACCCCAAAGACACCCGC-3'
HSPxTFAM ΔCG1	5'- CCCCTGCTAACCCCATACCCCGAACCAACCAAACCCCAAAGACACCCGC-3'
HSPxTFAM ΔCG2	5'- CCGCTGCTAACCCCATACCCCCAACCAACCAAACCCCAAAGACACCCGC-3'
HSPxTFAM ΔCG1+2	5'- CCCCTGCTAACCCCATACCCCCAACCAACCAAACCCCAAAGACACCCGC-3'
HSPtranscription	5'-CCATCCTACCCAGCACACACACACCGCTGCTAACCCCATACCCCGAAC CAACCAAACCCCAAAGATAAAATTTGTGGGCC-3'
HSPtranscription ΔCG1	5'-CCATCCTACCCAGCACACACACACCCCTGCTAACCCCATACCCCGAAC CAACCAAACCCCAAAGATAAAATTTGTGGGCC-3'
HSPtranscription ΔCG2	5'-CCATCCTACCCAGCACACACACACCGCTGCTAACCCCATACCCCCAAC CAACCAAACCCCAAAGATAAAATTTGTGGGCC-3'
HSPtranscription ΔCG1+2	5'-CCATCCTACCCAGCACACACACACCCCTGCTAACCCCATACCCCCAAC CAACCAAACCCCAAAGATAAAATTTGTGGGCC-3'

Appendix 2

Reverse transcription

Cell culture

- Plate cells into a 150 mm dish
- 48 hours before isolating RNA, feed the cells
- 24 hours before isolating RNA, split the cells into 2x150 mm dishes

Isolating RNA with TRIzol

- Wash the cells twice with PBS
- To each plate, add 4 mL of TRIzol
- Incubate for 5 minutes at room temp
- Pipet up and down, then transfer the TRIzol from both plates into a 15 mL conical tube
- Add 1.6 mL of chloroform and shake for 15 seconds
- Incubate at room temp for 3 minutes and centrifuge for 15 minutes at 12,000xg at 4^oC
- Transfer the aqueous (colorless) layer to a new tube and add an equal volume of chloroform
- Centrifuge for 15 minutes at 12,000xg at 4^oC
- Transfer the aqueous layer to a new tube
- Add 4 mL of isopropanol, mix, and incubate for 10 minutes at room temp
- Centrifuge for 10 minutes at 12,000xg at 4^oC
- Wash the pellet with 1 mL of 75% ethanol and centrifuge at 7,500xg at 4^oC for 5 minutes
- Air dry for 5 minutes at room temp, then resuspend in 50 uL HPLC H_2O
- Determine the RNA concentration using the NanoDrop

Reverse transcription with SuperScript III RT

- Mix the following for each reverse transcription primer x2 (one with RT and one no RT control)
    - 1 ug of RNA
    - 1 uL of a 2 uM primer dilution or 1 uL of random hexamers for control reactions
    - 1 uL 10 mM dNTP mix
    - HPLC H_2O to 10 uL
- Incubate at 65^oC for 5 minutes, then place on ice for at least 1 minute

- For each reaction, mix
    - 2 uL 10x RT buffer
    - 4 uL 25 mM $MgCl_2$
    - 2 uL 0.1 M DTT
    - 1 uL RNaseOUT
- Add 9 uL of the above mixture to the RNA mixtures
    - To the reverse transcription reactions, add 1 uL SuperScript III RT
    - To the negative controls, add 1 uL HPLC H_2O
- For random hexamer primed reactions, incubate at 25^oC for 10 minutes
- Incubate all reactions for 50 minutes at 50^oC
- Terminate the reactions at 85^oC for 5 minutes, then cool the reactions on ice
- Add 1 uL RNase H to each reaction and incubate at 37^oC for 20 minutes
- Store at -20^oC

End-point PCR

- Set up a PCR reaction for each reverse transcription reaction and no RT control + 1 no DNA control
- Mix
    - 12.5 mL HotStarTaq master mix
    - 1 uL forward primer
    - 1 uL reverse primer
    - 9.5 uL HPLC H_2O
    - 1 uL template or HPLC H_2O
- PCR cycling conditions
    1. 95 ^oC for 15 minutes
    2. 95 ^oC for 30 seconds
    3. Annealing temp (Primer melting temp - 5 ^oC) for 30 seconds
    4. 72 ^oC for 1 minute
    5. Go to step 2 39 times
    6. 72 ^oC for 5 minutes
    7. 4 ^oC forever
- Make a 1% Agarose gel with 1x TAE by mixing 0.5g agarose with 50 mL 1x TAE and microwaving to dissolve
- Add 3 uL EtBr to the gel mix and cast the gel
- Mix 5 uL of each PCR reaction with 1 uL 6x loading dye and load it onto the gel with 5 uL DNA ladder
- Run at 100V for 50 minutes and visualize on the UV box
- Bands should be present in the cDNA synthesis reactions with RT, but not in the reactions without RT or the H_2O reactions

qPCR

- Mix the qPCR reactions as the end-point reactions using the reverse transcribed samples and water controls
    - Use 12.5 uL Qiagen SybrGreen master mix
    - Prepare each reaction in triplicate

- PCR cycling conditions
    - 95 ^{o}C for 15 minutes
    - 95 ^{o}C for 30 seconds
    - Annealing temp (Primer melting temp - 5 ^{o}C) for 30 seconds
    - 72 ^{o}C for 1 minute
    - Go to step 2 39 times
    - 72 ^{o}C for 5 minutes
    - Melting curve: 40 ^{o}C-90 ^{o}C, hold for 1 second, read every 1 ^{o}C

Cell Fractionation

Cell culture

- Plate cells into a 150 mm dish
- 48 hours before cell fractionation, feed the cells
- 24 hours before cell fractionation, split the cells into 2x150 mm dishes

Fractionation

- Wash the cells 2x with cold PBS
- Scrape the cells and transfer them into a 15 mL conical tube – take 5% off and transfer it to a microfuge tube
- Spin the 5% of cells at 900xg at 4^{o}C for 5 minutes to pellet and resuspend in 5x weight/volume of SDS lysis buffer (example: 50 mg = 250 uL SDS lysis buffer)
- Spin the remaining cells at 900xg at 4^{o}C for 5 minutes to pellet and resuspend in 3 mL of mitochondrial homogenization buffer (0.25 M sucrose, 10 mM Tris-HCl, pH 7.0, 1 mM EDTA, pH 6.8) with protease inhibitors – add half a protease inhibitor cocktail tablet per 12.5 mL buffer
- Transfer resuspended cells to a dounce homogenizer on ice and incubate for 5 minutes
- Homogenize with 15 strokes, transfer to a 15 mL conical tube and centrifuge at 900xg at 4^{o}C for 5 minutes to pellet unbroken cells
- Transfer the supernatant to a new 15 mL conical tube labeled “post nuclear soup”
- Resuspend the pellet in 3 mL of homogenization buffer and repeat the homogenization and centrifugation twice more

Nuclear isolation

- Resuspend homogenized cells in 3 mL nuclear buffer (0.25 M sucrose, 10 mM $MgCl_2$)
- Layer the resuspended cells over 3 mL sucrose cushion (0.88 M sucrose, 0.5 mM $MgCl_2$)
- Spin at 2800xg for 5 minutes
- Resuspend pelleted nuclei in 5x weight/volume SDS lysis buffer

Mitochondrial isolation

- Spin the “post nuclear soup” at 900xg at 4^{o}C for 5 minutes
- Transfer supernatant to a 14 mL round bottom tube, leaving a couple mL behind to avoid contamination

- Spin the supernatant at 10,000xg for 15 minutes at 4^{o}C
- Transfer the supernatant to a new tube to isolate cytosolic proteins
- Wash the mitochondrial pellet with 1 mL of mitochondrial homogenization buffer without protease inhibitors
- Resuspend the pellet in 20x weight/volume Trypsin digestion buffer (10 mM HEPES-KOH, pH 7.4, 0.25 M sucrose, 0.5 mM EGTA, 2 mM EDTA, 1mM DTT)
- Add Trypsin-EDTA to 10 ug/mL and incubate for 20 minutes at room temp
- Add Bovine Trypsin inhibitor to 10 ug/mL and incubate on ice for 10 minutes
- Pellet the mitochondria by spinning at 10,000xg for 10 minutes at 4^{o}C
- Wash the pellet twice with 1 mL of mitochondrial homogenization buffer with protease inhibitors
- Resuspend the mitochondria in 10x weight/volume SDS lysis buffer

Cytoplasmic protein isolation

- To 5 mL of the saved mitochondrial supernatant, add 5 mL 20% TCA
- Incubate on ice for 20 minutes
- Spin at 6,000xg for 15 minutes
- Wash the pellet 3 times with 100% acetone, spinning at 6,000xg for 5 minutes
- Air dry the pellet on ice for 5 minutes
- Resuspend the pellet in 10x weight/volume SDS lysis buffer

Immunoblots

Bradford assay

- Turn on the spectrophotometer
- Add 35 uL BSA to 35 uL H_2O and mix
- Add water, lysis buffer, then BSA or sample to a glass borosilicate tube – prepare each mixture in duplicate

Sample	Sample Volume	Water	Lysis Buffer
BSA	0	799	1
BSA	2	797	1
BSA	4	795	1
BSA	6	793	1
BSA	8	791	1
BSA	10	789	1
Lysate	1	799	0

- Add 200 uL Biorad dye to each of the mixtures and mix by flicking them tube
- Incubate at room temp for 15 minutes
- Transfer samples into a plastic microcuvette and read the absorbance at 595 nm using both UV and visible on the spectrophotometer– re-use the microcuvette to reduce cost
- Use the slope of the standard curve to calculate the concentration of the lysates

Casting a gel

- Make fresh 10% APS by mixing 50 mg ammonium persulfate into 500 uL H_2O
- Mix the following reagents in a 50 mL conical tube (volumes are in mL)

Reagent	5% gel	10% gel	12% gel
H_2O	13	11.5	10.2
1.5 M Tris-HCl, pH 8.8	6	6	6
40% acrylamide 37.5:1	4.5	6	7.2
10% SDS	0.24	0.24	0.24
10% APS	0.24	0.24	0.24

- Using a stopper attached the vacuum flask tubing, de-gas the gel mixture for 10 minutes
- Clean the front and back gel plates (use 1.5mm plates for immunoblots) with 70% ethanol and assemble the casting apparatus
- Use parafilm on the grey foam part of the clamp to seal the bottom of the gel plates
- Test the seal with water and use Whatman paper to remove the water
- Add 24 uL of TEMED to the gel mixture, then pipet 8 mL into the gel plates
- Add 500 mL water-saturated butanol to the top of the gel and allow it to polymerize
- Mix the 4% stacking gel – volumes are in mL

Reagent	4% gel
H_2O	2.14
0.5 M Tris-HCl, pH 6.8	1.26
40% acrylamide 37.5:1	0.5
10% SDS	0.05
10% APS	0.05

- Using a stopper attached the vacuum flask tubing, de-gas the gel mixture for 10 minutes
- Use a Chemwipe to remove the butanol from the top of the resolving gel
- Add 5 uL of TEMED to the stacking gel mixture and mix
- Fill the remaining space between the gel plates with staking gel, then insert the comb at an angle so the bubbles can escape
- Allow the stacking gel to polymerize, then wrap in wet paper towels and cling film for storage at 4^oC for up to 3 days

Sample preparation

- Make Laemmli sample buffer by adding 25 uL BME to 475 uL Biorad Laemmli and vortexing
- Dilute lysates 1:1 in Laemmli sample buffer and adjust the samples to equal volume with SDS lysis buffer
- Boil the samples for 5 minutes, then spin the samples down
- Do not place the samples back on ice after boiling

SDS-PAGE

- Make 1L of 1x PAGE running buffer by adding 200 mL 5x Running buffer (30.2g Tris Base, 188g glycine, 10g SDS in 2L of ddH_2O) to 800 mL H_2O

- Clamp the gel(s) into the electrophoretic frame and place the unit in a gel box
- Fill the space within the frame completely with 1x running buffer, and fill the rest of the box about halfway
- Remove the comb and rinse the wells
- Load the boiled samples, along with 5 uL Biorad Precision Plus Dual Color marker
- Place the lid on the box and run the gels for ~1 hour (or until the dye front reaches the bottom of the gels) at 150V

Wet Transfer

- Prepare 1x Transfer buffer
    - 100 mL 10x Transfer buffer (16.879g Tris HCl, 17.299g Tris Base, 144.314g glycine, 10g SDS)
    - 200 mL MeOH
    - 700 mL H_2O
- Pour ~500 mL into a transfer box, place it in the cold room, and soak 2 sponges
- Wash the gel(s) with water, then equilibrate in ~50 mL of transfer buffer in the cold room for 15 minutes
- Cut a piece of PVDF slightly smaller than the front gel plate, soak it in MeOH for 1 minute, wash it in ddH_2O for 2 minutes, then equilibrate in ~50 mL of transfer buffer in the cold room for 15 minutes
- Assemble the transfer sandwich
    - Open a transfer plate and place it on the bench with the black side down
    - Place a wet sponge on top of the black plate and roll out the bubbles
    - Place 3 sheets of soaked Whatman paper, one at a time, on the sponge and roll out the bubbles
    - Float the gel onto the third sheet of Whatman paper
    - Place the membrane on the gel and roll out the bubbles
    - Place 3 sheets of soaked Whatman paper, one at a time, on the membrane and roll out the bubbles
    - Put the second sponge on top and close the plate
- Insert the plate into the transfer apparatus with the black plate facing the black side of the apparatus
- Place the apparatus into the cold box with a frozen spacer and a stir bar and fill the box with transfer buffer
- Put on the lid and run at 100V for one hour, on ice and with stirring
- After the transfer, disassemble the sandwich
- To check the transfer, soak the membrane in MeOH for one minute, then stain it with Ponceau S
    - Add Ponceau S to the membrane and shake until bands are visible
    - Rinse with ddH_2O until the background is white
- Check the gel for complete transfer by rinsing it with ddH_2O and staining with Coomassie

Probing the membrane

- Block the membrane in StartingBlock overnight at 4^{o}C or for 1 hour at room temp with gentle rocking
- Cut the membrane into the appropriate strips for the proteins of interest with a razor blade and the front plate for a gel as a straight edge
- Place the primary antibody dilution on the membrane for 1 hour at room temp with gentle rocking
- Remove the primary antibody and save it for future use
- Wash three times with TBS-T for 5 minutes with vigorous rocking
- Dilute the secondary antibody in the StartingBlock used to block the membrane
- Place the secondary antibody dilution on the membrane for 1 hour at room temp with gentle rocking
- Wash three times with TBS-T for 10 minutes with vigorous rocking
- Transfer membrane pieces to a dry container
- Mix 200 uL each of the two ECL reagents (SuperSignal West Dura) and pipet dropwise onto the membrane
- Incubate covered with foil for 5 minutes, then wrap in cling flim and develop using film or the Licor

mTERF Expression and purification

Growth of mTERF-expressing HMS174 cells

- Mix 25 uL Competent HMS174 cells with 50 ng of mTERF-pET32XT
- Incubate on ice for 5 minutes
- Heat shock at 42^{o}C for 30 minutes
- Incubate on ice for 2 minutes
- Add 125 uL SOC and incubate with 200 rpm shaking for 1 hour
- Plate onto an LB agar plate containing 50 ug/mL Carbenicillin
- Incubate overnight at 37^{o}C
- Pick a colony and inoculate 5 mL of LB media containing 50 ug/mL Carbenicillin
- Grow the 5 mL culture overnight at 37 degrees C with 250 rpm shaking
- Add the 5 mL culture to 95 mL of LB containing 50 ug/mL Carbenicillin
- Grow the 100 mL culture at 37 degrees C with 250 rpm shaking until it reaches an OD_{600} of 0.5 relative to a blank consisting of the growth media used for the 100 mL culture
- Split the 100 mL into 2x50 mL cultures, with one serving as an uninduced control
- Add IPTG to the induced culture to a final concentration of 1 mM
- Incubate culture with shaking at 20 degrees C for 18 hours
- After 18 hours, spin down the cells at 4000 x g for 10 minutes and discard the growth media

Lysis

- Weigh the cell pellets and resuspend in NiNTA lysis buffer (50 mM sodium phosphate, 300 mM NaCl) using 5 mL for every gram of pellet wet weight

- Add lysozyme to a final concentration of 1 mg/mL and incubate on ice for 30 minutes
- Lyse the cells on ice using a microtip sonicator on high for 3 minutes total sonication time – 45 seconds on, 3 minutes off
- Clear the lysate by spinning at 30,000xg for 30 minutes at 4^{o}C
- Transfer the soluble fraction (the supernatant) to a new tube and resuspend the pellet in an amount of 6M urea equal to the volume of the soluble fraction

NiNTA column purification

- Add 1 mL of 50% NiNTA resin slurry for every 4 mL of soluble fraction
- Incubate lysate/slurry mix with rotation in the cold room for 1 hour
- Add the lysate/slurry mix to a 10 mL plastic column and collect the flowthrough
- Wash the resin twice with ½ the starting lysate volume (or twice the 50% slurry volume) with lysis buffer +20 mM imidazole – collect the washes
- Elute the protein with ¼ the starting lysate volume of lysis buffer + 250 mM imidazole

TFAM Expression and purification

Growth of TFAM-expressing HMS174 cells

- Mix 25 uL Competent HMS174 cells with 50 ng of WT TFAM-pET28 or 300 ng mutant TFAM-pET28 and 300 ng of pEVOL plasmid for the desired unnatural amino acid
- Incubate on ice for 5 minutes
- Heat shock at 42^{o}C for 30 minutes
- Incubate on ice for 2 minutes
- Add 125 uL SOC and incubate with 200 rpm shaking for 1 hour
- Plate onto an LB agar plate containing the appropriate antibiotic(s) – 50 ug/mL Kanamycin for WT or 50 ug/mL Kanamycin and 25 ug/mL Chloramphenicol for mutants
- Incubate overnight at 37^{o}C
- Pick a colony and inoculate 5 mL of LB media containing the same antibiotics
- Grow the 5 mL culture overnight at 37 degrees C with 250 rpm shaking
- Add the 5 mL culture to 95 mL of LB containing the appropriate antibiotics and, for the mutants, a 0.5 mM concentration of the unnatural amino acid
- Grow the 100 mL culture at 37 degrees C with 250 rpm shaking until it reaches an OD_{600} of 0.5 relative to a blank consisting of the growth media used for the 100 mL culture
- Split the 100 mL into 2x50 mL cultures, with one serving as an uninduced control
- Add IPTG to the induced culture to a final concentration of 1 mM for WT. For the mutants, also add arabinose to a 0.2% final concentration
- Incubate culture with shaking at 20 degrees C for 18 hours
- After 18 hours, spin down the cells at 4000 x g for 10 minutes and discard the growth media

Lysis

- Weigh the cell pellets and resuspend in NiNTA lysis buffer (50 mM sodium phosphate, 300 mM NaCl) using 5 mL for every gram of pellet wet weight
- Add lysozyme to a final concentration of 1 mg/mL and incubate on ice for 30 minutes
- Lyse the cells on ice using a microtip sonicator on high for 3 minutes total sonication time – 45 seconds on, 3 minutes off
- Clear the lysate by spinning at 30,000xg for 30 minutes at 4^{o}C
- Transfer the soluble fraction (the supernatant) to a new tube and resuspend the pellet in an amount of 6M urea equal to the volume of the soluble fraction

NiNTA column purification

- Add 1 mL of 50% NiNTA resin slurry for every 4 mL of soluble fraction
- Incubate lysate/slurry mix with rotation in the cold room for 1 hour
- Add the lysate/slurry mix to a 10 mL plastic column and collect the flowthrough
- Wash the resin twice with ½ the starting lysate volume (or twice the 50% slurry volume) with lysis buffer +20 mM imidazole – collect the washes
- Elute the protein with ¼ the starting lysate volume of lysis buffer + 250 mM imidazole
- For the FPLC nickel column, the buffers are the same, but the wash is run until the Abs_{280} reaches baseline and the elution is run until the Abs_{280} reaches baseline, so the volumes vary.

EnrichS 5x50 mm column purification – 1 mL column volume

- Dialyze the elution fraction from an NiNTA column overnight in the cold room into 50 mM Hepes, pH 7.0, 50 mM NaCl, 1 mM DTT (Gangelhoff et al, 2009, NAR) – use at least 10x the elution fraction volume and change the dialysis buffer 2x
- Equilibrate the column with 5mL of the above buffer
- Load the dialyzed elution fraction onto the column and wash with 3 mL of the above buffer – collect the flowthrough and wash
- Run a 15 mL gradient from the starting 50 mM NaCl concentration to the above buffer + 0.5 M NaCl – collect 1 mL fractions
- Run 3 mL of the above buffer + 1 M NaCl to remove any remaining protein – collect this

Methylating and testing DNA

Annealing binding oligos

- Resuspend oligos in HPLC H_2O to 100 uM
- Mix 20 uL of each of the complimentary oligos
- Heat to 95^{o}C for 5 minutes
- Allow the mix to cool to room temperature on the bench
- Measure DNA concentration on the NanoDrop

Methylation reaction

- Dilute SAM from stock
    - SAM – 4 uL
    - HPLC H2O – 16 uL
- Reaction mix
    - 2 uL 10x NEBuffer 2
    - 2 uL diluted SAM (or water for unmethylated control sample)
    - 1 ug DNA
    - HPLC H2O to 19 uL
- Add 1 uL SssI and mix by pipetting
- Incubate at 37^{o}C overnight
- Stop reaction by incubating at 65^{o}C for 20 minutes

If you are not methylating the HSPtranscription DNA as your test DNA, set up a reactions using 1 ug of HSPtranscription with and without SAM to test methylation efficiency

Purifying the HSPtranscription test reactions

- Increase the volume of the HSPtranscription reactions with and without SAM to 100 uL with HPLC H2O
- Add 100 uL phenol, vortex, and spin at full speed in the 4^{o}C benchtop centrifuge
- Transfer aqueous (top) layer to a clean tube
- Add 100 uL HPLC H2O to the phenol layer, vortex, and spin at full speed in the 4^{o}C benchtop centrifuge
- Transfer aqueous (top) layer to the tube containing the previous aqueous layer
- Add 200 uL Chlorofom to the collected aqueous layers, vortex, and spin at full speed in the 4^{o}C benchtop centrifuge
- Transfer aqueous (top) layer to a clean tube
- Add 100 uL HPLC H2O to the chloroform layer, vortex, and spin at full speed in the 4^{o}C benchtop centrifuge
- Transfer aqueous (top) layer to the tube containing the previous aqueous layer
- To the collected aqueous layers (about 300 uL), add 900 uL 100% ethanol and 40 ug of glycogen (8 uL of the 5 mg/mL stock)
- Incubate at -80^{o}C for at least 20 minutes or -20^{o}C overnight
- Spin at full speed in the 4^{o}C benchtop centrifuge for 45 minutes
- Remove the supernatant from the pellet and wash the pellet with 100 uL 70% ethanol
- Spin at full speed in the 4^{o}C benchtop centrifuge for 10 minutes
- Remove the supernatant from the pellet and allow it to dry for 5 minutes
- Resuspend the pellet in 25 uL of HPLC H2O and check the concentration on the nanodrop

Diagnostic restriction digest with AciI

- Set up 4 restriction digest reactions – one with and without AciI for the reactions with and without SAM
- Reaction mix

    - 200 ng purified HSPtranscription DNA
    - 2 uL CutSmart Buffer
    - HPLC H2O to 19 uL
- Add 1 uL of AciI or HPLC H2O to the reactions
- Incubate at 37^{o}C for 1 hour
- Stop the reaction with a 20 minute, 65^{o}C incubation
- Check for cutting by running 15 uL (150ng) of each reaction on a 2% nusieve gel made in 1x TBE

qPCR to determine degree of protection from digestion

- For each PCR reaction, use 0.001 ng of digested DNA
    - Reactions are at 10 ng/uL, so perform two serial dilutions of 1:100 in HPLC H2O
- For each condition, set up qPCR reactions in triplicate with test and control primer pairs
    - Test primers – pcrHSPtranscripF and pcrHSPtranscripR
    - Control primers – pcrHSPtransquantF and pcrHSPtranscripR
- SsoFast single reaction mix
    - 10 uL 2x SsoFast master mix
    - 7.5 uL HPLC H2O
    - 0.75 uL forward primer
    - 0.75 uL reverse primer
    - 1 uL template
- qPCR protocol
    1. 98^{o}C for 00:02:30
    2. 98^{o}C for 00:00:10
    3. 58^{o}C for 00:00:20
    4. Plate read
    5. Go to Step 2 39 times
    6. Melting curve from 58^{o}C to 95^{o}C with plate reads every 1^{o}C, hold for 00:00:05
    7. End
- Analyse qPCR data using the deltadeltaC(t) method
    - Determine the average C(t) for the triplicate reactions
    - Subtract the average C(t) of the control primer reactions from the average C(t) of the test primer reaction for each condition to obtain the deltaC(t)
    - Subtract the deltaC(t) of the reactions with template that was not cut with AciI from the deltaC(t) of the reactions with template that was cut with AciI to determine the deltadeltaC(t)
    - Fold change = 2^-deltadeltaC(t)
    - Express the fold change as a percentage to determine the percent protection

TFAM EMSA

Radioactive labeling with T4 PNK for EMSAs

- Reaction mix
    - 5 pmol methylated or unmethylated DNA, as determined by length and concentration using the Promega Biomath Calculator
    - 1.5 uL [gamma-32P] ATP
    - 5 uL 10x T4 PNK buffer
    - 2 uL T4 PNK
    - HPLC H2O to 50 uL
- Incubate at 37^{o}C for 30 minutes
- Stop reaction by incubating at 65^{o}C for 20 minutes

Removing unincorporated ATP with a probeQuant column

- Break off bottom seal of illustra ProbeQuant column and loosen the cap ¼ turn
- Spin at 3000 rpm in the radioactive room centrifuge for 1 minute
- Transfer the column to a clean tube and pipette the T4 PNK reaction onto the column
- Spin at 3000 rpm in the radioactive room centrifuge for 2 minutes
- Discard column and determine CPM with the scintillation counter
- Store probes at -20^{o}C in small radioisotope freezer

Casting Native gels – to be done immediately before performing the EMSA

- Gel mix
    - 1.875 mL 40% acrylamide, 19:1
    - 2.5 mL 30% acrylamide, 37.5:1
    - 2.5 mL 5x TBE
    - 0.25 mL fresh 10% APS
- De-gas under vacuum for 5-10 minutes while setting up 0.75 mm plates
- Separate off 12.5 mL of the gel mix in case there is leakage
- To the other 12.5 mL of the gel mix, add 12.5 uL TEMED and fill plates
- Use 10 well, 0.75 mm comb
- After gels have polymerized, pre-run in 0.5x TBE at 100V for 1 hour in the cold room on ice

EMSA reactions

- Reaction buffer – 1x
    - 20 mM Tris-HCl, pH 8
    - 10 mM MgCl2
    - 60 mM NaCl
    - 15% glycerol
    - 1 mM EDTA
    - 1 mM DTT
- Make a 2x concentration for use in EMSA reactions
- Dilute rmtTFA 1:10 in 1x reaction buffer
- Make a mastermix for methylated and unmethylated probe – (Single reaction below) x (Number of reactions +1)
    - 5 uL 2x reaction buffer

    - 1 uL 1 mg/mL BSA
    - 1 uL H_2O
- To each master mix, add (Number of reactions + 1) uL of labeled probe
- Aliquot 8 uL of the reaction mix + probe into low bind 0.6 mL tubes
- Add 1 uL H_2O to the probe-only reactions and 1 uL of the diluted rmtTFA to binding reactions
- For cold competitor reactions, add 1 uL
    - H_2O for no competitor reactions
    - 10 nM cold probe for 1x reactions
    - 100 nM cold probe for 10x reactions
- Incubate at 22^{o}C for 30 minutes
- Rinse the wells of the gel with running buffer before loading
- Add 2 uL of 15% Ficoll + 0.25% bromophenol blue + 0.25% xylene cyanol to the probe only reactions, and 2 uL of 15% Ficoll to the binding reactions
- Load the gel and run on the bench on ice for 10 minutes at 100V
- Move the gel to the cold room and run for 2.5 hours, or until the bromophenol blue has just run off the bottom of the gel
- Disassemble the gel and place on a sheet of Whatman paper
- Dry for 2 hours at 60^{o}C in the vacuum dryer
- Expose in a phosphorscreen cassette for 1 hour to overnight and scan using the Typhoon

TFAM Fluorescence Polarization

Preparing the FP probes

- Prepare 10 ug of methylated FAM-probe in 10 x 1 ug methylation reactions (see Methylating and Testing DNA)
- Equilibrate the ENrich Q column with 5 mL of 20 mM Tris, pH 8.0
- Turn off the UV lamp and wrap the column in aluminum foil
- Dilute the probe to a volume of 1 mL in 20 mM Tris, pH 8.0
- Load the diluted probe onto the ENrich Q column using the 1 mL loading loop and 5 mL of 20 mM Tris, pH 8.0, collecting the flowthrough
- Run a 15 mL gradient from 20 mM Tris, pH 8.0 to 20 mM Tris, pH 8.0 + 1 M NaCl over the column and collect 1 mL fractions
- Run 5 mL 20 mM Tris, pH 8.0 + 1 M NaCl over the column and collect 1 mL fractions
- Check the DNA concentrations in the fractions by NanoDrop – the double-stranded probe is usually present in fraction 15
- To the DNA-containing fraction(s), add 3 mL 100% ethanol and 40 ug of glycogen (8 uL of the 5 mg/mL stock)
- Incubate at -80^{o}C for at least 20 minutes or -20^{o}C overnight
- Aliquot into 2 mL microfuge tubes and spin at full speed in the 4^{o}C benchtop centrifuge for 45 minutes
- Remove the supernatant from the pellet and wash the pellet with 100 uL 70% ethanol

- Spin at full speed in the 4^{o}C benchtop centrifuge for 10 minutes
- Remove the supernatant from the pellet and allow it to dry for 5 minutes
- Resuspend the pellet in 25 uL of HPLC H2O and check the concentration on the nanodrop
- Prepare a 50 nM stock of the purified FAM probes for use in FP

Fluorescence Polarization reaction

- Reaction buffer – 1x
    - 20 mM Tris-HCl, pH 8
    - 10 mM MgCl2
    - 60 mM NaCl
    - 15% glycerol
    - 1 mM EDTA
    - 1 mM DTT
- Make a 2x concentration for use in FP reactions
- Dilute purchased rmtTFA 1:20 in 1x reaction buffer
- Prepare each reaction in triplicate – 1 3x reaction is
    - 150 uL 2x reaction buffer
    - 3 uL 50 nM purified FAM oligo
    - Diluted rmtTFA to the desired concentration
    - H_2O to 300 uL
- Incubate at 22^{o}C for 30 minutes
- Place the reactions on ice and take them up to the PheraStar in Sanger Hall
- Transfer the reactions to a black 96 well OptiPlate with flat wells, 100 uL per well
- Take an end-point reading with the FP module at an optical distance of 5.6
- Subtract the average polarization value of reactions without TFAM from those containing TFAM to determine the ΔmP